NTNU – Trondheim
Norwegian University of
Science and Technology

Comparative Study On Dynamic Responses of a Semi-submersible Wind Turbine Using a Simplified Aerodynamic Model and a BEM Model

Rui Zhang

Marine Technology
Submission date: June 2013
Supervisor: Torgeir Moan, IMT

Norwegian University of Science and Technology
Department of Marine Technology

NTNU Trondheim
Norwegian University of Science and Technology
Department of Marine Technology – Group of Marine Structures

MSC THESIS IN MARINE TECHNOLOGY

SPRING 2013

FOR

STUD.TECHN. Rui Zhang

Comparative study on dynamic responses of a semi-submersible wind turbine using a simplified aerodynamic model and a BEM model

Sammenlignende studie av dynamiske effekter av en halvt nedsenkbar vindturbin med forenklet aerodynamisk modell og en BEM modell

Background

Dynamic responses of floating wind turbines in turbulent wind and random waves are of interest for design purpose. Aerodynamic loads acting on wind turbine rotor, in particular the integrated thrust force, may induce large resonant motions in pitch and/or surge for floating concepts. A simplified thrust force model for wind turbine aerodynamics has been developed and combined with Simo/Riflex to predict global motion response of floating wind turbines. This tool is called Simo/Riflex/TDHMILL. It has been validated for spar wind turbines by comparison with the analysis tool HAWC2 in which the Blade Element Momentum (BEM) theory is used for aerodynamics. The objective of this MSc thesis is to compare this simplified model for a semi-submersible wind turbine with Simo/Riflex/Aerodyn. The WindFloat concept will be considered for comparison.

This MSc thesis work aims at comparing the aerodynamic model TDHMILL and Aerodyn using the same WindFloat model developed in Simo/Riflex and should be carried out in cooperation with the PhD candidate Chenyu Luan at CeSOS.

Assignment

The following tasks should be addressed in the thesis:

1. Literature review on semi-submersible wind turbines with focus on the WindFloat concept, aerodynamic model (both simplified and refined models), methods for hydrodynamic analysis and global motion analysis.

2. Establish a complete WindFloat model in Simo/Riflex with the help from Chenyu Luan. The model should include a rigid-body formulation for the semi-submersible floater and beam models for tower, blades and mooring lines.

3. Select representative long-term wind and wave conditions. For short-term time domain simulations, the same turbulent wind field generated by TurboSim and random waves generated in Simo should be used for comparison.

4. Compare the analysis tools Simo/Riflex/TDHMILL and Simo/Riflex/Aerodyn for global dynamic responses of the WindFloat. The response parameters should include thrust force, rigid-body motions of the floater and mooring line tension. The comparison should be made based on response time series, spectra and statistics.

5. Conclude the work and give recommendations for future work on the use of simplified and refined aerodynamic models.

The work scope could be larger than anticipated. Subject to approval from the supervisors, topics may be deleted from the list above or reduced in extent.

In the thesis the candidate shall present his personal contribution to the resolution of problem within the scope of the thesis work.

Theories and conclusions should be based on mathematical derivations and/or logic reasoning identifying the various steps in the deduction.

The candidate should utilize the existing possibilities for obtaining relevant literature.

The thesis should be organized in a rational manner to give a clear exposition of results, assessments, and conclusions. The text should be brief and to the point, with a clear language. Telegraphic language should be avoided.

The thesis shall contain the following elements: A text defining the scope, preface, list of contents, summary, main body of thesis, conclusions with recommendations for further work, list of symbols and acronyms, reference and (optional) appendices. All figures, tables and equations shall be numerated.

The supervisor may require that the candidate, in an early stage of the work, present a written plan for the completion of the work. The plan should include a budget for the use of computer and laboratory resources that will be charged to the department. Overruns shall be reported to the supervisor.

The original contribution of the candidate and material taken from other sources shall be clearly defined. Work from other sources shall be properly referenced using an acknowledged referencing system.

The thesis shall be submitted in two copies as well as an electronic copy on a CD:

- Signed by the candidate
- The text defining the scope included
- In bound volume(s)
- Drawings and/or computer prints which cannot be bound should be organized in a separate folder.

Supervisors: Professor Torgeir Moan, PhD candidate Chenyu Luan, Dr. Zhen Gao, NTNU

Torgeir Moan

Deadline: 10.06.2013.

Preface

This report presents my master thesis work in NTNU. The thesis work is done in accordance to all the tasks and requirements proposed in the thesis description, with detailed discussions and comments on relevant contents.

This thesis cannot be completed without great support from many people at Marine Technology Department and the Center for Ships and Offshore Structures of NTNU.

First of all, I would like to thank my supervisor Prof. Torgeir Moan, who has provided support on my thesis and my master's project throughout the final year of my master study. Special thanks to Dr. Zhen Gao, for his guidance on the thesis content and discussions on the results. Special thanks to PhD candidate Chenyu Luan, for his help with the computation tools and key modeling considerations.

Gratitude is also given to Ms. Marit Irene Kvittem, for her help on the mooring system design, Ms. Lin Li, for her help on the environmental statistic information in Norwegian Sea, Mr. Qinyuan Li, for his help with wind input file generation tools, and Mr. Shengsheng Fan, for his help on Matlab data processing.

Rui Zhang

June, 2013

Trondheim, Norway

Abstract

Due to the high potential of offshore wind energy, a lot of research work is being done around the world on offshore wind turbines. Currently mainly two types of model are used in Marine Technology Department of NTNU to estimate wind effect on the turbine. A simplified method with computation tool TDHmill, and a refined method with computation tool Aerodyn. No detailed analysis has yet been performed to show the difference between these two methods on a semi-submersible floating offshore wind turbine.

In this thesis, the comparison between these models is performed.

Two models are set up in the Simo-Riflex dynamic response calculation code with exactly the same floater and mooring system. Wind turbines in the two models are set up with the two different computation tools. Environmental conditions are chosen based on the wind turbine specification and wave statistics in Norwegian Sea. Wind input files in the two models are transformed from one origin and thus are exactly the same.

The models are checked to show that they are similar with regard to all features except wind turbine models, and the two models are reasonable in engineering reality.

The results are analyzed based on the response time series, mean value and standard deviation and response spectrum. It is shown that mean values of thrust force, floater motion and mooring line tension are similar in the two models but TDHmill model shows a slightly larger response. Generally TDHmill model shows less variation than Aerodyn model, with significant difference. In extreme conditions, conclusions can be drawn that TDHmill gives poor estimation of the wind effect, the mooring line tension response is slightly smaller in TDHmill model, and wave effect is more important than wind effect. Computation time for TDHmill is much shorter than for Aerodyn model.

It can be concluded that TDHmill can be used in any environment in turbine working conditions, when mean value is the value of interest and accuracy requirement is not very strict. And TDHmill cannot be used in extreme condition analysis, or when extreme value or oscillation range is the value of interest. Neither can it be used when accuracy requirement is strict.

Table of Contents

List of Figures

List of Tables

List of Symbols

Symbol	Description
ρ	Density of sea water
V	Displacement of the floater
R_x	Radius of gyration in x direction
R_y	Radius of gyration in y direction
R_z	Radius of gyration in z direction
C_D	Drag coefficient in Morison Equation
I_{ij}	Moment of inertia
∇	Displacement
T_H	Thrust force
K	Parameter in thrust force formula
C_T	Thrust force coefficient
U_{REL}	Relative wind velocity
u_T	Reference wind velocity
R	Radius of wind turbine
A	Added mass
K	System stiffness
ζ	Damping ratio
δ	Logarithmic decrement
x_0	Original displacement
x_n	Displacement maxima of the n-th cycle
ω_d	Damped natural frequency
ω_n	Natural frequency
U_{10}	Mean wind speed at 10m height
$U(z)$	Mean wind speed at z m height
I	Turbulence intensity
U_w	Mean wind speed
H_s	Significant wave height
T_p	Peak period
γ	Peak enhancement factor

List of Acronyms and Abbreviations

NREL	National Renewable Energy Laboratory
COG	Center of gravity
CeSOS	Centre for Ships and Ocean Structures
DNV	Det Norske Veritas
BEM	Beam element momentum
RAO	Response amplitude factor
GM	Metacentric height
BM	Metacentric radius
GK	Center of gravity height
BK	Center of buoyancy height
IEC	International Electrotechnical Commission
NTMs	Normal Turbulence Models
FFT	Fast Fourier Transformation
PDF	Probability density function
CDF	Cumulative distribution function
ULS	Ultimate limit state
ALS	Accidental limit state
WAFO	Wave Analysis for Fatigue and Oceanography

Chapter 1. Introduction

1.1 Background

As the demand for energy is increasing and focus is shifted towards non-polluting renewable energy sources, wind energy has emerged as a good alternative. Wind energy has been utilized for power production for decades and for agricultural purposes for centuries. Offshore wind energy has a large potential in terms of space, larger average wind speeds and less turbulence than onshore. For large water depths floating wind turbines might be the most cost effective solution Floating wind turbines is a new technology. Land based turbines on the other hand are a proven technology but have met a lot of resistance because of their aesthetics and impact on nature. Offshore wind turbines do not have the same problem, but reducing the costs to a reasonable level is a challenge.

Therefore, a lot of research work is being done currently to estimate the performance of offshore floating wind turbine. One of the most important parts of offshore wind turbine time domain simulation is how to model the wind effect on the turbine.

1.2 Motivation

Currently two types of models are used in Marine Technology Center at NTNU to estimate wind effect on the turbine. In the first method, an external force is applied at the rotor point, and the tower and turbine are regarded as part of the rigid floater. The computation code for this method is called TDHmill, developed by Statoil. In the second method, the turbine and tower are modeled as beams, and the wind is applied at each element on the blades. The computation code for this method is called Aerodyn, developed by NREL.

The first method is a simplified method, while the second one is believed to be a refined method. Up to now, no detailed study has been performed to show the difference between these two models on semi-submersible wind turbines.

Further analysis of Wind Turbines based on these two methods is expected to continue in the future. Thus it is interesting to conduct an assessment of the performance of these two wind turbine models.

1.3 Objective

The objective of this thesis project is to compare the performance of the two models and show the feasibility of the simplified method.

Wind thrust force, floater motion and mooring line tension are taken as the parameters to be studied. Load cases are taken from different wind speeds from the cut-in speed to cut-out speed and the wind speed corresponding to the extreme condition in Norwegian Sea.

1.4 Outline of the report

There are mainly 3 parts in this project.

Chapters 1-3 is the introduction part, which introduces the basis for this thesis project, including calculation method and tools, models and thesis outline.

Chapter 4-6 is the simulation preparation part. This is a very important part of the project. First in this part, all the input files are set up for the two models. Next, verification work is done to make sure that the two models are the same and the models are physically reasonable. Then, study cases are selected based on the turbine specifications and the probability distribution of wind and wave.

Chapter 7-10 is the result presentation part. Here different kinds of results are presented with discussions. A few sample time series are first given to show an overall idea of the response in the two models. Next, mean value and standard deviation of thrust force, floater motion and mooring line tension are compared with discussion. Finally, spectral analyses are performed for sample cases, and stochastic uncertainty is considered for extreme conditions.

Chapter 11 is the conclusion part. Conclusions are summarized here, and future work is recommended.

Chapter 2. Description of WindFloat 5 MW Semi-submersible

2.1 Summary

Many concepts have been proposed for different water depths in the offshore wind industry, including jackets, floating structures, TLPs or spars. One of the well-developed concepts is the WindFloat 2MW semi-submersible design by PrinciplePower (US)[1], which has already been constructed and is now in operation outside Portugal. A similar design WindFloat 5MW has then been proposed, with some analysis and test results open to public. The WindFloat 5MW will be used as the basic model in our project, and the available results will be used for comparison.

In this chapter, the WindFloat 5MW concept and its main parameters will be introduced, including the main structures, floater specifications, mooring system and wind turbine information.

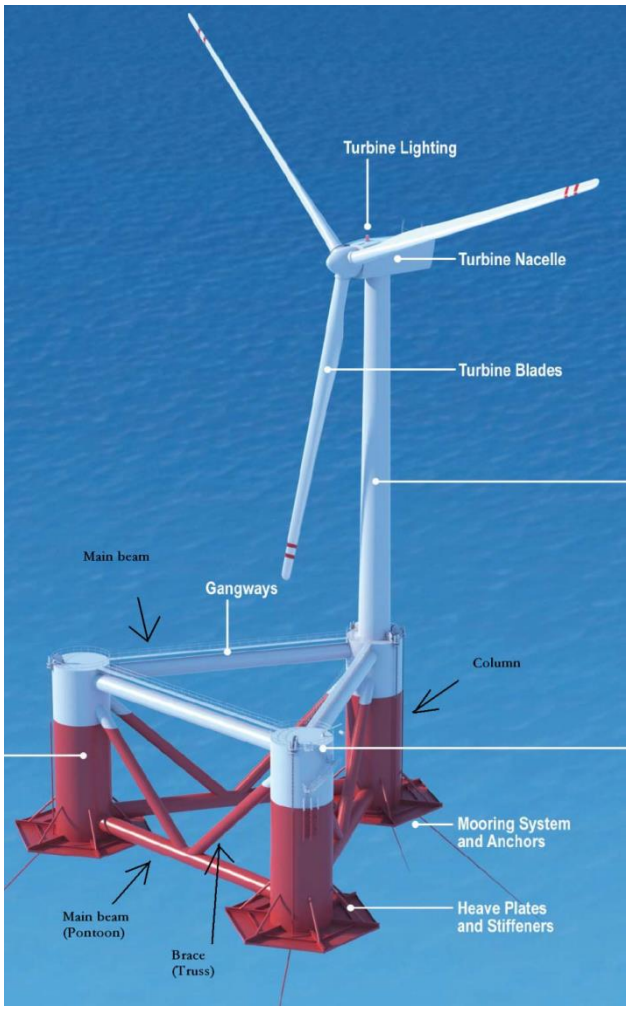

Figure 2-1 WindFloat concept

The WindFloat 5 MW design consists of a 3-column stabilized offshore platform with water-entrapment plates and an asymmetric mooring system. A wind turbine tower is positioned directly

[1] Principle Power. Inc. http://www.principlepowerinc.com/products/windfloat.html Windfloat description

above one of the stabilizing columns. See the Figure 2-1 above for a brief illustration of the structures.[1]

2.2 Floater

The main particulars of the WindFloat floater are presented below.

	Unit	Value
Column diameter	m	10
Pontoon diameter	m	2.1
Length of heave plate edge	m	15
Draft	m	17
Column center to center	m	46
Thickness of heave plate	m	0.1

Table 2-1 Main particulars of the WindFloat

The mass distribution of the whole structure is shown in the table.

		Value	Units
Displacement	ρV	4.64E06	kg
Coordinate of the center of gravity	X	-0.278	m
	Y	0	m
	Z	3.728	m
Radius of Gyration	Rx	34.9	m
	Ry	34.7	m
	Rz	26.5	m

Table 2-2 Mass properties of WindFloat 5MW

The top view and side view of the underwater part of the semi-submersible is presented below.

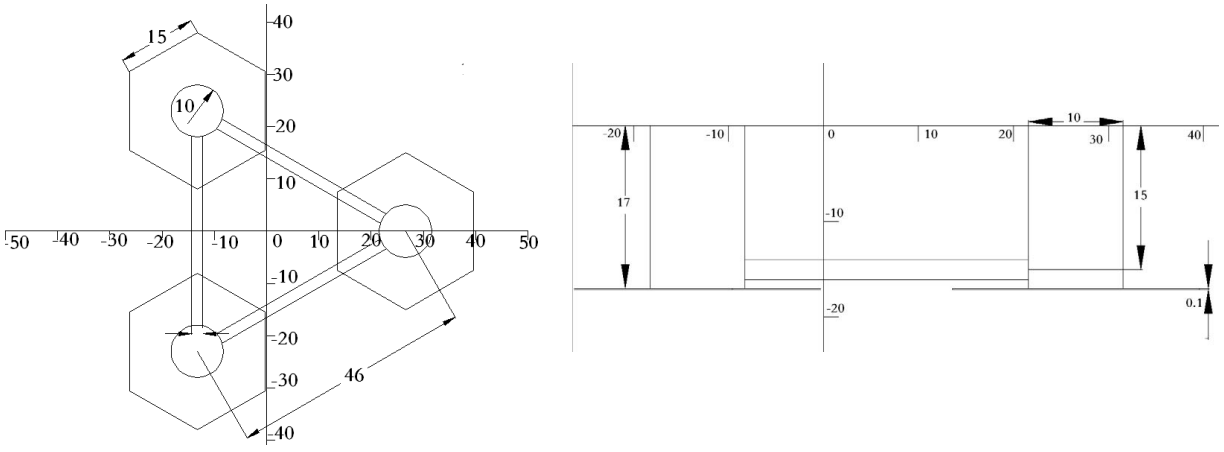

Figure 2-2 Top view and side view of the underwater part of the model

[1] Roddier D, Peiffer A. A Generic 5 MW Windfloat for Numerical Tool Validation & Comparison Against a Generic Spar. OMAE2011-50278, Rotterdam: 2011.

The mass information provided in the above table already takes into account tower and turbine, and it is only useful in the TDHmill-Simo-Riflex model. This means when doing the modeling for the Aerodyn-Simo-Riflex model, this part of mass must be extracted and new mass, COG, radius of gyration needs to be calculated again.

The floater has shown very good dynamic performance in previous work, a similar design has already been constructed and is now in operation outside Portugal.

2.3 Mooring system

According to the original design, the WindFloat is positioned with a catenary morring, which consists of 4 mooring lines, two on column 1, which carries the turbine, and one on each other column. Each line is made of 3 sections:

- 80m of 3-inch chain at the fairlead
- 718m of 5-inch chain polyester rope
- 80m of 3-inch chain to the anchor

A clump weight is attached to the upper chain section and the polyester rope to control the tension. The pretension on the mooring lines is 535kN.

The fairleads and anchor locations with respect to the platform region, and the mooring line weights, and the mooring line tension at rest are presented in the tables below.

	x	*y*	*z*
Fairlead1	29.578	-5.51	-16.8
Fairlead2	29.578	5.51	-16.8
Fairlead3	-16.379	28.37	-16.8
Fairlead4	-16.379	-28.37	-16.8
Anchor1	600	-600	-319.9
Anchor2	600	600	-319.9
Anchor3	-600	600	-319.9
Anchor4	-600	-600	-319.9

Table 2-3 Fairlead and anchor locations with respect to the platform origin

	Mass per unit (kg/m)	Weight in air (kN/m)	Weight in water (kN/m)	Extensional stiffness (kN)
Top chain	127	1.247	1.083	586450
Polyester	18	0.176	0.045	100000
Bottom chain	127	1.247	1.083	586450

Table 2-4 Line weight

	Fairlead1	Fairlead2	Fairlead3	Fairlead4
Mooring line tension at rest	539	539	531	531

Table 2-5 Line pretension

However, the line tension at rest cannot be obtained in the Simo-Riflex model, which will be used in this project. This has been shown in previous work by the author.

In order to achieve the correct mooring line tension at rest, as well as the correct stiffness features of the mooring system, modifications to the mooring line length and clump weight have been done by Marit Irene Kvittem at CeSOS. The corrected mooring system shows very good consistence in terms of dynamic performance with the original design. This will be demonstrated later in Chapter 4 and 5.

2.4 Wind turbine and tower

The wind turbine used in this project is known as the "NREL offshore 5-MW baseline wind turbine". It is the reference wind turbine provided by National Renewable Energy Laboratory (NREL) in the USA. It is a three-bladed upwind turbine. The turbine has a cut-in wind speed of 3m/s which is the wind speed required to start power production. The maximum wind speed for power production is 25m/s. this is the cut-out wind speed and the blades are pitched to produce minimum lift ad stops rotating. At the speed of 11.2m/s the thrust force is at its maximum when the turbine is running. The rotor speed is kept constant between rated speed (11.2m/s) and the cut-out speed (25m/s) while the thrust force is decreasing in this interval. The thrust force and power curves are given below.

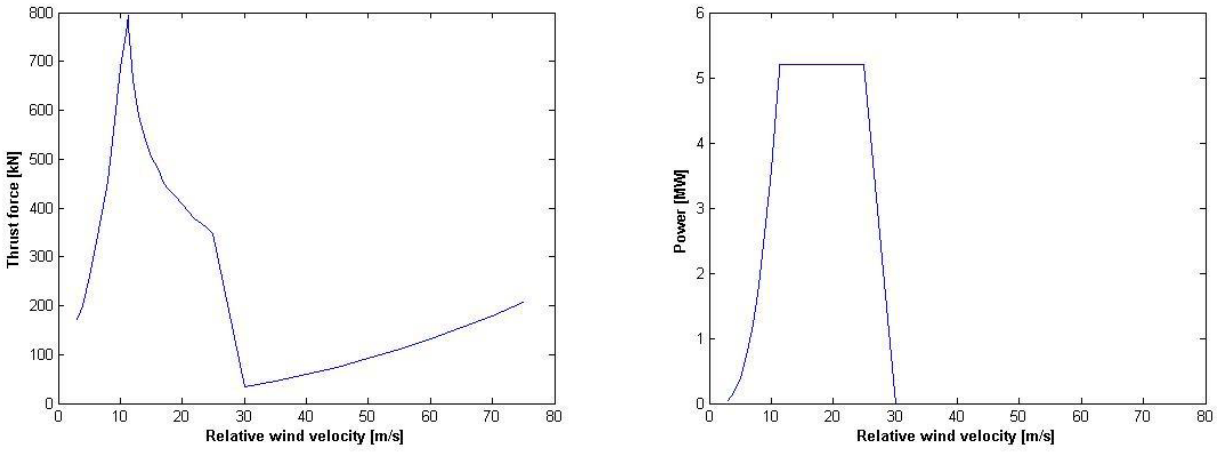

Figure 2-3 Force and power curves for NREL 5MW[1]

All specifications of the blade structural properties, blade aerodynamic properties and hub and nacelle properties, as well as the control system properties are also provided for this reference wind turbine. The reference wind turbine is directly applicable to AeroDyn model. However, a transformation should be done before it can be used in the TDHmill model in terms of response features and control system.

[1] Jonkman J, Butterfield S. Definition of a 5 MW Reference Wind Turbine for Offshore System Development. Technical Report NREL/TP-500-38060. 2009.

It should be noted here that we are changing the original wind turbine on WindFloat 5MW to the reference turbine NREL 5MW, of which more information is available. These two turbines are not exactly the same. However, the blade length are similar (63m and 61.5m), and the generator power are the same (5MW), so the combination of these two will still make a reasonable model.

The basic properties of this reference wind turbine are shown below.

Rating	5 MW
Rotor Orientation, Configuration	Upwind, 3 Blades
Control	Variable Speed, Collective Pitch
Drivetrain	High Speed, Multiple-Stage Gearbox
Rotor, Hub Diameter	126 m, 3 m
Hub Height	90 m
Cut-In, Rated, Cut-Out Wind Speed	3 m/s, 11.4 m/s, 25 m/s
Cut-In, Rated Rotor Speed	6.9 rpm, 12.1 rpm
Rated Tip Speed	80 m/s
Overhang, Shaft Tilt, Precone	5 m, 5º, 2.5º
Rotor Mass	110,000 kg
Nacelle Mass	240,000 kg
Tower Mass	347,460 kg
Coordinate Location of Overall CM	(-0.2 m, 0.0 m, 64.0 m)

Table 2-6 Specifications of the wind turbine[1]

The modeling of the wind turbine will be shown in Chapter 4.

[1] Jonkman J, Butterfield S. Definition of a 5 MW Reference Wind Turbine for Offshore System Development. Technical Report NREL/TP-500-38060. 2009.

Chapter 3. Brief Theory Review and Introduction of Computation Tools

3.1 Summary

In this chapter, the theoretical knowledge used in this project will be introduced briefly. Introduction of computation tools used in this project will also be given.

The theories in this project concerns computation of the dynamic response, different methods to calculate wind effect on the turbine, as well as wind turbine control method.

The computation tools used in this project include: GeniE, HydroD, Simo, Riflex, TDHmill, Aerodyn and Turbsim. Matlab is also used for data process.

3.2 Dynamic response theory

The nonlinear dynamic equilibrium equation can be expressed as

$$\boldsymbol{M}(\boldsymbol{r})\ddot{\boldsymbol{r}} + \boldsymbol{D}(\dot{\boldsymbol{r}})\dot{\boldsymbol{r}} + \boldsymbol{K}(\boldsymbol{r})\boldsymbol{r} = \boldsymbol{Q}(\boldsymbol{t}, \boldsymbol{r}, \dot{\boldsymbol{r}})$$

where ***M*** is the mass matrix, ***D*** is the damping matrix, ***K*** is the stiffness matrix, ***Q*** is the load vector and ***r*** is the response deformation vector.

Given the system features (***M***, ***K***, ***D***), the load history (***Q***) and the initial conditions ($\boldsymbol{r_0}$), the response can be calculated by step by step integration. And after getting the response vector ***r***, other unknowns like the motion of the floater and mooring line tension can be obtained from geometric relationship, displacement-strain relationship and strain-stress relationship.

3.3 Basic wind turbine theory

3.3.1 Wind spectrum

The wind velocity $\tilde{u}$ can be split up into a mean and a fluctuating part:

$$\tilde{u} = U + u$$

where *u* is the fluctuation and *U* is the mean value or time average:

$$U = \frac{1}{T}\int_0^T \tilde{u}dt$$

T is the time considered, which should be larger than any significant period of the fluctuations.[1]

The turbulence intensity is defined as the ratio between the standard deviation of the wind speed and the mean wind speed:

$$I_{Turb} = \frac{\sigma_{\tilde{u}}}{U}$$

[1] H. Tennekes and J.L Lumley. A First Course in Turbulence. The MIT Press, 1972.

The wind and how the wind turbulence is distributed between different frequencies can be expressed through a wind spectrum. According to DNV[1], the Harris and Kaimal spectrum is commonly used. In this project, Kaimal model is used to generate the wind time series for different mean wind speeds and turbulence intensities.

The Kaimal wind spectrum is given as[2]:

$$S_K(f) = \frac{4\sigma_{\tilde{u}} \frac{L_K}{U_{hub}}}{\left(1 + \frac{6L_k f}{U_{hub}}\right)^{5/3}}$$

where

$$\sigma_{\tilde{u}} = I_{Turb}(0.75U_{hub} + 5.6)$$

$$L_K = 8.1\lambda$$

are the standard deviation and integral length scale.

U_{hub} is the mean wind velocity at hub height and is the spectral parameter.

3.3.2 Thrust force from 1-D momentum theory

In the TDHmill model, only the rotor thrust force is calculated with a simple method. To give some understanding about how the rotor thrust force can be calculated in a simple manner the 1-D momentum theory will be briefly discussed.

The simple 1-D model is shown in the following figure. The rotor is considered as an ideal, frictionless disc and the wake behind it is not rotating. The flow is incompressible, steady and inviscid. The pressure far downstream of the rotor is equal to the atmospheric pressure also found far upstream, P_0.

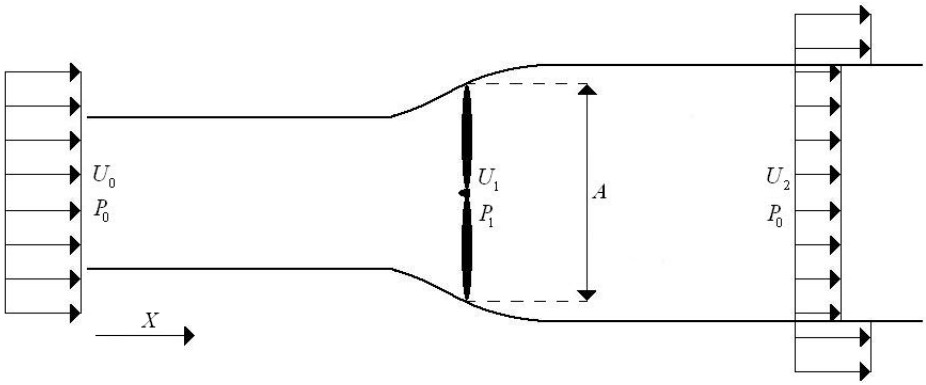

Figure 3-1 1-D momentum model[3]

[1] DNV/Risø. Guidelines for design of wind turbines, second edition. Jydsk Centraltrykkeri, Denmark 2002.
[2] Rune Yttervik. TDHMILL3D User documentation. Statoil internal document, 2009.
[3] Jonkman J, Butterfield S. Definition of a 5 MW Reference Wind Turbine for Offshore System Development. Technical Report NREL/TP-500-38060. 2009.

There is a pressure drop over the rotor. Using Bernoulli's equation upstream and downstream of the rotor gives the following expression for the change in pressure:

$$\Delta P = \frac{1}{2}\rho(U_0^2 - U_1^2)$$

where ρ is the mass density of air.

An expression for the thrust force is then obtained by multiplying the pressure drop with the swept rotor area.

$$T = \Delta P A$$

To determine the magnitude of the velocity behind the rotor, U_2, the momentum equation will be used together with the conservation of mass. The thrust force can be expressed as:

$$T = -\sum F_x = \dot{m}_0 U_0 - \dot{m}_2 U_2$$

$\dot{m}_0$ and $\dot{m}_2$ is the mass flow rate at location 0 and 2 in the figure. The flow is steady and the conservation of the mass then gives:

$$\dot{m}_0 = \dot{m}_2 = \dot{m}_1 = \rho U_1 A$$

The thrust force then becomes:

$$T = \rho U_1 A(U_0 - U_2)$$

And so the velocity at the rotor reads:

$$U_1 = \frac{1}{2}(U_0 + U_2)$$

The axial induction factor, a, is defined as the ratio of the reduction in fluid velocity between location 0 and 1 and the velocity at location 0:

$$U_1 = (1 - a)U_0$$

So,

$$U_2 = (1 - 2a)U_0$$

And the final expression for the thrust force:

$$T = \frac{1}{2}\rho U_1 A(U_0 - U_2) = 2\rho {U_0}^2 Aa(1 - a) = \frac{1}{2}\rho {U_0}^2 A C_T$$

where C_T is defined as thrust coefficient:

$$C_T = 4a(1 - a)$$

According to experiments, the momentum theory and the assumptions of an ideal rotor is valid only for an axial induction factor less than 0.4, M. Hansen.[1] The reason for this is that for values of *a* exceeding this value, the free shear layer at the edge of the wake becomes unstable and starts to transport momentum into the wake.

The axial induction factor is large when the wind speed is low and the wake is broad. This also means that the thrust coefficient is large when the wind speed is low. Further details on this can be found in chapter 4 in Hansen's book.

3.3.3 Blade element momentum theory

Balde element momentum theory is used in the Aerodyn model. It is relatively complex because all the blade structures with corresponding aerodynamic coefficients are calculated and used in the calculation. In this subsection, only the basic principles of the blade element momentum theory are given, no detailed matrix formulas and iteration methods are provided. The following information is extracted from Aerodyn Theory Manual[2]. See the manual for more detailed information.

Blade element momentum (BEM) theory is one of the oldest and most commonly used methods for calculating induced velocities on wind turbine blades. This theory is an extension of actuator disk theory, first proposed by the pioneering propeller work of Rankine and Froude in the late 19th century. The BEM theory, generally attributed to Betz and Glauert (1935), actually originates from two different theories: blade element theory and momentum theory (see Leishman 2000). Blade element theory assumes that blades can be divided into small elements that act independently of surrounding elements and operate aerodynamically as two-dimensional airfoils whose aerodynamic forces can be calculated based on the local flow conditions. These elemental forces are summed along the span of the blade to calculate the total forces and moments exerted on the turbine. The other half of BEM, the momentum theory, assumes that the loss of pressure or momentum in the rotor plane is caused by the work done by the airflow passing through the rotor plane on the blade elements.

Using the momentum theory, one can calculate the induced velocities from the momentum lost in the flow in the axial and tangential directions. These induced velocities affect the inflow in the rotor plane and therefore also affect the forces calculated by blade element theory. This coupling of two theories ties together blade element momentum theory and sets up an iterative process to determine the aerodynamic forces and also the induced velocities near the rotor.

In practice, BEM theory is implemented by breaking the blades of a wind turbine into many elements along the span. As these elements rotate in the rotor plane, they trace out annular regions, shown in the figure above, across which the momentum balance takes place. These annular regions are also where the induced velocities from the wake change the local flow velocity at the rotor plane. BEM can also be used to analyze stream tubes through the rotor disk, which can

[1] Martin O. L. Hansen. Aerodynamics of Wind Turbines, second edition. Earthscan, 2008.

[2] P.J. Moriarty. AeroDyn Theory Manual

be smaller than the annular regions and provide more computational fidelity. However, as currently written, AeroDyn only allows analysis using annular regions.

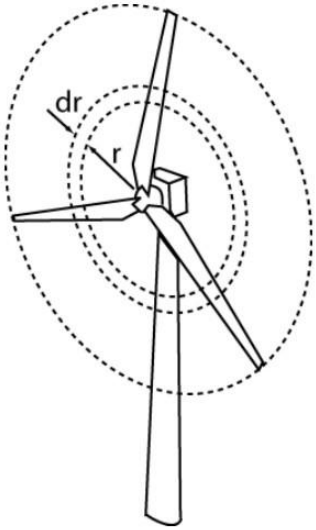

Figure 3-2 Annular plane used in blade element momentum theory

3.3.4 Wind turbine control method

Floating wind turbines equipped with a control system designed for conventional land based turbines may for wind speeds above the rated speed experience large resonant motions. The wind forces may amplify the wave motions and this can be considered as a negative damping effect. The power curve and thrust curve for this turbine is shown in Figure 3-3. Above the rated wind speed of 11.2m/s the power output is kept constant by controlling the blade pitch. From the corresponding thrust force curve, we see that the thrust force decreases for wind speeds above rated. This can explain the negative damping effect. Consider a case with wind speed above rated. If the turbine is surging/pitching towards the wind, the relative wind speed will increase and the thrust force according to the curve will decrease, leading to a smaller force against the movement. If the turbine is moving away from the wind the opposite will happen.

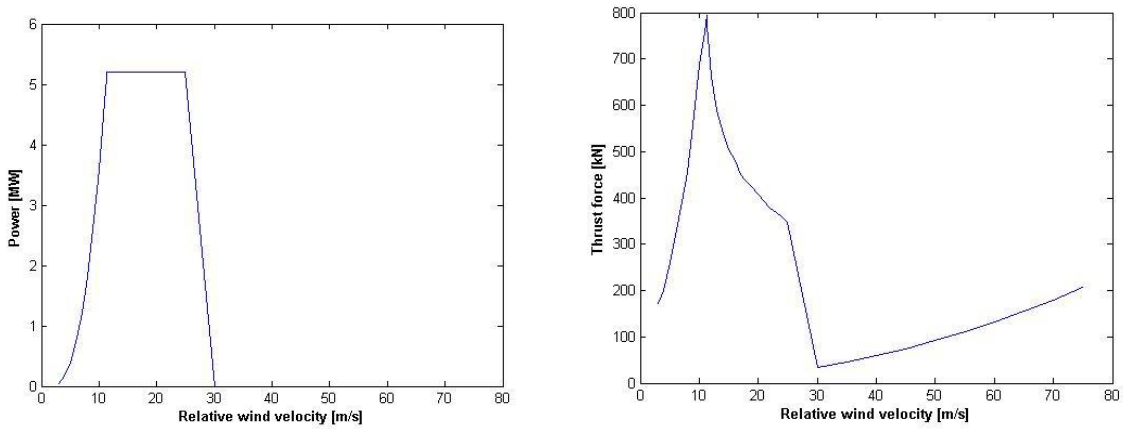

Figure 3-3 Power and thrust force curve

Especially for floating wind turbines of the spar/semi-sub type this is a problem because the pitch motions are large and the wind contains significant energy around the typical pitch natural frequencies. For floating wind turbines it is therefore necessary to have a wind turbine control system designed to overcome this issue.

In this project, the pitch control is used in the Aerodyn model, while in the TDHmill mill the turbine control is not modeled in detail, but the information of control is included through the set of thrust coefficients.

3.4 Introduction to computation tools

HydroD

Sesam HydroD is a tool for hydrostatic and hydrodynamic analysis. The module used in this project to do linear response calculation is Wadam.

Wadam is based on widely accepted linear methods for marine hydrodynamics the 3-D radiation-diffraction theory employing a panel model and Morison equation in linearized form employing a beam model. Only the single body model corresponding to the radiation-diffraction theory is applied in this project.

HydroD is used to calculate the hydrodynamic coefficients and RAOs for the floater. This information is then imported to DeepC for further use.

DeepC

Sesam DeepC is a tool for mooring and riser design as well marine operations of offshore floating structures. It can perform mooring analysis separately or when including the coupled effects from risers and vessels. Furthermore, Sesam DeepC may be used for riser design where the risers are analyzed separately or when considering coupling effects. Marine operations may be simulated in the time domain for a study of motions and station keeping of multi-body systems.

In this project, DeepC is used to write the input files for riflex and Simo. The mooring system, including mooring line deployment and line features, is modeled in DeepC. After the input files are obtained from DeepC, they are modified manually, and then put into computation by Riflex and Simo, together with TDHmill or Aerodyn.

Simo[1]

SIMO is a time domain simulation program for study of motions and station keeping of multibody systems. Flexible modelling of station keeping forces and connecting force mechanisms (anchor lines, ropes, thrusters, fenders, bumpers, docking guide piles) is included.

The results from the program are presented as time traces, statistics and spectral analysis of all forces and motions of all bodies in the analysed system.

[1]SINTEF. Simo introduction. http://www.sintef.no/upload/MARINTEK/PDF-filer/Sofware/Simo.pdf

Riflex

RIFLEX is a tailor-made computer program system for static and dynamic analysis of flexible riser systems. User friendliness is achieved by taking advantage of the simple geometry of flexible risers which allows for very simple input/output specifications and automatic mesh generation. Special input/output specifications are available for standard riser systems such as the Free Hanging, Steep Wave, Lazy Wave, Steep S and Lazy S configurations. Several alternatives are available for static and dynamic analyses from very simple methods which are useful in the early stage design, to advanced 3-D analyses of arbitrary flexible riser systems.[1]

In addition to the original aim of this code, it can also be used to calculate static and dynamic features of system with flexible beams.

The combination of Simo and Riflex are applied in order to calculate the time domain dynamic response for both rigid bodies and flexible structures. Simo is used to calculate rigid bodies including the floater, nacelle and hub, while Riflex is used to calculate flexible structures like the blades, tower and mooring lines.

Aerodyn

AeroDyn is a series of routines written to perform the aerodynamic calculations for aeroelastic simulations of horizontal axis wind turbine configurations. Craig Hansen and researchers at the University of Utah and Windward Engineering originally developed these routines for wind turbine simulation work, and the complexity of the algorithms has gradually increased with time. Recently, researchers at the National Renewable Energy Laboratory (NREL) have further developed these routines and changes are ongoing. This report provides users of these routines with the aerodynamic theories behind the various algorithms in AeroDyn. It also provides some insight into the limits of each aerodynamic model, which may provide ideas for further improvement. This report is not intended to be a user's guide for the routines, however. That kind of guide (Laino and Hansen 2002) is available for downloading at the NREL design codes Web site (http://wind.nrel.gov/designcodes/).

Currently, the routines of AeroDyn interface with several aeroelastic simulation codes: YawDyn, FAST, SymDyn, and ADAMS. The differences between these codes lie mainly in the structural dynamics, and since each of them uses AeroDyn, the aerodynamic calculations between them are identical. Further explanation and user's guides for each of these codes are also on the NREL design codes Web site.[2]

The Aerodyn-Simo-Riflex model has been developed by CeSOS, and is proved to give satisfactory calculation results. The detailed wind turbine should be modeled in Simo-Riflex model and Aerodyn will provide wind force to the Simo-Riflex structural response model.

---

[1] MARINTEK. Rifelx. http://www.sintef.no/home/MARINTEK-old/Software-developed-at-MARINTEK/RIFLEX/

[2] P.J. Moriarty. AeroDyn Theory Manual

TDHmill

TDHmill is a simplified computer tool for analysis of floating wind power facilities developed by MARINTEK. It is a numerical model of thrust from a wind turbine rotor onto the nacelle. The model consists of coefficients for thrust (force in the axial direction of the rotor axis) tabulated as a function of relative velocity between rotor and the wind. Gyro-moments from the rotor when it is rotating about an axis in the rotor plane are also included.[1]

TDHmill is designed to work together with the MARINTEK computer program SIMO. Force models for wind turbine rotors do not exist in SIMO today. TDHmill provides an external force that is caused by the wind turbine and put that into the SIMO calculation.

Turbsim[2]

The TurbSim stochastic inflow turbulence tool has been developed to provide a numerical simulation of a full-field flow that contains coherent turbulence structures that reflect the proper spatiotemporal turbulent velocity field relationships seen in instabilities associated with nocturnal boundary layer flows and which are not represented well by the IEC Normal Turbulence Models (NTM). Its purpose is to provide the wind turbine designer with the ability to drive design code (e.g., FAST or MSC.Adams®) simulations of advanced turbine designs with simulated inflow turbulence environments that incorporate many of the important fluid dynamic features known to adversely affect turbine aeroelastic response and loading.

[1] Statoil. TDHMILL3D User Documentation

[2] Kelley N, Jonkman B. TurbSim description. http://wind.nrel.gov/designcodes/preprocessors/turbsim/

Chapter 4. Modeling

4.1 Summary

In this project, two complex models must be set up. The model concerns floater, mooring line, tower and turbine. For the floater, same hydrodynamic model can be used for both models (added mass, RAO etc.). Mass model from HydroD can be used directly in TDHmill Model (here and after noted as Model A), but turbine mass must be extracted in the Aerodyn Model (here and after noted as Model B). The tower and the turbine must be modeled in detail in Aerodyn Model. No structure model of the tower and the turbine is required in Model A, but turbine specifications must be transformed. Wind files must be generated for Model B and then processed to files that can be loaded into TDHmill.

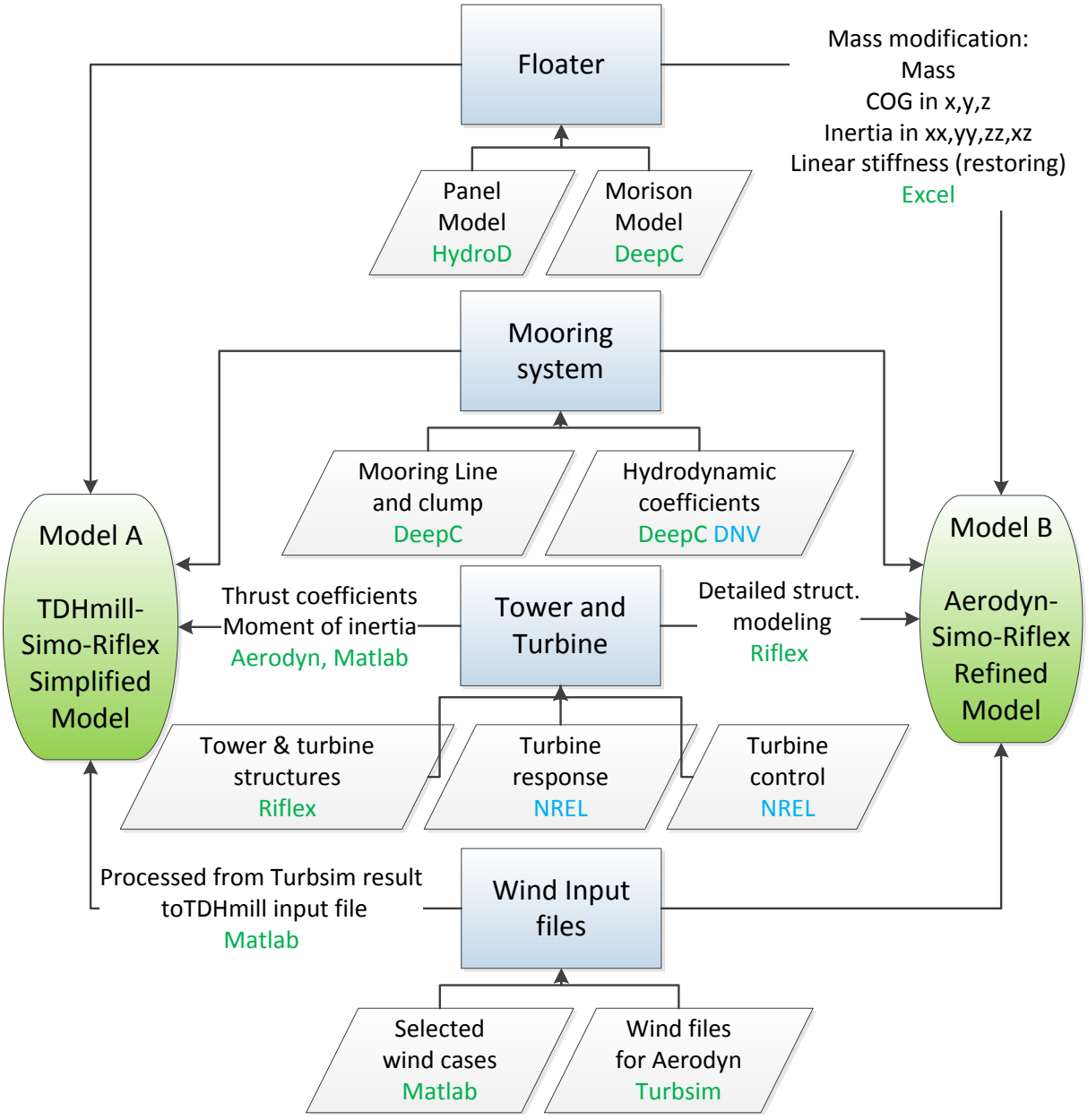

Figure 4-1 Modeling set up process structure

The figure above shows an overall idea of how the models are set up. The four rectangular boxes are the main steps, the parallelograms denote information input, the lines mark information flow, and the notes on the lines show the modifications or calculations needed for modeling. Green letters denote software or tools used, and blue letters are references from which the information is obtained.

4.2 Floater

4.2.1 Panel model

The model established by Luan in his previous work is based on the same model in our study case, and has shown quite satisfactory results. Thus his panel model established in GeniE is used directly in this project.

However, since extreme condition calculation is associated with larger significant wave height (up to 16m) and larger peak period (up to 20s), Luan's hydrodynamic model which calculated period up to 30 seconds will not be accurate enough for this project. And thus Luan's model needs to be extended to broader period band.

So, the linear response calculation is performed again with HydroD, with the same panel model but calculation periods extended to 50s.

A figure of the panel model is shown below.

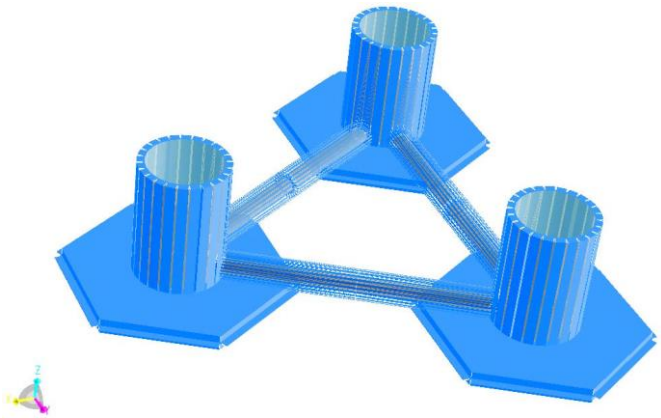

Figure 4-2 Panel model for floater[1]

4.2.2 Morison model

As Luan has done in his previous project, a Morision model is established in DeepC in this project in order to consider viscous effects.

Viscous force can be estimated by Morison's equation:

$$dF = \frac{1}{2}\rho C_D D dz|v|v$$

[1] Chenyu Luan. Pre-project for Master's Thesis. Norwegian University of Science and Technology: 2010.

where:

dF is the viscous force on a strip of length dz of a vertical rigid circular cylinder.
D is diameter of the cylinder.
v is the relevant velocity.
C_D is the drag coefficient.

The parameters of Morison model is shown in the table below. This information is also extracted from Luan's work.

		Column			Heave plate			Pontoon		
	strip No.	30	30	30	1	1	1	60	60	60
end1(m)	*x*	26.56	-13.3	-13.3	26.56	-13.3	-13.28	-13.3	-13.3	-13.3
	y	0	23	-23	0	23	-23	-23	-23	23
	z	-17	-17	-17	-17.1	-17.1	-17.1	-15	-15	-15
end2(m)	*x*	26.56	-13.3	-13.28	26.56	-13.28	-13.28	-13.3	26.6	26.6
	y	0	23	-23	0	23	-23	23	0	0
	z	0	0	0	-17	-17	-17	-15	-15	-15
viscous coefficients (N*s^2/m^3)	*x*	538	538	538	2.3E+07	2.3E+07	2.3E+07	75.4	75.4	75.4
	y	5381	5381	5381	2.1E+06	2.1E+06	2.1E+06	754	754	754
	z	5381	5381	5381	2.1E+06	2.1E+06	2.1E+06	754	754	754

Table 4-1 Parameters of the Morison model[1]

4.2.3 Hydrodynamic features

Applying the panel model in HydroD, all the required hydrodynamic coefficients can be obtained and can be used in the following analysis.

Hydrodynamic features like added mass coefficients, RAO and so on are used in both models. The mass information of Model A is given by HydroD results and can be used directly. The mass information of Model B needs to be cauculated, the mass information is modified and thus the hydrodynamic calculation is performed once again to obtain the correct linear stiffness coefficients. See Section 4.5 and 4.6.

Later analysis will also show that the hydrodynamic features of the TDHmill model agrees with the results from Roddier et al.

4.3 Mooring system

4.3.1 Original mooring line deployment

WindFloat is originally designed with a catenary mooring system. The following information in this subsection is extracted from Roddier's report.

[1] Chenyu Luan. Pre-project for Master's Thesis. Norwegian University of Science and Technology: 2010.

The WindFloat is positioned with a catenary mooring, which consists of 4 mooring lines, two on column 1, which carries the turbine, and one on each other column. Each line is made of 3 sections.

- 80m of 3-inch chain at the fairlead
- 718m of 5-inch chain polyester rope
- 80m of 3-inch chain to the anchor

A clump weight is attached to the upper chain section and the polyester rope to control the tension. The pretension on the mooring lines is 535kN.

The fairleads and anchor locations with respect to the platform region, and the mooring line weights, and the mooring line tension at rest are presented in the tables below.

	x	*y*	*z*
Fairlead1	29,578	-5,51	-16,8
Fairlead2	29,578	5,51	-16,8
Fairlead3	-16,379	28,37	-16,8
Fairlead4	-16,379	-28,37	-16,8
Anchor1	600	-600	-319,9
Anchor2	600	600	-319,9
Anchor3	-600	600	-319,9
Anchor4	-600	-600	-319,9

Table 4-2 Fairlead and anchor locations with respect to the platform origin

	Mass per unit (kg/m)	Weight in air (kN/m)	Weight in water (kN/m)	Extensional stiffness (kN)
Top chain	127	1,247	1,083	586450
Polyester	18	0,176	0,045	100000
Bottom chain	127	1,247	1,083	586450

Table 4-3 Line weight

	Fairlead1	Fairlead2	Fairlead3	Fairlead4
Mooring line tension at rest	539	539	531	531

Table 4-4 Line pretension

A clumped mass of 30000kg and 1.6m^3 is placed in the connection point between the top part and the middle part of each mooring line so that the pretension can be as large as the wanted. This is done by adding a 'buoy' in the line in DeepC and defining the mass and buoyancy to achieve the correct clump force acting downward.

It is shown in the later analysis that this clump weight will result in a much larger pretension in the mooring line, and thus the mass value is modified so that the pretension can be correct.

4.3.2 Modification of the mooring line

Based on this mooring line deployment, large error between the mooring line pretention and system natural period will occur. A close look at the clump weight of 30t with a volume of just 1.6m^3 shows that the clump weight has an unreasonably dense. And the mooring line is not langer enough than the distance between the anchor point and the fairlead to actually form a catenary mooring system. Thus a modification of the mooring line is necessary.

Marit Irene Kvittem from CeSOS has given a recommendation for a more reasonable mooring system, with modification for the fairleads and the anchor point and mooring line length, as well as clump weight. Here is the changed mooring system. It gives natural periods fairly close to the WindFloat system. Compared to earlier, the clump weight has a new volume, the top chain is longer and the spread angle is changed from 40 to 45 degrees. The details are shown below. The clamp weight is then changed to 30t, 3.8 m^3.

	x	*y*	*z*
Fairlead 1	31.56	0	-17
Fairlead 2	-15.78	-27.33	-17
Fairlead 3	-15.78	27.33	-17
Fairlead 4	31.56	0	-17
Anch 1	738.07	-706.51	-320
Anch 2	-721.76	-733.31	-320
Anch 3	-721.76	733.31	-320
Anch 4	738.07	706.51	-320

Table 4-5 New mooring line anchor point and fairlead

Part	Material	length
1	Chain	80
2	Polyester	769.8
3	Chain	232.58

Table 4-6 New mooring line

Later analysis will show that this mooring system gives good results in terms of mooring line pretension and line stiffness.

4.3.3 Mooring line profile

Apart from the basic information provided in the subsection above, several coefficients are needed for the load calculation.

The following figures are captured from the DeepC software window. The most important coefficients are shown in the above figures, including outer diameter, quadratic drag coefficients, added mass and hydrodynamic diameter.

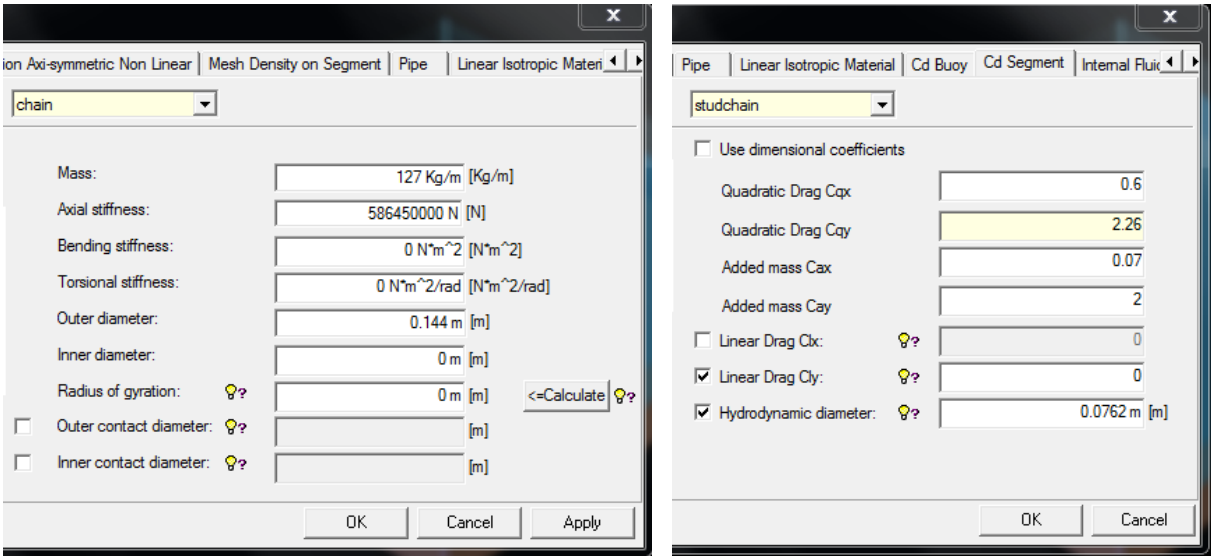

Figure 4-3 Coefficients for chain

The above coefficients should be entered precisely because they are components of the matrices in the equilibrium equation and can have large effect on the results.

For the chain part of the mooring line, coefficients need to be chosen according to the equivalent diameter. This information is not provided in DeepC User Manuel. Reference has been made to DNV-OS-E301 and Orcaflex documentation. (Orcaflex is a similar software as DeepC based on the same theory and formulations.) The coefficients shown in Figure 5 are chosen such that both recommendations are considered. For example, the quadratic coefficient is recommended to be 2.2-2.6 for chain in DNV standard and a value of 2.26 is proposed by Orcaflex documentation, and in this project it is taken as 2.26.

4.3.4 Specified force

To achieve the correct mooring line pretension, and to reduce the static deviation of the floater position when attached to mooring lines, a specified force acting upward should be added at each fairlead of the floater.

The specified force is chosen by running a few static analyses in the model, and a value of 402kN at each fairlead for Model A and 848kN for Model B show best performance with regard to line pretension and floater position, and thus are chosen as the specified upward force.

4.4 Difference in modeling for Model A and Model B

After the above modeling work done with DNV software package SESAM, input files for Simo and Riflex are generated and ready for feature use.

The files are then made into two copies for the two different models. Model A is used for the TDHmill model, and Model B is used for the Aerodyn Model. And from this moment DeepC is not used any more. The following modeling work is done by changing Simo and Riflex input files manually.

4.4.1 Model A description

In Model A the tower and turbine are not modeled with details. Only the mass information is taken. The floater-tower-turbine is considered as one rigid body in this system. And the wind is added as an external force by the TDHmill module.

Mass information is provided for the rigid body as a whole by Roddier et al. However, features of the wind turbine must be calculated before the simulation.

4.4.2 Model B description

In Model B the tower and turbine are modeled in detail. Information about NREL 5MW wind turbine is given and the tower and turbine input files are also provided by Jonkman et al.

The floater in this system is excluding tower and turbine, and thus the mass, center of gravity, radius of gyration and restoring terms for the floater should be changed.

4.5 Mass model

It is provided the mass model used for the TDHmill model in Roddier's work. That means we already have the mass information for floater, tower and turbine as a whole rigid body, i.e. the mass model for Model A. And so what is needed is to calculate the mass information of the floater without tower or turbine for Model B.

It should be noted that there is unknown ballast water in the floater, and thus calculation for the mass information by adding up weight of the floater steel structures is not possible.

The detailed information of tower and turbine of NREL 5 MW is also given by Jonkman. And so the only way to calculate the mass model for the floater only is by extracting the tower and turbine from the floater-tower-turbine mass model.

The position of the tower is on one of the column, which is also assumed to be 10 m above water. This gives the base point of the tower (26.56, 0, 10).

The undistributed properties of turbine blade, nacelle, hub and tower are shown below. These tables are taken from Jonkman's book.

Undistributed Blade Structural Properties

Length (w.r.t. Root Along Preconed Axis)	61.5 m
Mass Scaling Factor	4.536 %
Overall (Integrated) Mass	17,740 kg
Second Mass Moment of Inertia (w.r.t. Root)	11,776,047 kg•m^2
First Mass Moment of Inertia (w.r.t. Root)	363,231 kg•m
CM Location (w.r.t. Root along Preconed Axis)	20.475 m
Structural-Damping Ratio (All Modes)	0.477465 %

Undistributed Tower Properties	
Height above Ground	87.6 m
Overall (Integrated) Mass	347,460 kg
CM Location (w.r.t. Ground along Tower Centerline)	38.234 m
Structural-Damping Ratio (All Modes)	1 %

Nacelle and Hub Properties	
Elevation of Yaw Bearing above Ground	87.6 m
Vertical Distance along Yaw Axis from Yaw Bearing to Shaft	1.96256 m
Distance along Shaft from Hub Center to Yaw Axis	5.01910 m
Distance along Shaft from Hub Center to Main Bearing	1.912 m
Hub Mass	56,780 kg
Hub Inertia about Low-Speed Shaft	115,926 kg•m^2
Nacelle Mass	240,000 kg
Nacelle Inertia about Yaw Axis	2,607,890 kg•m^2
Nacelle CM Location Downwind of Yaw Axis	1.9 m
Nacelle CM Location above Yaw Bearing	1.75 m
Equivalent Nacelle-Yaw-Actuator Linear-Spring Constant	9,028,320,000 N•m/rad
Equivalent Nacelle-Yaw-Actuator Linear-Damping Constant	19,160,000 N•m/(rad/s)
Nominal Nacelle-Yaw Rate	0.3 °/s

Table 4-7 Information for blades, hub, nacelle and tower[1]

The mass for the floater is then directly obtained as

$$m = m_{with\ turbine} - m_{tower} - m_{blade} \times 3 - m_{hub} - m_{nacell}$$

$$= 4640 - 347.46 - 17.74 \times 3 - 56.78 - 240 = 3942.54$$

However, the center of gravity, especially the moments of inertia will be difficult to obtain from the information above. Thus a detailed calculation is applied based on the distributed properties.

The center of gravity of several components is calculated by

$$x = \sum_{1}^{n} \frac{m_i}{m_{total}} x_i$$

$$y = \sum_{1}^{n} \frac{m_i}{m_{total}} y_i$$

$$z = \sum_{1}^{n} \frac{m_i}{m_{total}} z_i$$

The moment of inertia of several components is calculated by

[1] Jonkman J, Butterfield S. Definition of a 5 MW Reference Wind Turbine for Offshore System Development. Technical Report NREL/TP-500-38060. 2009.

$$I_{xx} = \sum_{i}^{n} I_{xx,i} + m_i x_i^2$$

$$I_{yy} = \sum_{i}^{n} I_{yy,i} + m_i y_i^2$$

$$I_{zz} = \sum_{i}^{n} I_{zz,i} + m_i z_i^2$$

$$I_{xz} = \sum_{i}^{n} I_{xz,i} + m_i x_i z_i$$

Now, the tower and each blade are regarded to be composed of several elements. The moment of inertia for each element with regard to the element central position is neglected.

I_{xy} and I_{yz} are zero due to symmetry with respect to x-z plane. The blades can result in some asymmetry, but as the blade mass is small compared with the tower and the floater, and the blades are turning at working conditions and thus can be regarded as symmetric.

By applying the above equations for hub and nacelle and each element of the blades and the tower, the mass model of the floater can be obtained.

The calculation is applied with an excel sheet. Detailed calculation can be found in Appendix 1.

The mass information for Model B is listed below.

	weight/t	COGx/m	COGy/m	COGz/m	I_{xx}/tm^2	I_{yy}/ tm^2	I_{zz}/ tm^2	I_{xz}/ tm^2
Result	3995.143	-4.58624	4.44E-08	-6.78005	2.16E+06	1.69E+06	2.80E+06	-1.18E+06

Table 4-8 Mass model results for Model B

4.6 Linear stiffness coefficients

As in the previous section, the stiffness, or restoring terms for Model A is obtained previously by HydroD.

Stiffness coefficients are directly related to the metacentric height GM, which can be obtained from the following formula.

$$GM = BM + BK - GK$$

where

$$BM = \frac{I_{water\ plain}}{\nabla}$$

Due to center of gravity change, GK of the new floater body is different from the original floater-tower-turbine body. So modifications of the coefficients are also needed.

The coefficients are obtained by doing the HydroD calculation again for the same floater structure with different mass and center of gravity.

4.7 Tower and wind turbine

4.7.1 Model B

NREL 5MW provides the input file for Aerodyn. However, the tower and turbine must be modeled in detail as beams in Riflex. So are the two bodies associated with the turbine. This is done by modifying the inpmod.inp file of Riflex. Here is an illustration of modeling of the turbine.

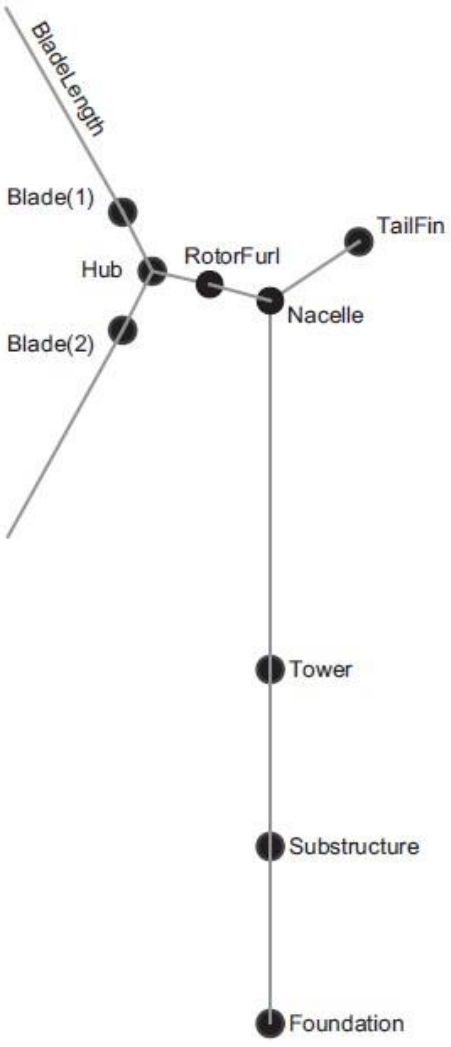

Figure 4-4 Modeling of tower and turbine[1]

There are three rigid bodies in this model, floater, nacelle and hub. The tower is modeled by a beam with 17 sections, the mass and diameter of the section is decreasing from the bottom to top. The detailed data is provided by Jonkman et al. The three blades are modeled with two beams, a

[1] Erin Bachynski. Simo-Riflex-Aerodyn User's Manual. January, 2012

small beam near the rotor, and a long beam with 17 sections on the outer side. The beam between the nacelle and the rotor is divided into two sections with a FLEX joint in the middle, so that the turbine will be able to turn during the simulation.

Information of the rigid bodies is modeled in the sys-file for SIMO.

4.7.2 Model A

For Model A, a simplified method for calculating wind force is applied. Therefore besides the basic information like radius of the turbine, many other coefficients are also required. The moment of inertia of the blades about the rotor axis, the rotation speed and the thrust coefficients are important in this project.

The moment of inertia is calculated by integration of the blade elements with the formula below.

$$I = \sum_{i}^{n} I_i + m_i r_i^2$$

where I_i is neglected, and i denotes the elements.

The result of moment of inertia is 35460 in this case.

The rotational speed is used for calculating the procession moment. As this value is relatively small when calculating the dynamic response, a common value of 12 rounds per minute is taken.

The thrust coefficient is defined below:

$$T_H(t) = K \cdot C_T(u_T) \cdot U_{REL}^2(t)$$

where C_T is the thrust coefficient and T_H is the thrust force, K is defined as

$$K = \frac{1}{2}\pi\rho R^2$$

where ρ is the air density and R is the radius of the turbine.

29 cases with the same significant wave height (0.01m) and different wind speed constant wind (from 3 to 40 m/s) are performed with the Aerodyn model, and thus 29 series of thrust force is obtained. For each wind speed, the mean value of this time series can be taken as the thrust force.

The simulation is run for 1000s. The mean value of thrust force results from 400s to 1000s are taken to be the thrust force value, because transient effect is significant at the beginning of the simulation, and the response is stable after 400s. More discussions about transient effect can be found in the result analysis chapters. The thrust force can be obtained by applying the two inversed formulas:

$$C_T(u_T) = \frac{T_H(t)}{K \cdot U_{REL}^2(t)}$$

The result for thrust coefficients is listed below.

Wind speed m/s	Thrust coefficient	Wind speed m/s	Thrust coefficient
3	1.0894E+00	20	1.1132E-01
4	1.0194E+00	21	9.7100E-02
5	9.3945E-01	22	8.5444E-02
6	8.8097E-01	23	7.5799E-02
9	7.9246E-01	24	6.7732E-02
10	7.8182E-01	25	6.0799E-02
11	7.5333E-01	26	5.4931E-02
12	5.8017E-01	27	4.9901E-02
13	4.1975E-01	28	4.5491E-02
14	3.2488E-01	29	4.1694E-02
15	2.5991E-01	30	3.8338E-02
16	2.1280E-01	33	3.0264E-02
17	1.7748E-01	34	2.8154E-02
18	1.5034E-01	40	1.8773E-02
19	1.2879E-01		

Table 4-9 Thrust coefficient

Matlab is used to process the data. See Appendix 2 for the data processing Matlab code.

4.8 Modeling of wind

The selection of wind cases will be shown in Chapter 6.

For each selected mean wind and turbulence intensity, the wind field must be generated for Aerodyn calculation usage. This is done by software Turbsim from NREL. See Appendix 10 for an example of the TurbSim input file.

The *TurbSim* stochastic inflow turbulence code was developed to provide a numerical simulation of a full-field flow that contains bursts of coherent turbulence (organized turbulent structures in the flow that have a well-defined spatial relationship) that reflect the proper spatiotemporal turbulent velocity field relationships seen in instabilities associated with nocturnal boundary layer flows. Such features are not simulated well by the International Electrotechnical Commission (IEC) Normal Turbulence Models (NTMs). Its purpose is to provide the wind turbine designer with the ability to drive design code (FAST, MSC.ADAMS®, or YawDyn) simulations of advanced turbine designs with simulated inflow turbulence environments that incorporate many of the important fluid dynamic features known to adversely affect turbine aeroelastic response and loading. The purpose of this document is to provide the user with a generalized overview of how the code has been developed and some of the theory behind that development.[1]

[1] Statoil. TDHMILL3D User Documentation

Kaimal is chosen as the turbulence model. Mean wind force and turbulence intensity are chosen in the next chapter and also are applied as input in Turbsim.

The output of Turbsim is a .wnd file, which can be used directly in Aerodyn calculations.

In order to make the wind in TDHmill exactly the same as it is in Aerodyn calculation, the wind input file for TDHmill must be the same as it is for Aerodyn. However, the two input files require different information and different formats.

First of all, by changing one control parameter in Turbsim input file, we can get an output file containing only the wind speed series at any point in the blade area in a certain direction. Manual copy and paste work is needed in order to get it into a more organized format. See figures below. After that, the time, wind speed in the rotor center and mean wind speed at the blade area is taken and written into a new wind file, as required by the TDHmill wind input file format.

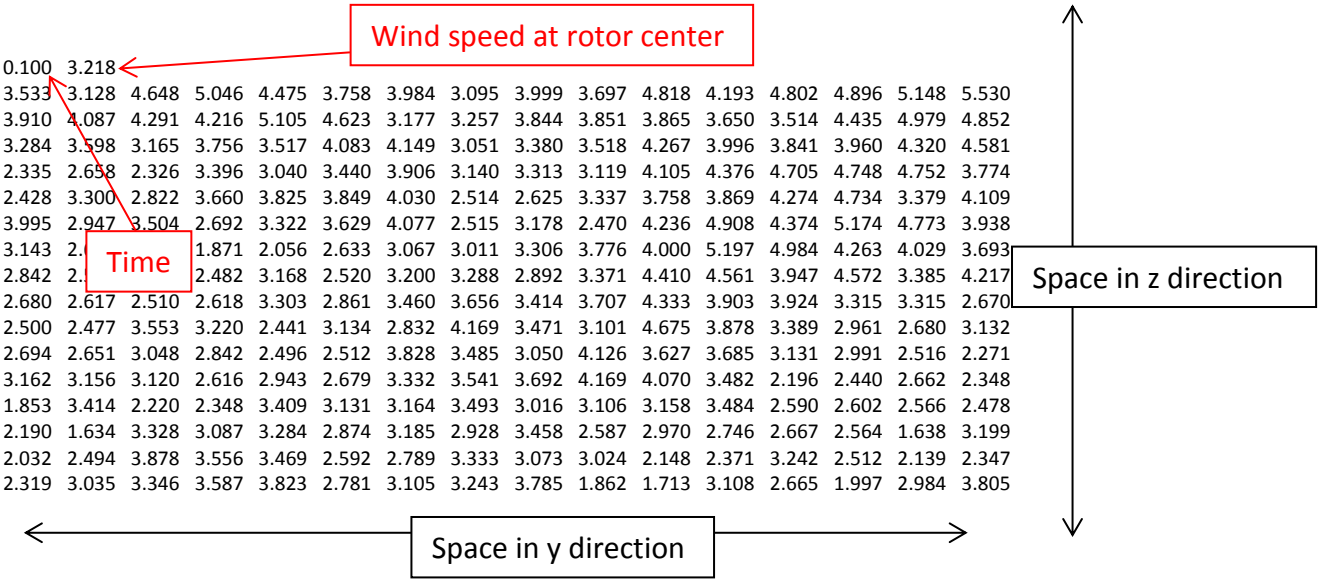

Figure 4-5 Sample of wind speed file from Turbsim

The wind speeds are transformed into an input file with the following format, by applying Matlab.

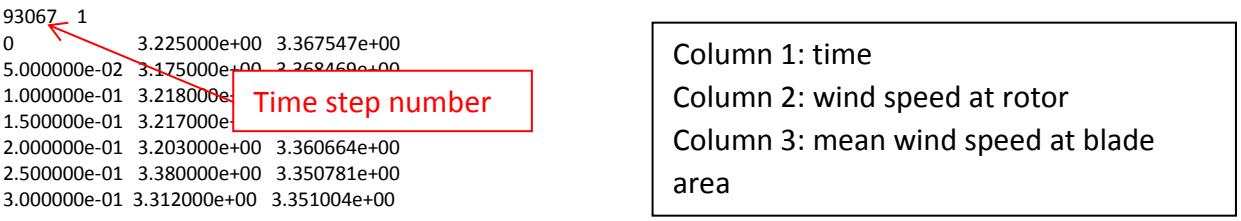

Figure 4-6 Sample of wind input file for TDHmill

The Matlab code for transformation of wind input file for TDHmill is shown in Appendix 3.

Chapter 5. Model Verification

5.1 Summary

In this chapter, the two models will be checked.

Two things are needed to be verified. One is whether the model is reasonable compared to the original design; the other is whether the two models are the similar compared with each other.

The items checked and compared, and the numerical tests performed are shown in the chart below.

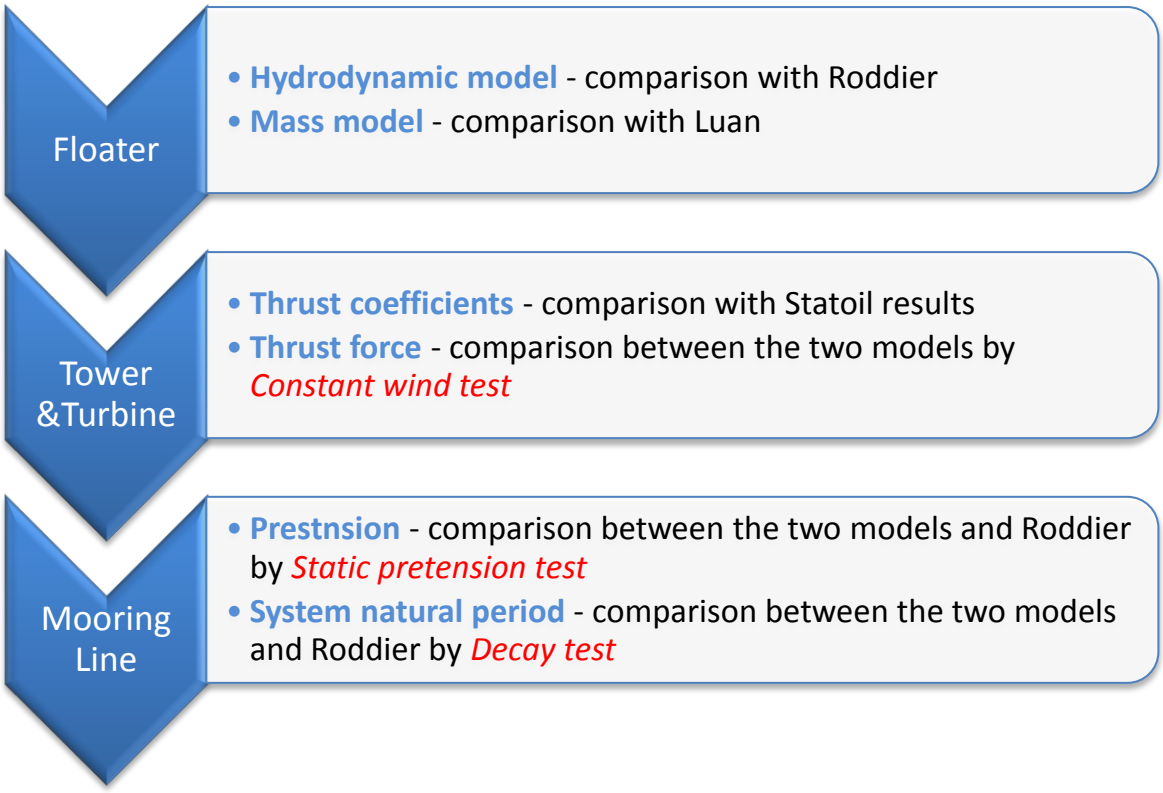

Figure 5-1 Model verification procedures

5.2 Hydrodynamic model

As mentioned in the previous chapter, Luan's model is directly used in this project, the linear response analysis in HydroD is performed again, and the periods are extended to 50s.

First, the peak periods for heave, roll and pitch at wave direction 0 are taken for comparison with the analysis done by Roddier et al, which is considered as reliable.

The results are shown below. The sign denotes whether the results are larger (+) or smaller (-).

d.o.f.	Roddier's model (reference)	Model used in this project	difference
Heave	19.9 s	20 s	-0.5%
Roll	43.3 s	46 s	-6.2%
Pitch	43.2 s	46 s	-6.5%

Table 5-1 Comparison of the natural period of floater

Another important part that needs to be compared is the added mass terms. Since only added mass at resonance are available from Roddier et al., only these values are to be compared here. But the comparison of added mass at resonance can also verify that the method applied is warranted. See the results below.

d.o.f.	Roddier's model (reference)	Model used in this project	difference
Heave	1.90E7	1.969E+07	-3.63%
Roll	7.76E9	8.050E+09	-3.99%
Pitch	7.76E9	8.046E+09	-3.69%

Table 5-2 Comparison of the added mass at resonance

The hydrostatic stiffness (restoring) are also compared as shown below.

d.o.f.	Roddier's model (reference)	Model used in this project	difference
Heave	2.37E6	2.353E+06	+0.71%
Roll	2.83E8	2.528E+08	+10.67%
Pitch	2.83E8	2.528E+08	+10.67%

Table 5-3 Comparison of the hydrostatic stiffness

As shown in the tables above, the overall performance of the panel model used in this project has shown nice agreement with the analysis done by Roddier et al[1]. Only restoring stiffness has shown a difference of a bit more than 10%. However, surge, sway and yaw motion are of more importance when doing mooring analysis, and thus 10% can also be regarded as a satisfactory value. Moreover, the aim of this project is to compare the aerodynamic computation codes Aerodyn and TDHmill, and thus our model doesn't have to be exactly the same with the reference model, it is good enough as long as the floater model is reasonable.

The natural period are obtained from the following equation.

$$T = 2\pi\sqrt{\frac{A+m}{K}}$$

When the stiffness is large, the natural period is small. If we neglect the added mass difference (the difference is small and the floater mass is reducing this small difference), the difference in restoring stiffness (+10%) and natural period (-6%) shows a good agreement with this formula. This again can prove that the hydrodynamic calculation gives reasonable result.

5.3 Mass model and stiffness coefficients

Mass model for the floater in Model A is given, while the following parameters are modified for the floater in Model B: mass, center of gravity, radius of gyration and linear stiffness.

[1] Roddier D, Peiffer A. A Generic 5 MW Windfloat for Numerical Tool Validation & Comparison Against a Generic Spar. OMAE2011-50278, Rotterdam: 2011

A similar work has been done by Luan, and thus comparison between his result and the result in this project is provided below.

	Result	Luan's result	difference
weight/t	3995.143	4000	-0.1%
COGx/m	-4.58624	-4.53	1.2%
COGy/m	4.44E-08	0	-
COGz/m	-6.78005	-6.71	1.0%
I_{xx}/tm^2	2.16E+06	2150000	0.5%
I_{yy}/tm^2	1.69E+06	1660000	1.8%
I_{zz}/tm^2	2.80E+06	2790000	0.4%
I_{xz}/tm^2	-1.18E+06	-1160000	1.7%

Table 5-4 Comparison of mass calculation results

All results are within 2% of difference, which demonstrates that the mass calculation is good.

5.4 Thrust force coefficients

Tower and turbine information input to Model A is obtained from Model B, one for each wind speed. The available turbine input file for TDHmill is based on another turbine design called Hywind, and is not exactly the same as NREL 5MW that is used in this project, and thus the comparison between these two can only provide reference.

It is seen that the moment of inertia is similar to the previous calculation.

The thrust coefficients are then compared as shown below. As the wind speed values for calculation are not exactly the same between the two calculations and there are many values to be compared, a figure is drawn to better show the difference.

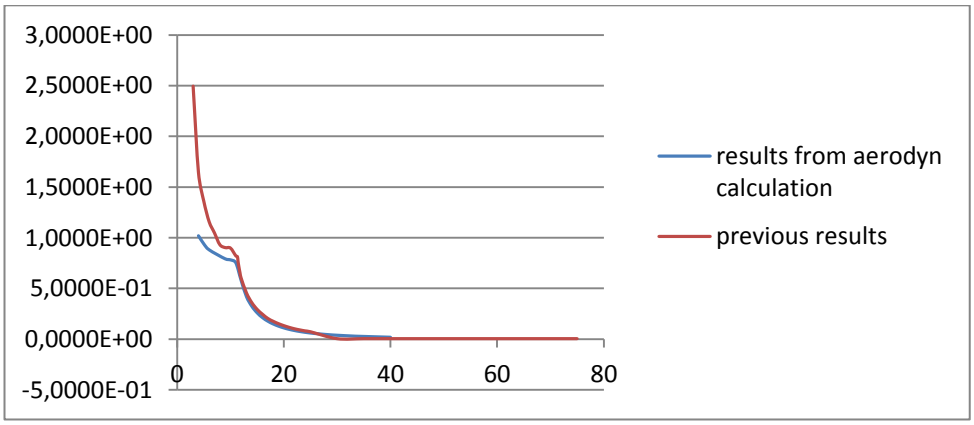

Figure 5-2 Comparison of thrust coefficients

There is relatively large difference between these calculation results, (up to 15% in the working conditions and very large at small or large wind speed). However, since the two turbines are not exactly the same, we may conclude that the obtained thrust coefficients are within reasonable range. The thrust coefficients can then be verified by constant wind test.

5.5 Constant wind test

Constant wind tests are performed for 5 sample wind speeds to confirm the correct computation of the thrust coefficients. The simulation is run with no wave (simulated by significant wave height 0.01m) and constant wind speed. The data in Model B is processed similar as when the thrust coefficients are obtained. In Model A the data is processed with first printing the external force with Simo Outmod, and then taking the mean value of results from time 400s to 1000s with Matlab. See Appendix 4 for the Matlab codes.

The constant wind test results are presented below.

Wind speed/ m/s	Thrust in Model A/ kN	Thrust in Model B/ kN	Difference
6	229.8533	231.0103	-0.50%
11.2	658.4517	652.8718	0.85%
14	478.4097	463.8263	3.14%
20	326.6711	324.3407	0.72%
40	219.6068	218.7731	0.38%

Table 5-5 Constant wind test results

Very good agreement is shown between the two models. There is 3% larger thrust force in Model A than in Model B at wind speed 14m/s. This may result from the truncation time (400s-1000s) and increasing the simulation time may give better results. But 3% is a small value (under 5%), and the two models are considered equivalent in terms of thrust force.

5.6 Mooring line static features

5.6.1 Pretension

The pretension of the system is obtained by running a static analysis with no wave (simulated by significant wave height 0.01m), and the result is shown as below.

Line Number	Pretension in the original model / kN	Pretension in Model A / kN	Pretension in Model B / kN	difference between model A and B
1	539	513.37	517.4	0.78%
2	539	513.37	517.4	0.78%
3	531	513.31	517.2	0.75%
4	531	513.31	517.2	0.75%

Table 5-6 Comparison of line pretensions

It can be seen that the mooring line pretension between the two models are similar.

5.6.2 Static stiffness

The static stiffness of the mooring system is obtained by running several static analyses with different specified force acting on the corresponding direction.

Here is presented the reaction force as a function of the floater displacement in surge direction for Model A.

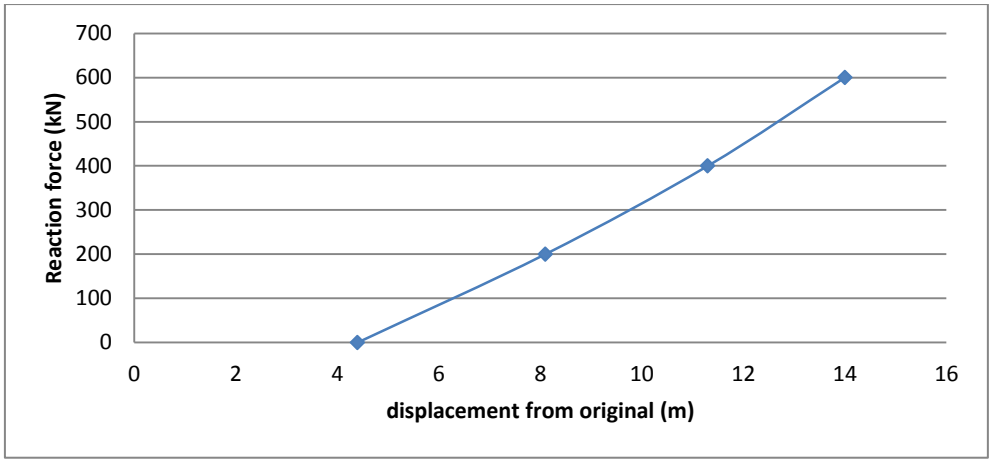

Figure 5-3 Static stiffness in surge direction

The static stiffness in this direction is approximately 60kN/m. A relatively large difference exists between this value and the Roddier's 'equivalent mooring stiffness'. However, the 'equivalent mooring stiffness' in Roddier's work is a specially defined parameter which takes into account damping and other dynamic effects, and thus it is expected to be different from what we have here. So comparison between these results is meaningless. What is shown is that the static stiffness we have is in the same order as the 'equivalent stiffness', and thus it is qualitatively reasonable.

Reference results are not available in other directions either, so stiffness in other directions will not be shown in this report.

5.7 Decay test

Decay test for both models are performed. The decay test is used to verify that the two models are the same in terms of mass distribution and hydrodynamic performance and the mooring system is reasonable.

Decay tests are performed in surge, sway and yaw directions.

In a decay test, a system is set free from a predefined displacement. The system then will oscillate until it is damped to very small amplitude. The time series of the interesting parameters are recorded and can be used for analysis. Usually, the aim of decay test is to find the damping ratio and natural frequency of an oscillating system. The damping ratio can be obtained from the following formula.

$$\zeta = \frac{1}{\sqrt{1 + \left(\frac{2\pi}{\delta}\right)^2}}$$

where δ is the logarithmic decrement defined as

$$\delta = \frac{1}{n} \ln\left(\frac{x_0}{x_n}\right)$$

The natural frequency can then be obtained from the damped frequency and the damping ratio by

$$\omega_d = \frac{2\pi}{T}$$

$$\omega_n = \frac{\omega_d}{\sqrt{1-\zeta^2}}$$

5.7.1 Surge decay test

The surge decay test is performed by giving a specified force in x-direction for the first 200 seconds and then removing it. The test is done for 1000 seconds in total.

The x-direction motion time series for the two models are given below.

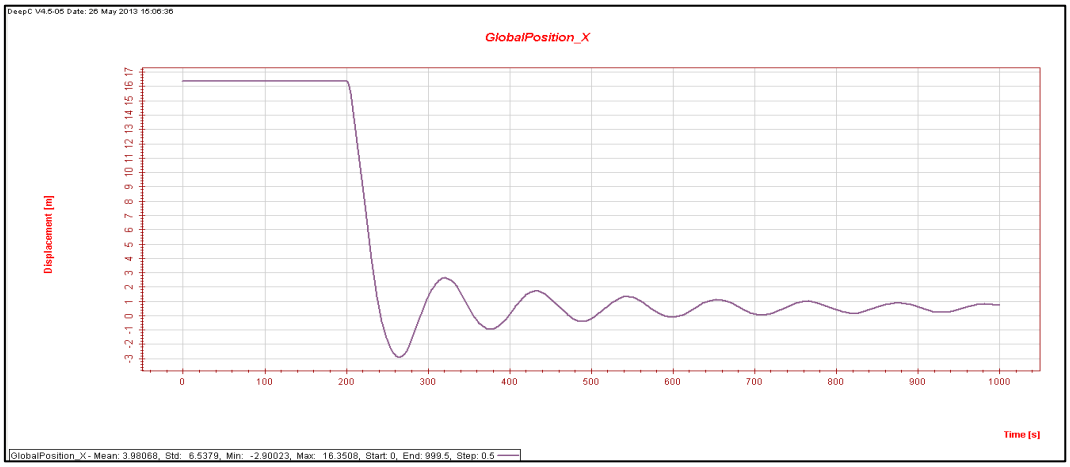

Figure 5-4 Surge decay test result in Model A

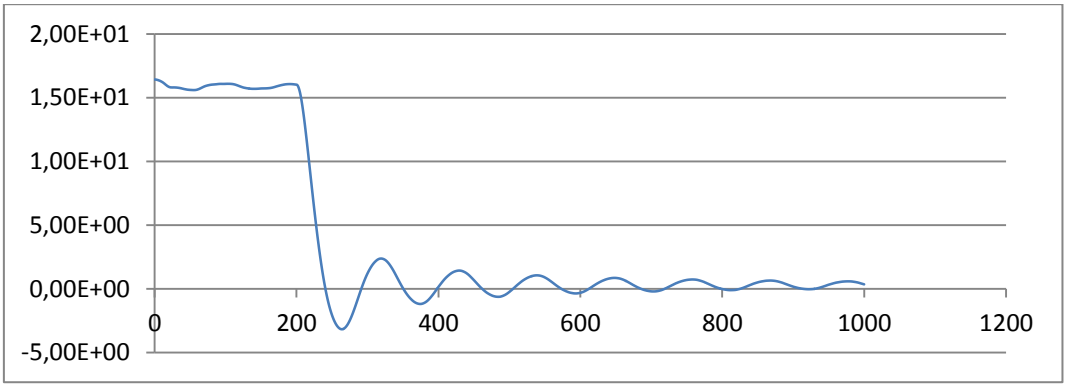

Figure 5-5 Surge decay result in Model B

The comparison between the two results and the result given by Roddier is below.

Natural period in Model A/ s	Natural period in Model B/ s	Roddier's result (reference model)/ s	Difference between Model A and Model B
106.78	106.31	108.6	0.4%

Table 5-7 Results of surge natural period

Again it is worth noting that the model used in this analysis is not exactly the same as it is used in Roddier's research. The result of Roddier is only used for a reference.

The natural periods obtained by the two models are almost the same, and thus the two models can be considered equivalent with regard to the hydrodynamic performance and mooring system. The result for the beginning period, however, is a bit unstable in Model B. This is because static calculation cannot give a very accurate solution within a reasonable calculation time. However, this error does not affect the model verification.

5.7.2 Sway decay test

The sway decay test is performed by giving a specified force in y-direction for the first 200 seconds and then removing it. The test is done for 1000 seconds in total.

The y-direction motion time series for the two models are given below.

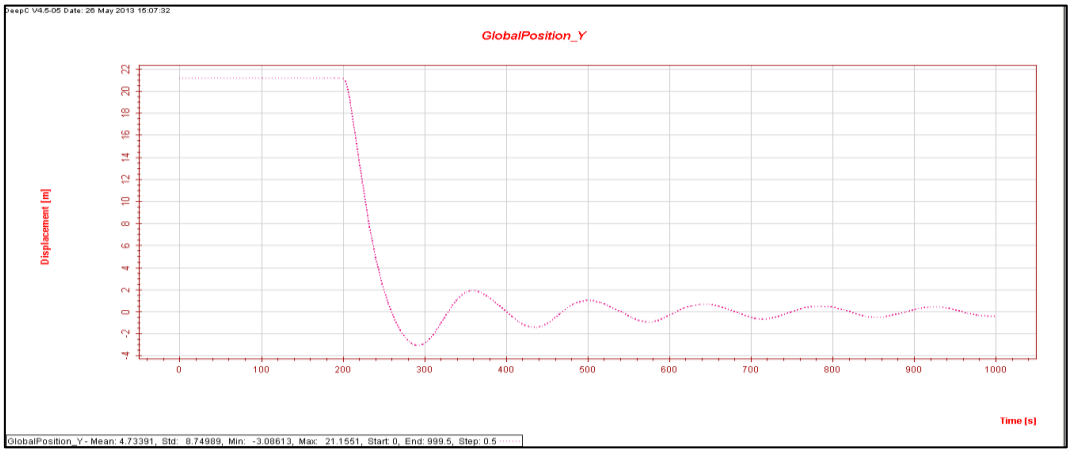

Figure 5-6 Sway decay test in model A

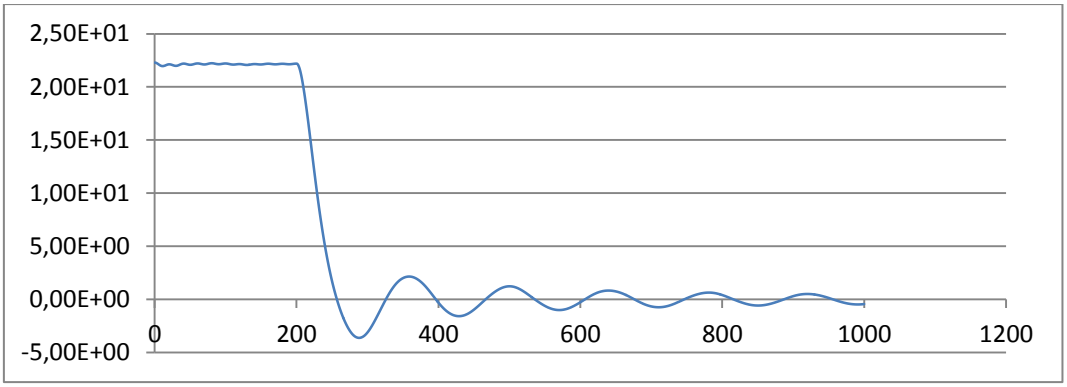

Figure 5-7 Sway decay test in model B

The comparison between the two results and the result of Roddier is shown below.

Natural period in Model A/ s	Natural period in Model B/ s	Roddier's result (reference model)/ s	Difference between Model A and Model B
143.83	144.17	135.7	0.22%

Table 5-8 Results of sway natural periods

The periods in the two models show very good agreement. The static value in Model 2 is a bit higher than in Model 1 (about 22 vs. 21.6). Again, this is very likely to be caused by the static calculation. However, the difference is very small and is not very relevant in this test.

We can conclude that the models are equivalent to each other.

5.7.3 Yaw decay test

The yaw decay test is performed by giving a force pair around the COG for the first 200s and then removing the force pair. The test is done for 1000 seconds in total.

The y-direction motion time series for the two models are given below.

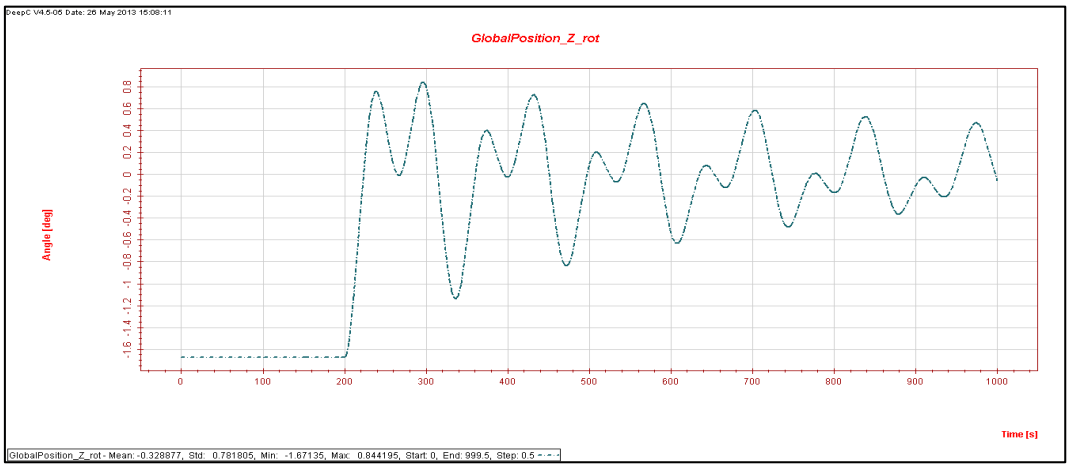

Figure 5-8 Sway decay test in Model A

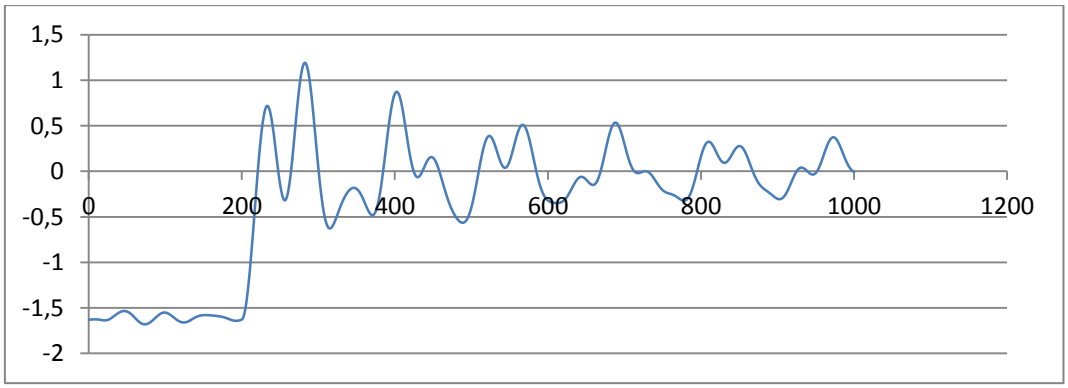

Figure 5-9 Sway decay test in Model B, original

Seen from the figures above, we can see there is serious coupling.

There is also large difference between the two models. This is because of the accuracy in static model analysis. More coupling problems exist in Model 2. In order to see the natural frequency for yaw, frequency transformation is needed.

The power spectrum of the wave height is obtained from FFT (Fast Fourier Transformation) in Matlab. The result is presented below for the two Models. See Appendix 5 for the Matlab code.

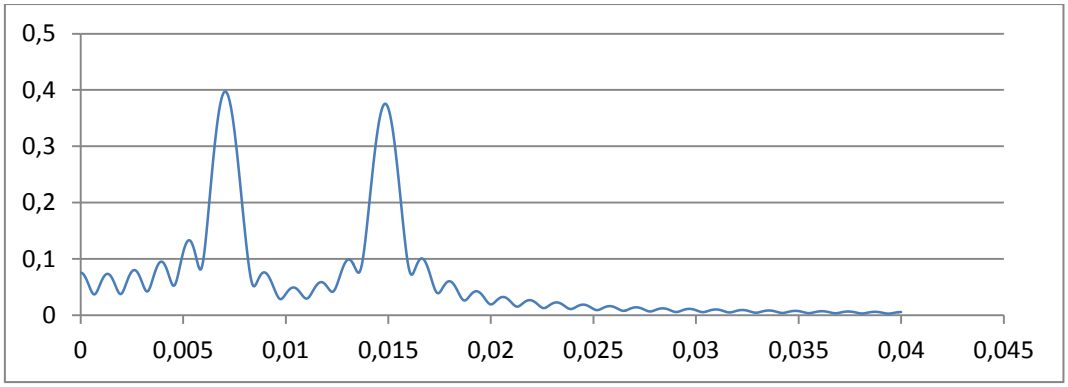

Figure 5-10 Spectrum of yaw decay for Model A

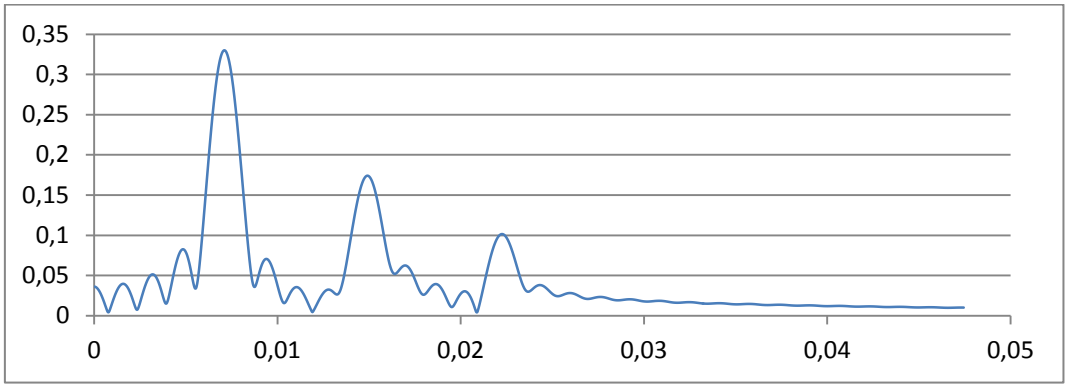

Figure 5-11 Spectrum of yaw decay for Model B

The results of these frequencies are listed below

	Natural frequency / Hz	Natural period / s	Relevant d.o.f.
maximum 1	0.00706	141.6431	sway
maximum 2	0.01484	67.38544	yaw

Table 5-9 Natural frequencies in Model A

Natural frequency for maximum 1 in Model A is 141.6431s, which is near the natural frequency of sway (143.83s), and thus the coupling with sway is serious. The second maximum then corresponds to yaw natural frequency.

	Natural frequency / Hz	Natural period / s	Relevant d.o.f.
maximum 1	0.0071	140.8451	sway
maximum 2	0.0149	67.11409	yaw
maximum 3	0.02225	44.94382	pitch

Table 5-10 Natural frequencies in Model B

There is more complex coupling in Model B, which involves yaw, sway (natural period around 140s), and pitch (natural period without mooring line, 46s).

In order to better see the coupling effect, the following are presented sway and pitch motion of both models in yaw decay test.

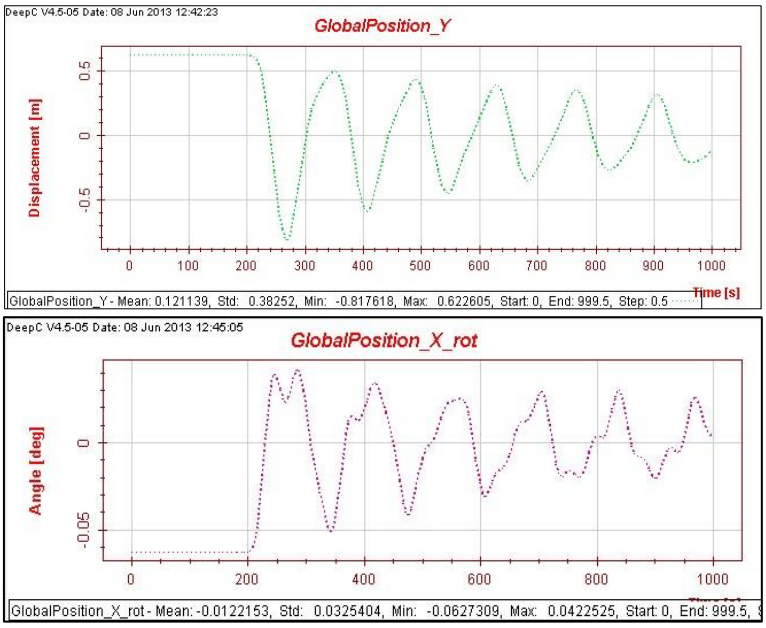

Figure 5-12 Sway and pitch motion of Model A in yaw decay test

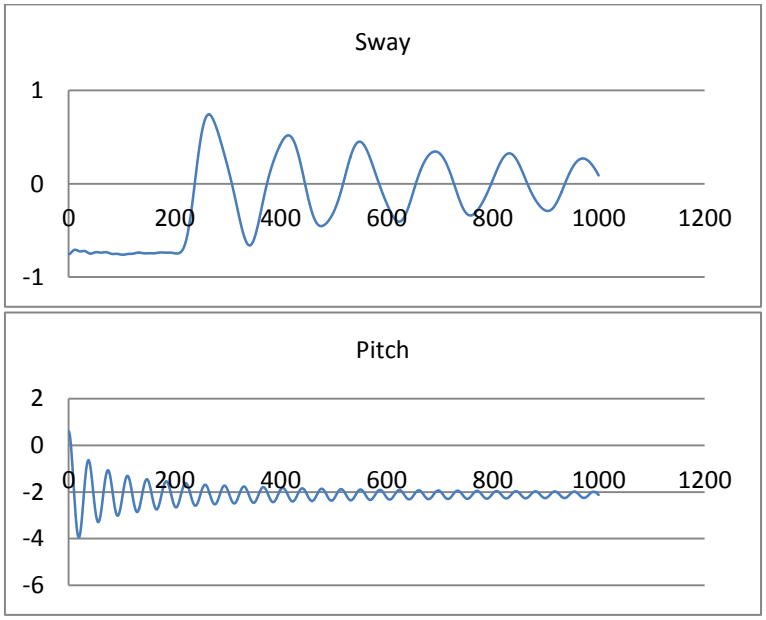

Figure 5-13 Sway and pitch motion of Model B in yaw decay test

We first observe large sway motion in both models. This means sway coupling is serious in both models. Pitch motion in Model A is very small (smaller than 0.05 deg), and thus does not have a significant effect on the results. However, the pitch motion in Model B is relatively large. These observations agree with the spectral analysis for yaw motion results.

It can also be seen that pitch motion starts at time 0s rather than 200s. This means the pitch motion is not induced by the specified force during the first 200 seconds. It is very probably caused by the errors introduced in static calculation. When more load steps and iteration steps are applied in the static calculation, the coupling problem in pitch is reduced, but cannot be avoided within a reasonable computation time.

Coupling with the other degrees of freedoms also exist, but with much smaller effect.

The results for yaw natural periods are then presented below.

Natural period in Model A /s	Natural period in Model B /s	Roddier's result (reference model) /s	Difference between Model A and Model B
67.38544	67.11409	71.3	0.4%

Table 5-11 Results of yaw natural periods

Again, the models are equivalent with regard to yaw natural period.

Chapter 6. Load Case Selection

6.1 Summary

In this chapter, the load cases are selected according to the following process: wind – significant wave height – peak period.

First of all, 14 wind speeds are selected according to the wind turbine specification and the extreme environmental condition. Then, 5%, 50% and 95% exceedance significant wave heights are selected for each wind. Finally the most probable peak period is selected for each significant wave height. The total load case number is 42.

The environment information including all distributions is provided by Li Lin's work on statistics.

6.2 Reference wind speed

The marginal mean wind speed is given in Li's work. However, in order to study the different performances and feasibility of the two calculation models, only the wind speeds where the turbine can operate and the extreme wind speed are of interest.

For the extreme condition, the mean wind speed is given at 10 m above sea level, so the following formula needs to be used to get the wind speed at rotor.

$$U(z) = U_{10}\left(\frac{z}{10}\right)^{a}$$

Where z represents the height, U_{10} is the mean wind speed at 10 m above sea level. In this project, the Norwegian Sea extreme wind is 33.3m/s, exponent a equal to 0.1 can be used.[1]

$$U_{extreme} = 33.3 \cdot \left(\frac{89}{10}\right)^{0.1} = 41.8$$

The wind speeds at rotor are then selected as follow:

Number	Wind Speed (m/s)	Note	Number	Wind Speed (m/s)	Note
1	3	Cut-in speed	8	13	
2	6		9	14	
3	8		10	16	
4	9		11	18	
5	10		12	20	
6	11.2	Rated speed	13	25	Cut-out speed
7	12		14	41.8	Extreme wind speed

Table 6-1 Wind speed selection

[1] Li L, Gao Z, Moan T. Environmental Data at Five Selected Sites for Concept Comparison. CeSOS: 2012

The wind speeds listed above are wind speed at rotor height, which can be used in thrust force calculation. In order to decide which wave profile to use, the corresponding wind speed at 10m above sea level must also be obtained. Applying $U(z) = U_{10}\left(\frac{z}{10}\right)^{a}$, the wind speed for 10m height can be calculated with

$$U_{10} = U(z)\left(\frac{z}{10}\right)^{-a}$$

The result is then obtained and listed below.

Number	Wind Speed rotor (m/s)	Wind Speed 10m (m/s)	Number	Wind Speed (m/s)	Wind Speed 10m (m/s)
1	3	2.410917	8	13	10.44731
2	6	4.821834	9	14	11.25095
3	8	6.429112	10	16	12.85822
4	9	7.232751	11	18	14.4655
5	10	8.03639	12	20	16.07278
6	11.2	9.000757	13	25	20.09097
7	12	9.643668	14	41.8	33.3

Table 6-2 Wind speed at rotor height and 10m height

6.3 Turbulence intensity factor

The information below is extracted from Li Lin's work.[1]

Wind speed in longitudinal direction (i.e. the main wind direction) is represented by the mean wind speed *U* plus the dynamic part $u_1(t)$, which is a Gaussian random process with mean value of zero and standard deviation of σ_1. For wind turbines, the turbulence intensity factor *I* is normally used, which is defined as the standard deviation divided by the mean wind speed at hub height,

$$I = \frac{\sigma_1}{U_{hub}}$$

where U_{hub} is the mean wind speed at hub height, which is already obtained in the previous section.

The turbulence intensity factor is different for different mean wind speeds. Even for a given mean wind speed, the turbulence intensity factor may vary, but follows a distribution. For wind turbines in operational conditions (i.e. when the mean wind speed is between the cut-in and cut-out speeds), IEC-61400-1[1] suggests the following formula to estimate the characteristic value of the turbulence intensity factor as function of mean wind speed.

$$I = I_{ref}\left(0.75 + \frac{5.6}{U_{hub}}\right)$$

[1] Li L, Gao Z, Moan T. Environmental Data at Five Selected Sites for Concept Comparison. CeSOS: 2012, P.12-13.

Where I_{ref}=0.12 is the expected value of turbulence intensity factor at reference wind speed of 15m/s for offshore site.

In extreme conditions, wind turbines are parked. For such conditions, IEC-61400-1[1] suggests a fixed value of 0.11 for the turbulence intensity factor.

Based on the information above, the turbulence intensity factors are added into the wind profile table.

Number	Wind Speed rotor (m/s)	Turbulence intensity factor	Wind Speed 10m (m/s)	Number	Wind Speed (m/s)	Turbulence intensity factor	Wind Speed 10m (m/s)
1	3	0.314	2.410917	8	13	10.44731	10.44731
2	6	0.202	4.821834	9	14	11.25095	11.25095
3	8	0.174	6.429112	10	16	12.85822	12.85822
4	9	0.164667	7.232751	11	18	14.4655	14.4655
5	10	0.1572	8.03639	12	20	16.07278	16.07278
6	11.2	0.15	9.000757	13	25	20.09097	20.09097
7	12	0.146	9.643668	14	41.8	33.59211	33.3

Table 6-3 Wind selections

6.4 Selection of sea state

According to Li[1], the conditional PDF (probability density function) of H_s is given as

$$f_{H_s|U_w}(h|u) = \frac{\alpha_{HC}}{\beta_{HC}}\left(\frac{h}{\beta_{HC}}\right)^{\alpha_{HC}-1} \exp\left[-\left(\frac{h}{\beta_{HC}}\right)^{\alpha_{HC}}\right]$$

Where α_{HC} and β_{HC} are the shape and scale parameters, which are given as function of u,

$$\alpha_{HC} = a_1 + a_2 u^{a_3}$$

$$\beta_{HC} = b_1 + b_2 u^{b_3}$$

Where the parameters have been obtained by Li's analysis to the raw data outside the Norwegian Sea (site 14), as are shown below.

a1	2.136	b1	1.816
a2	0.013	b2	0.024
a3	1.709	b3	1.787

Table 6-4 Values for parameters in the conditional distribution of Hs

The corresponding cumulative distribution function (CDF) is then

[1] Li L, Gao Z, Moan T. Environmental Data at Five Selected Sites for Concept Comparison. CeSOS: 2012, P.7

$$F_{H_s|U_w}(h|u) = \int_0^h f_{H_s|U_w}(\bar{h}|u)\mathrm{d}\bar{h} = \int_0^h \frac{\alpha_{HC}}{\beta_{HC}}\left(\frac{\bar{h}}{\beta_{HC}}\right)^{\alpha_{HC}-1} \exp\left[-\left(\frac{\bar{h}}{\beta_{HC}}\right)^{\alpha_{HC}}\right]\mathrm{d}\bar{h}$$

$$\Rightarrow \qquad F_{H_s|U_w}(h|u) = 1 - \exp\left[-\left(\frac{h}{\beta_{HC}}\right)^{\alpha_{HC}}\right]$$

In this project, we take the medium and 90% boundaries for comparison study, in order to cover more cases. That means, for each wind speed, 3 significant wave heights are taken when

$$1 - \exp\left[-\left(\frac{h}{\beta_{HC}}\right)^{\alpha_{HC}}\right] = 5\%$$

$$1 - \exp\left[-\left(\frac{h}{\beta_{HC}}\right)^{\alpha_{HC}}\right] = 50\%$$

$$1 - \exp\left[-\left(\frac{h}{\beta_{HC}}\right)^{\alpha_{HC}}\right] = 95\%$$

The h then can be obtained by

$$h = \beta_{HC}\sqrt[\alpha_{HC}]{-\ln(1-F)}$$

The significant wave heights are obtained by using an Excel sheet. After that, the most probable peak period for each significant wave height can be obtained from the conditional distribution given by

$$f_{T_p|H_s}(t|h) = \frac{1}{\sqrt{2\pi}\sigma_{LTC}t}\exp\left(-\frac{1}{2}\left(\frac{\ln(t)\mu_{LTC}}{\sigma_{LTC}}\right)^2\right)$$

where μ_{LTC} and σ_{LTC} are the parameters in the conditional lognormal distribution, i.e. the mean value and standard deviation of ln(T_p) conditional on H_s. They are given as functions of h.

$$\mu_{LTC} = c_1 + c_2 h^{c_3}$$

$$\sigma_{LTC}{}^2 = d_1 + d_2\exp(d_3 h)$$

where the parameters are

c1	1.886	d1	0.001
c2	0.365	d2	0.105
c3	0.312	d3	-0.264

Table 6-5 Values for parameters in the conditional distribution of Tp

It is not of much interest in this project to calculate many peak periods, and so for each significant wave height, we take only the peak period with largest probability, i.e. when $f_{T_p|H_s}(t|h)$ is at maximum. The maximum of $f_{T_p|H_s}(t|h)$ can then be obtained by numerical method. First, give a

reasonable series of t (in this project it is taken t=1:0.01:50), then find the maximum corresponding f. The final list for study cases are listed below.

case number	wind speed at rotor	wind speed at 10m	I	H_s /m (5%, 50%, 95% values)	T_p /s
1	3	2.410917	0.314	0.499025	7.789
2				1.634543	9.191
3				3.184681	10.294
4	6	4.821834	0.202	0.618183	8.004
5				1.892353	9.409
6				3.549359	10.504
7	8	6.429112	0.174	0.73833	8.193
8				2.138156	9.6
9				3.887242	10.688
10	9	7.232751	0.164667	0.811614	8.298
11				2.282206	9.706
12				4.081035	10.79
13	10	8.03639	0.1572	0.894238	8.409
14				2.440052	9.817
15				4.290158	10.897
16	11.2	9.000757	0.15	1.00629	8.55
17				2.647423	9.958
18				4.560256	11.03
19	12	9.643668	0.146	1.089136	8.647
20				2.796423	10.055
21				4.751398	11.123
22	13	10.44731	0.141692	1.202208	8.772
23				2.994639	10.179
24				5.002271	11.24
25	14	11.25095	0.138	1.326197	8.901
26				3.206024	10.307
27				5.265964	11.361
28	16	12.85822	0.132	1.608285	9.168
29				3.667791	10.57
30				5.830198	11.609
31	18	14.4655	0.127333	1.937822	9.445
32				4.180753	10.841
33				6.441465	11.863
34	20	16.07278	0.1236	2.316729	9.731
35				4.74399	11.119
36				7.097876	12.124
37	25	20.09097	0.11688	3.488192	10.47
38				6.36632	11.833
39				8.928444	12.791
40	41.8	33.59211	0.11	9.797777	13.085
41				13.92168	14.335
42				16.96126	15.152

Table 6-6 Calculation cases for comparison

Selection of peak periods is processed by Matlab. See Appendix 6.

Another parameter needed for the input of these cases is the peak enhancement factor Υ, which can be obtained by

$$\gamma = \begin{cases} 5 & for\ \frac{T_p}{H_s} \leq 3.6 \\ \exp\left(5.75 - 1.15\frac{T_p}{H_s}\right) & for\ 3.6 < \frac{T_p}{H_s} \leq 5 \\ 1 & for\ \frac{T_p}{H_s} > 5 \end{cases}$$

Wind input files are handed with software, see Chapter 4 for wind modeling. And wave input information is given in the input files for Simo and Riflex.

Chapter 7. Comparison of Sample Time Series

7.1 Summary

In this chapter, sample cases are selected to present the different time series of both Models. Responses in thrust force, floater surge motion and mooring line tension are presented with discussions on time series features. The time series of the first sample is discussed in detail, while the other two are briefly commented.

The main purpose of this chapter is to have a direct look at the time series of some sample cases. A general trend can be obtained from these time series.

More analytical and detailed analysis can be found in the next chapter, comparison of statistical results.

7.2 Sample 1 – medium wind, small wave

First, we take a sample case of a medium wind speed with relatively small wave for comparison. Case 10 is selected for this purpose. The environmental information of Case 10 is listed below.

H_s (m)	T_p (s)	U_{mean} (m/s)	I
0.811614	8.298	9	0.164677

Table 7-1 Sample case information, Case 10

7.2.1 Thrust force

The thrust force series for Case 10 in Model A and Model B is shown below.

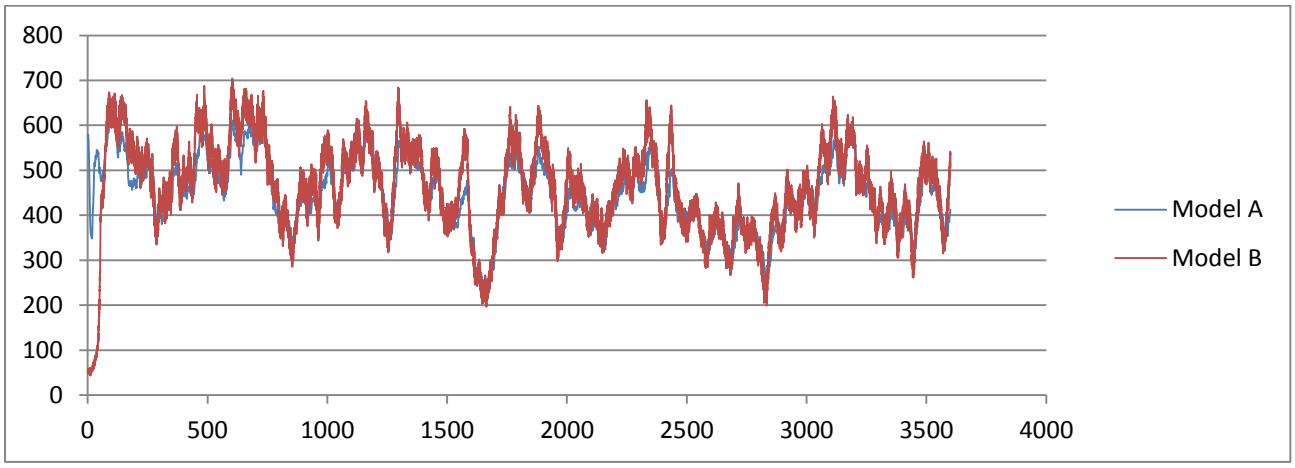

Figure 7-1 Thrust force in Case 10 of Model A and Model B

Seen from the above figure, we notice that generally there is no big difference between these two thrust force time series.

In the beginning period, Model A starts from a certain thrust force while Model B starts from almost zero thrust force. This is because of the calculation method between these two models. Thus when doing analysis, the transient effect must be considered for Model B.

A careful look at the time series also shows that Model A gives a thrust force slightly smaller than Model B. But this difference is not significant. Further statistical analysis will show more information.

7.2.2 Surge motion

The surge motion series for the sample case in Model A and Model B are shown below.

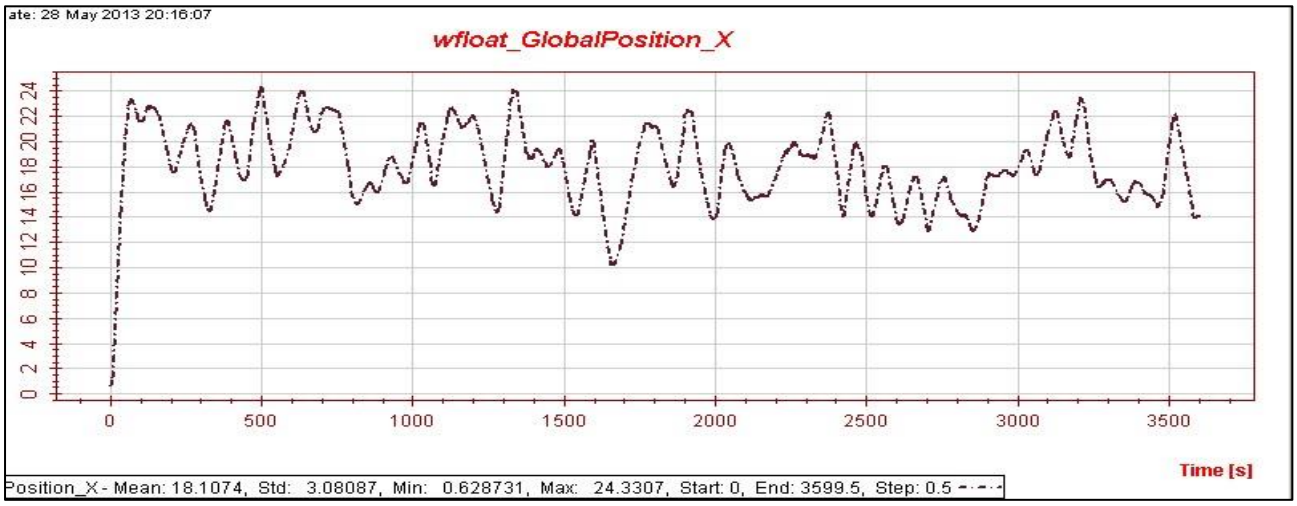

Figure 7-2 Surge in Case 10 for Model A

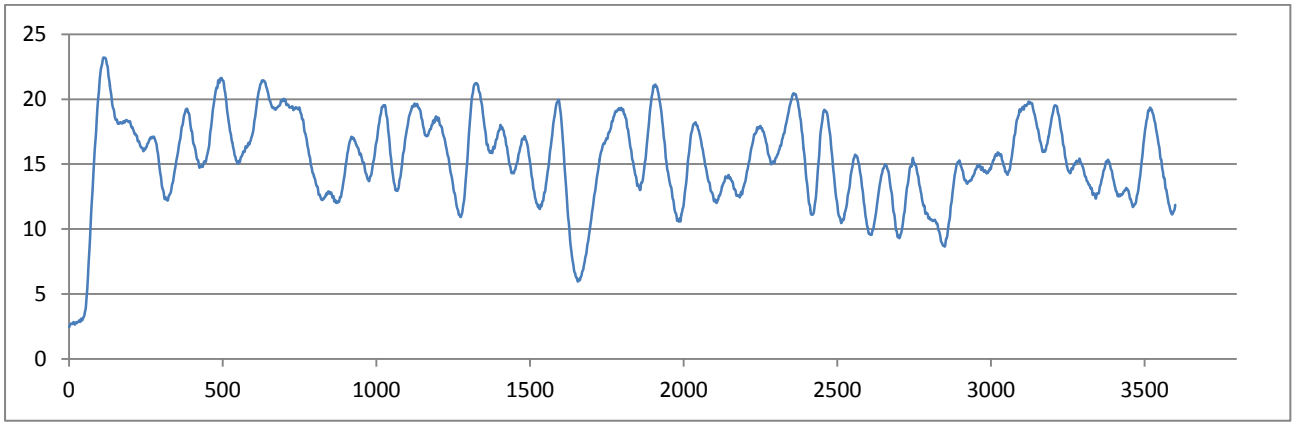

Figure 7-3 Surge in Case 10 for Model B

It is seen from the two figures that the general trend of the response is similar, but in some local points there is some difference, for example, at the negative maxima around 1600s, it reads around 10 m in Model A and just 6 m in Model B.

The two models are based on different calculation methods, the differences in these two time series are thus reasonable.

It is also seen that Model A tend to give a slightly larger response than Model B, and the variation in Model B is larger. Statistical analysis will show this difference with regard to mean value and standard deviation.

The response time series curve for surge motion is smooth compared with that for thrust force. This is because the mass of the system is large, and the high-frequency variation in thrust force will not induce large response.

7.2.3 Mooring line tension

Mooring line tension for Line 3 (mooring line in up wind direction) is presented below.

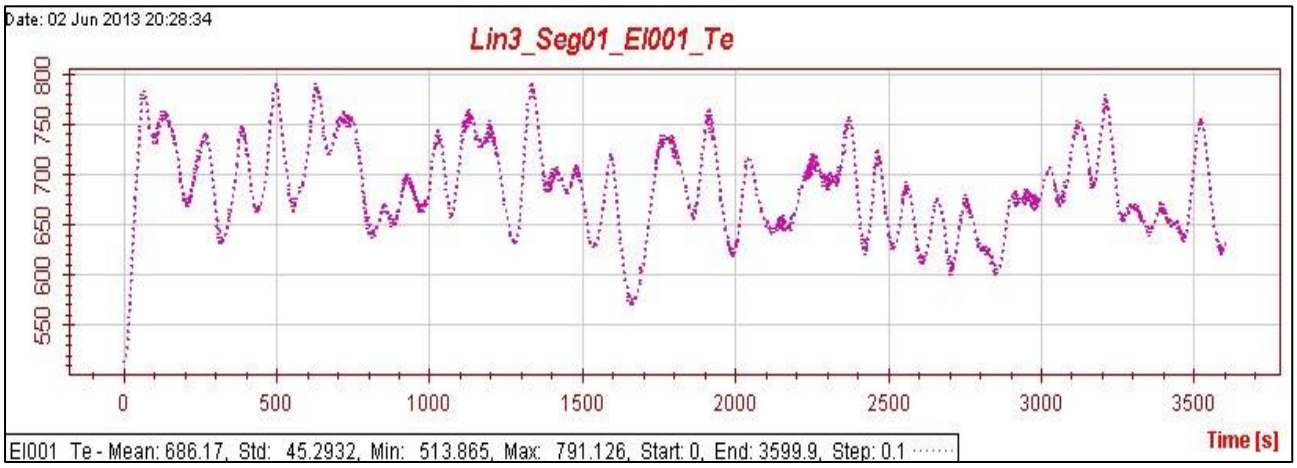

Figure 7-4 Mooring line tension for Case 10 in Model A

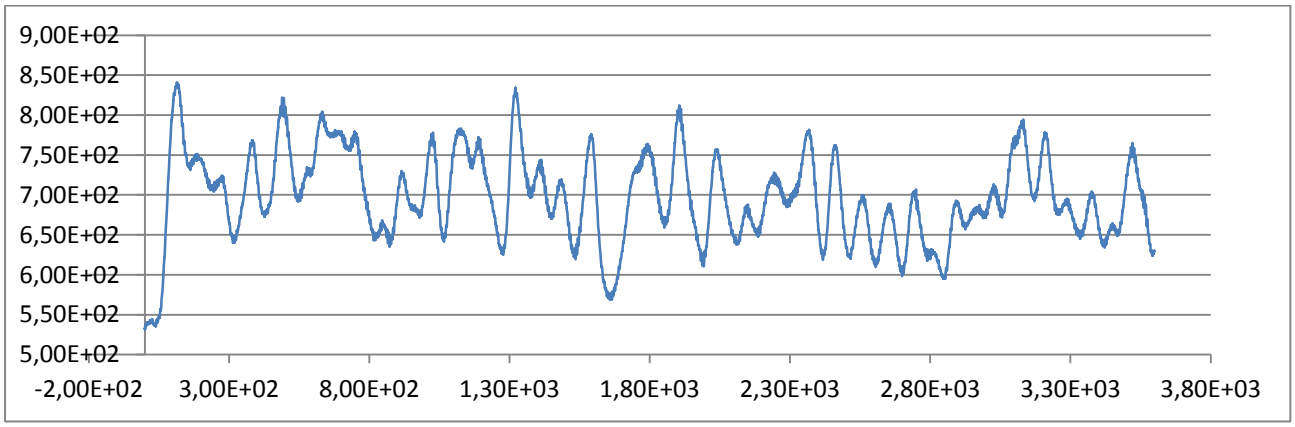

Figure 7-5 Mooring line tension for case 10 in Model B

Similar trend is shown in these two figures. The mooring line tension shows more small-period variations which is due to wave effect. This is because the wave effect on the mooring line can result in certain response in mooring line tension, but very limited floater motion.

7.3 Sample 2 – medium wind, large wave

Similarly, we take a sample case of a medium wind speed with relatively large wave for comparison. Case 12 is selected for this purpose, which is with the same wind information but larger wave than Case 10. The environmental condition of Case 12 is listed below.

H_s (m)	T_p (s)	U_{mean} (m/s)	I
4.081035	10.79	9	0.164677

Table 7-2 Sample case information, Case 12

The thrust force, surge motion and mooring line tension is shown below.

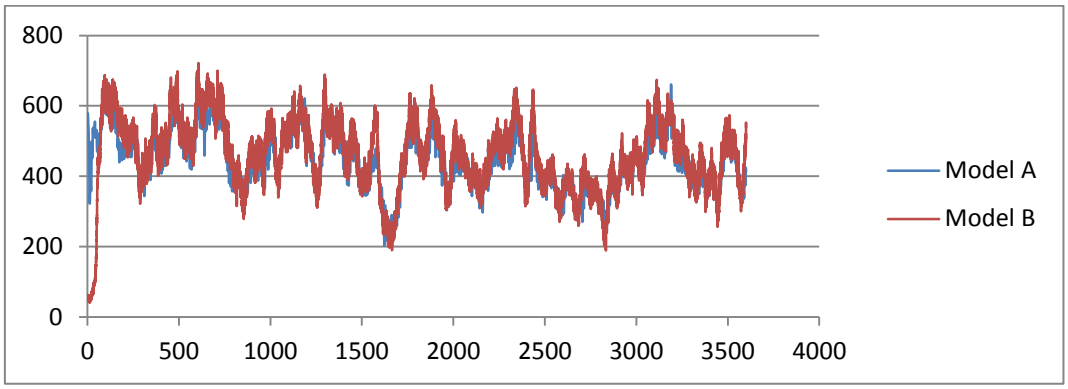

Figure 7-6 Thrust force in Case 12 for Model A and B

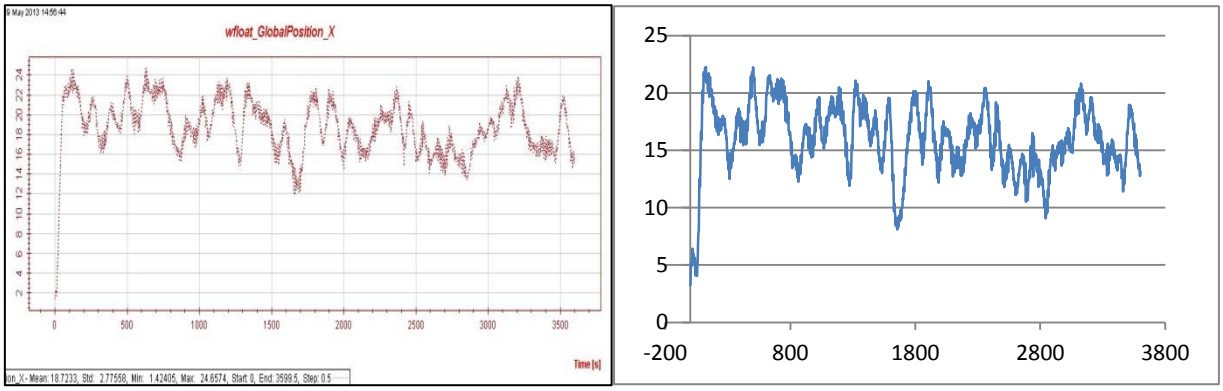

Figure 7-7 Surge in Case 12 for Model A (left) and B (right)

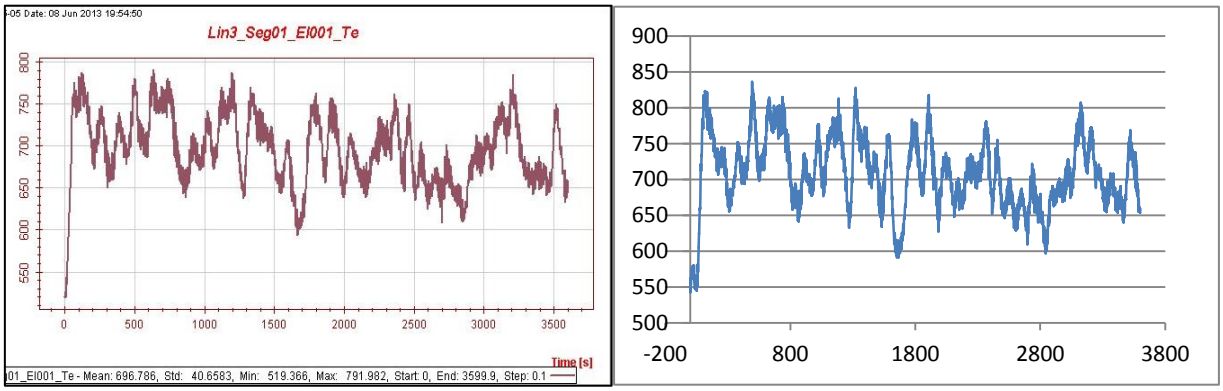

Figure 7-8 Mooring line tension for Case 12 in Model A (left) and B (right)

The short-period oscillations are larger. Since the wind used in this case is the same as in the previous one, it must be the wave effect that caused the increase in short-period oscillations. Wind effect is still dominating the response, and therefore the general trends between these two results are similar.

The surge motion and mooring line tension change is mainly due to thrust force change. And thus we see similar trends among these three results.

This is a very representative case in this project. Response time series in other regular cases are quite similar to this one, except for the extreme case, when wave is dominating the response.

7.4 Extreme condition comparison

In this project, Case 42 is the extreme condition. The load condition is below.

H_s (m)	T_p (s)	U_{mean} (m/s)	I
4.081035	10.79	9	0.164677

Table 7-3 Sample case information, Case 42

The thrust force, surge motion and mooring line tension is shown below.

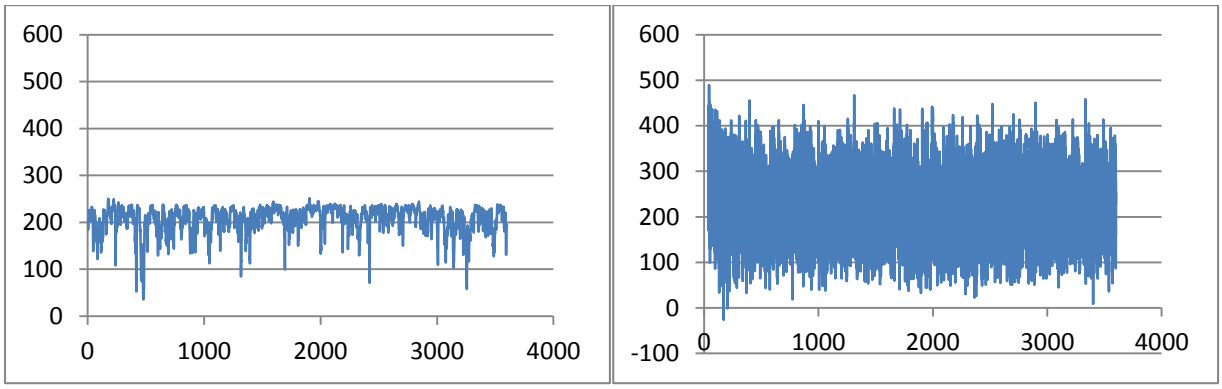

Figure 7-9 Thrust force in Case 42 for Model A (left) and B (right)

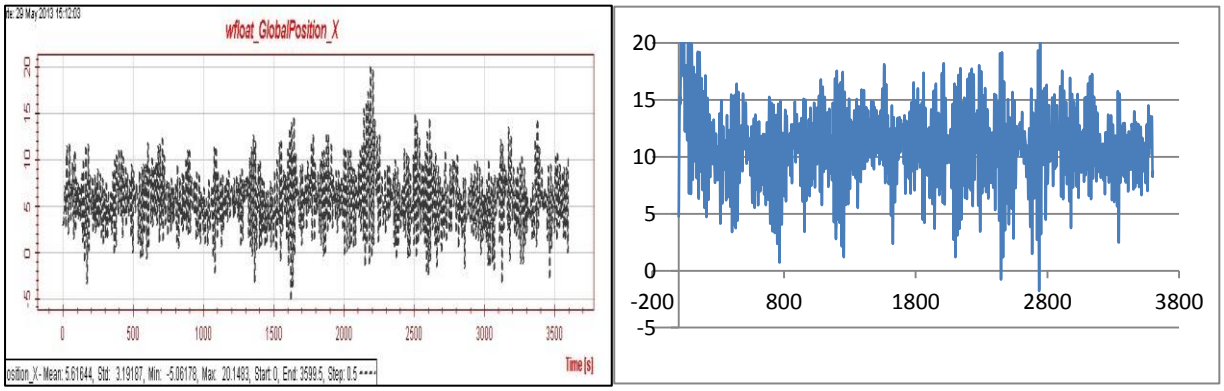

Figure 7-10 Surge in Case 42 for Model A (left) and B (right)

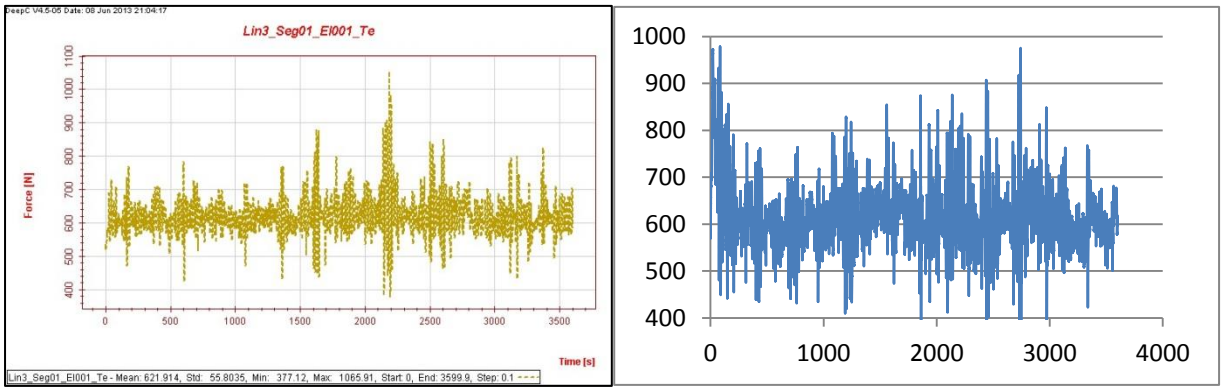

Figure 7-11 Mooring line tension in Case 42 for Model A (left) and B (right)

In the extreme condition, the turbine blades are stalled and the turbine is not in operation. The wind is large and associated with large turbulence, which means the wind is changing largely along the blade plain and with time. The force acting on the blades are quite complex and the total thrust

force can be calculated correctly only by the refined method. TDHmill model is too simple to reflect the complex wind field and wind turbine response in the extreme case. Because of this, seen from the thrust force time series, we observe much larger variance in Model B than in Model A. The mean value of thrust force seems to be similar.

Due to large difference in thrust force, surge motion and mooring line tension are also quite different.

Wave effect under extreme condition is also large. We cannot easily see it from the results above because wind is also involved in.

We may conclude that TDHmill cannot reflect the wind effect very well in extreme conditions. More detailed analysis will be given in the next few chapters.

Chapter 8. Comparison of Statistical Results

8.1 Summary

In this chapter, statistical results (mean and standard deviation) of thrust force, floater motion and mooring line tension will be shown for all cases. Computation time is also shown at last in this chapter.

Discussions are made on these results including observations, error analysis and conclusions for model feasibility.

The results show that responses between these two models are quite similar in terms of mean value, but significant difference is shown in terms of standard deviation.

8.2 Thrust force

Thrust force statistic values are processed with Matlab and presented below. Data from 1600s to 3600s are taken into analysis. See Appendix 7 for the Matlab code.

Case	Mean thrust force in Model A	Standard deviation in Model A	Mean thrust force in Model B	Standard deviation in Model B	difference for mean	difference for standard deviation
1	72.202	21.654	77.361	26.559	-7%	-18%
2	72.259	22.075	77.389	26.673	-7%	-17%
3	72.400	23.113	77.420	26.959	-6%	-14%
4	223.856	42.258	227.315	56.042	-2%	-25%
5	223.921	42.879	227.298	56.216	-1%	-24%
6	224.078	44.257	227.222	56.555	-1%	-22%
7	365.751	66.378	372.358	86.665	-2%	-23%
8	365.798	67.014	372.455	86.876	-2%	-23%
9	365.880	68.712	372.343	87.285	-2%	-21%
10	445.502	76.137	460.170	102.293	-3%	-26%
11	445.567	76.863	460.162	102.569	-3%	-25%
12	445.717	78.349	460.053	103.123	-3%	-24%
13	531.204	78.533	550.949	108.850	-4%	-28%
14	531.122	79.235	550.927	108.875	-4%	-27%
15	530.892	80.336	550.670	109.307	-4%	-27%
16	594.438	61.240	593.390	103.390	0%	-41%
17	594.651	61.379	593.491	103.872	0%	-41%
18	594.201	61.628	593.121	104.295	0%	-41%
19	592.327	61.242	574.605	109.154	3%	-44%
20	593.347	61.482	574.234	109.174	3%	-44%
21	593.029	61.717	573.651	109.500	3%	-44%
22	554.292	77.110	520.013	104.291	7%	-26%
23	554.337	75.432	519.334	104.474	7%	-28%
24	554.452	73.901	518.678	105.536	7%	-30%
25	505.970	78.600	469.808	92.508	8%	-15%

Table to be continued next page.

Case	Mean thrust force in Model A	Standard deviation in Model A	Mean thrust force in Model B	Standard deviation in Model B	difference for mean	difference for standard deviation
26	505.074	76.268	469.146	93.293	8%	-18%
27	504.206	74.200	468.477	94.887	8%	-22%
28	422.371	55.583	397.947	71.565	6%	-22%
29	421.851	54.359	397.701	74.140	6%	-27%
30	421.907	54.361	397.323	77.607	6%	-30%
31	370.373	35.057	351.983	58.276	5%	-40%
32	370.360	35.171	351.643	61.821	5%	-43%
33	370.490	35.533	351.309	66.139	5%	-46%
34	336.091	24.899	321.261	56.473	5%	-56%
35	336.138	25.125	320.955	60.711	5%	-59%
36	336.210	25.360	320.737	64.178	5%	-60%
37	283.872	14.763	273.902	66.354	4%	-78%
38	283.916	14.896	273.697	68.726	4%	-78%
39	283.982	15.078	273.553	71.596	4%	-79%
40	206.555	27.308	229.701	107.193	-10%	-75%
41	206.699	27.361	229.428	107.959	-10%	-75%
42	206.785	27.841	228.853	108.900	-10%	-74%

Table 8-1 Thrust force comparison

8.2.1 Mean value analysis

Seen from the above, we observe the first of all, very good agreement between the thrust forces at the rated speed (Case 16,17,18). However, the difference between the thrust force mean values at some other wind speeds are a bit large.

For the cut-in speed 3m/s (Cases 1,2,3), Model A gives 7% smaller mean thrust forces than in Model B. At the wind speed higher than rated wind speed, 14m/s (Cases 25,26,26), Model A gives 8% larger mean thrust forces than in Model B. The general trend is that when wind speed is small, Model A underestimates the thrust force, while it overestimates the thrust force when wind speed is large. However, the largest difference is 8%, and thus the simplified model is applicable only for rough estimation.

At the extreme conditions (Case 40,41,42), the wind turbine blades are stalled, and Model A shows a mean thrust force 10% smaller than Model B.

8.2.2 Standard deviation analysis

Generally, there is significant standard deviation difference between the two models, up to 40% for working conditions and 70% for extreme conditions. That means TDHmill model cannot be used for analyses concerning the standard deviation, for example, fatigue analysis. TDHmill shows a significant underestimation of the thrust force standard deviation.

8.2.3 Error discussion

The difference thrust force between the two models may result from the following contributions:

The thrust coefficients in TDHmill can introduce significant error. The coefficients have been carefully calculated in this project. However, longer Aerodyn simulation time for each coefficient, and more wind speed-coefficient points are needed to give more accuracy. Especially in cut-in and cut-out conditions, it takes a bit time for the turbine to enter steady control condition, and the transient effect lasts in this case about 400s.

Truncation errors are also important. The period truncated for analysis (in this case 1600s-3600s) is usually not a complete cycle of oscillation. For example, if there is a wave component or wind component with a period of 1000s, then the result may probably be inaccurate. This error can be reduced by either carefully selecting the period of interest or increasing simulation time.

Wind input file processing method may introduce error. The wind input file in TDHmill is processed from the wind input file in Aerodyn, so that it is confirmed that the two wind files come from the same wind. In TDHmill, for each time step, the wind speed at rotor and the mean wind speed at the turbine area are required. Mean wind speed at turbine area is calculated with limited discretized points at this area, and so increasing the number of sample points at the area will give more accuracy.

Waves used in these two models are not the same. Although the wave parameters used in these two models (including random generation seed) are exactly the same, the generated waves are not the same probably due to different software version. The statistic uncertainty of wave load is also a contribution to the error.

Statistical uncertainty may also introduce some error. This means that the statistical results usually may change with different random seeds. Actually mean value and standard deviation is not very sensitive to statistical uncertainty, but running more cases will still reduce this type of error.

All of the above may contribute to the difference between these two models, some are significant errors and some errors are not of importance. However, apart from the above uncertainties, the most important reason for the difference in the results is the systematic error in these two calculation models. The inertia force and damping of the wind turbine and tower has a significant effect on the response results in some load conditions. TDHmill uses a simple external force as the wind effect, and thus a lot of significant dynamic effects are neglected.

8.3 Floater surge and pitch motion

A direct result of the thrust force difference is the difference in floater positions.

Floater motion statistic results are processed with the same Matlab code as used in thrust force analysis. See Appendix 7. The results are shown in the table on the next page.

	Model A				Model B				Difference			
	surge mean	surge std	pitch mean (deg)	pitch std	surge mean	surge std	pitch mean (deg)	pitch std	surge mean	surge std	pitch mean	pitch std
1	3.075	0.930	1.315	0.422	3.036	1.070	0.962	0.427	1%	-13%	37%	-1%
2	3.253	0.900	1.322	0.447	3.229	1.001	0.968	0.436	1%	-10%	37%	3%
3	3.601	0.952	1.342	0.532	3.600	1.027	0.986	0.500	0%	-7%	36%	6%
4	8.215	1.912	3.530	0.881	8.131	2.326	3.112	0.898	1%	-18%	13%	-2%
5	8.425	1.769	3.540	0.890	8.350	2.139	3.119	0.894	1%	-17%	14%	0%
6	8.801	1.752	3.559	0.936	8.732	1.981	3.137	0.927	1%	-12%	13%	1%
7	12.678	2.683	5.603	1.379	12.703	3.118	5.200	1.418	0%	-14%	8%	-3%
8	12.917	2.510	5.612	1.377	12.980	2.914	5.208	1.408	0%	-14%	8%	-2%
9	13.277	2.448	5.636	1.416	13.401	2.714	5.227	1.424	-1%	-10%	8%	-1%
10	15.012	2.936	6.763	1.590	15.288	3.478	6.451	1.660	-2%	-16%	5%	-4%
11	15.259	2.746	6.773	1.584	15.579	3.261	6.460	1.652	-2%	-16%	5%	-4%
12	15.638	2.619	6.793	1.601	15.997	3.049	6.479	1.663	-2%	-14%	5%	-4%
13	17.403	3.036	8.010	1.672	17.844	3.616	7.749	1.775	-2%	-16%	3%	-6%
14	17.643	2.849	8.018	1.656	18.125	3.385	7.756	1.762	-3%	-16%	3%	-6%
15	17.989	2.722	8.031	1.659	18.518	3.180	7.775	1.777	-3%	-14%	3%	-7%
16	19.120	2.416	8.917	1.727	19.050	3.273	8.380	1.902	0%	-26%	6%	-9%
17	19.398	2.218	8.928	1.584	19.316	3.034	8.392	1.859	0%	-27%	6%	-15%
18	19.772	2.123	8.947	1.465	19.691	2.852	8.413	1.821	0%	-26%	6%	-20%
19	19.071	2.410	8.888	1.995	18.526	3.514	8.151	2.041	3%	-31%	9%	-2%
20	19.393	2.188	8.913	1.722	18.784	3.168	8.159	1.978	3%	-31%	9%	-13%
21	19.780	2.093	8.933	1.582	19.169	2.907	8.178	1.927	3%	-28%	9%	-18%
22	18.041	2.578	8.340	2.882	17.024	3.244	7.424	1.989	6%	-21%	12%	45%
23	18.372	2.358	8.350	2.403	17.313	2.885	7.431	1.912	6%	-18%	12%	26%
24	18.815	2.258	8.380	2.005	17.717	2.666	7.455	1.868	6%	-15%	12%	7%
25	16.769	2.545	7.645	2.854	15.664	2.801	6.745	1.811	7%	-9%	13%	58%
26	17.103	2.319	7.646	2.382	15.997	2.494	6.756	1.719	7%	-7%	13%	39%
27	17.527	2.241	7.667	2.029	16.438	2.353	6.783	1.665	7%	-5%	13%	22%
28	14.522	2.057	6.438	1.894	13.673	2.103	5.760	1.382	6%	-2%	12%	37%
29	14.940	1.894	6.444	1.504	14.104	1.917	5.780	1.321	6%	-1%	11%	14%
30	15.364	1.901	6.482	1.466	14.529	1.912	5.815	1.333	6%	-1%	11%	10%
31	13.077	1.541	5.680	1.185	12.374	1.555	5.124	1.146	6%	-1%	11%	3%
32	13.566	1.488	5.706	1.057	12.873	1.455	5.149	1.097	5%	2%	11%	-4%
33	13.987	1.634	5.759	1.143	13.293	1.557	5.192	1.149	5%	5%	11%	-1%
34	12.136	1.240	5.182	0.882	11.520	1.232	4.686	1.069	5%	1%	11%	-18%
35	12.700	1.285	5.219	0.889	12.113	1.256	4.722	1.030	5%	2%	11%	-14%
36	13.078	1.507	5.274	1.035	12.488	1.454	4.780	1.115	5%	4%	10%	-7%
37	10.771	0.980	4.433	0.641	10.321	1.084	4.054	1.061	4%	-10%	9%	-40%
38	11.357	1.269	4.495	0.837	10.930	1.333	4.125	1.142	4%	-5%	9%	-27%
39	11.707	1.660	4.592	1.081	11.256	1.682	4.217	1.292	4%	-1%	9%	-16%
40	9.400	1.880	3.534	1.248	10.306	1.875	3.055	1.664	-9%	0%	16%	-25%
41	9.954	2.664	3.880	1.720	10.822	2.642	3.379	1.983	-8%	1%	15%	-13%
42	10.221	3.323	4.183	2.096	10.877	3.249	3.644	2.259	-6%	2%	15%	-7%

Table 8-2 Vessel motion comparison

Again, almost no difference is shown in mean surge motion for the rated speed condition (Cases 16,17,18). At the wind speed where there is large thrust force difference, there is correspondingly

large difference in floater surge motion (up to 7%). There is strong correlation between the thrust force difference and the floater surge motion difference.

Larger difference is obtained for floater pitch motion (up to 11% in regular conditions, 37% at cut-in wind speed, and 16% at extreme condition). However, the exact difference value is not so large, and the pitch motion mean value of Model A is always around 0.5 deg larger than that of Model B. This is due to the difference in modeling. An error of 0.5 deg in the static condition is introduced due to inaccurate calculation for mass model or restoring coefficients. The static 0.5 deg error is small and tolerable for mass calculation. However, since the exact value of the pitch motion is also small (from 1 deg to 7 deg), the difference in percentage is then relatively large.

The standard deviation in this case is a bit difficult to explain. There is no obvious trend of the standard deviation change with load cases. Generally, it is still Model A that is associated with smaller deviation. However, in some cases, the standard deviation in Model A is the same as in B or even a bit larger. The standard deviation is related to the random seed used in wave and wind generation, so the generated wind and wave may differ from case to case. And the response from TDHmill or Aerodyn are different with different wind and wave cases, and that again confirms that TDHmill should not be used in calculations related to standard deviation, for example, fatigue problems.

8.4 Mooring line tension

The mean force and standard deviation comparison for mooring line tension are listed below. Line 1 is the down-wind mooring line and Line 3 is the up-wind mooring line.

Mooring line tension statistics are extracted from the Riflex dynmod result file dynmod.res.

	Model A				Model B				Difference			
	Line1 mean	Line 1 std	Line3 mean	Line 3 std	Line1 mean	Line 1 std	Line3 mean	Line 3 std	Line1 mean	Line 1 std	Line3 mean	Line 3 std
1	492.9	6.7	535.3	8.5	496.9	8.2	541.6	10.5	-1%	-19%	-1%	-19%
2	491.6	7.0	537.1	8.8	492.8	9.5	547.3	10.9	0%	-26%	-2%	-20%
3	489.0	8.9	540.6	9.9	495.5	8.0	543.5	10.2	-1%	11%	-1%	-3%
4	459.2	10.8	589.6	22.1	463.4	14.6	595.1	27.6	-1%	-26%	-1%	-20%
5	457.9	10.3	592.1	20.8	462.0	13.6	597.6	25.4	-1%	-24%	-1%	-18%
6	455.7	11.2	597.0	21.1	459.7	13.4	602.2	23.9	-1%	-16%	-1%	-12%
7	436.4	12.6	649.5	37.5	440.0	16.1	655.3	44.2	-1%	-22%	-1%	-15%
8	435.1	12.0	653.0	35.3	438.5	15.1	659.1	41.4	-1%	-20%	-1%	-15%
9	433.5	12.6	658.7	34.7	436.4	14.7	665.4	38.9	-1%	-14%	-1%	-11%
10	426.3	12.4	686.2	45.3	428.8	16.3	695.5	54.1	-1%	-24%	-1%	-16%
11	425.1	11.9	690.1	42.5	427.3	15.3	699.9	51.0	-1%	-22%	-1%	-17%
12	423.5	12.4	696.8	40.7	425.5	14.9	706.8	48.1	0%	-17%	-1%	-15%
13	417.0	12.0	727.6	50.7	418.6	16.3	738.8	60.1	0%	-26%	-2%	-16%
14	416.0	11.7	731.9	47.4	417.4	15.4	743.5	56.7	0%	-24%	-2%	-16%
15	414.7	12.3	738.6	45.1	415.8	15.1	750.5	53.5	0%	-19%	-2%	-16%

Table to be continued next page.

	Model A				Model B				Difference			
	Line1 mean	Line 1 std	Line3 mean	Line 3 std	Line1 mean	Line 1 std	Line3 mean	Line 3 std	Line1 mean	Line 1 std	Line3 mean	Line 3 std
16	410.7	9.5	758.8	40.4	414.2	14.8	759.6	56.0	-1%	-36%	0%	-28%
17	409.7	9.3	764.3	36.8	413.0	13.7	764.2	51.8	-1%	-32%	0%	-29%
18	408.4	10.3	772.3	35.2	411.5	13.7	771.3	48.9	-1%	-25%	0%	-28%
19	411.0	9.3	757.9	41.1	416.1	14.7	750.0	63.5	-1%	-37%	1%	-35%
20	409.7	9.1	764.2	37.0	414.8	13.4	754.0	57.2	-1%	-32%	1%	-35%
21	408.4	10.2	772.4	35.2	413.2	13.4	760.9	52.5	-1%	-24%	2%	-33%
22	414.7	9.8	738.9	44.0	421.0	13.3	721.5	58.5	-2%	-26%	2%	-25%
23	413.3	9.7	745.1	40.2	419.6	12.2	725.8	52.3	-2%	-20%	3%	-23%
24	411.7	11.0	754.0	38.4	417.9	12.8	732.7	48.3	-1%	-14%	3%	-20%
25	419.3	10.0	715.8	42.1	425.6	12.1	696.3	48.9	-1%	-17%	3%	-14%
26	417.8	9.9	721.7	38.5	424.0	11.3	701.3	44.0	-1%	-12%	3%	-12%
27	416.2	11.4	729.9	37.3	422.2	12.5	708.8	41.4	-1%	-8%	3%	-10%
28	427.9	8.9	677.1	32.1	430.6	10.4	668.2	31.6	-1%	-15%	1%	1%
29	426.0	9.5	684.1	29.6	428.8	12.8	675.2	31.3	-1%	-26%	1%	-5%
30	424.3	11.8	691.8	29.1	430.6	10.4	668.2	31.6	-1%	14%	4%	-8%
31	434.0	7.7	654.2	21.9	437.2	9.3	640.9	23.4	-1%	-17%	2%	-6%
32	431.7	9.2	662.1	21.2	434.8	10.1	648.2	22.1	-1%	-9%	2%	-4%
33	430.0	12.6	669.5	22.6	433.0	13.4	654.8	23.1	-1%	-6%	2%	-2%
34	438.2	7.1	640.2	16.4	440.0	9.1	628.6	18.1	0%	-22%	2%	-9%
35	435.6	9.7	649.1	17.1	437.3	10.7	637.1	18.4	0%	-10%	2%	-7%
36	434.0	13.8	655.7	18.9	435.7	14.9	642.9	20.5	0%	-7%	2%	-7%
37	444.9	7.5	621.6	12.5	443.3	9.7	612.1	19.1	0%	-23%	2%	-35%
38	442.0	12.5	630.6	15.2	440.5	13.7	620.2	20.6	0%	-9%	2%	-26%
39	440.7	18.5	636.5	19.3	439.3	19.5	624.9	24.7	0%	-5%	2%	-22%
40	452.8	22.1	606.3	25.9	445.9	23.3	673.3	39.4	2%	-5%	-10%	-34%
41	451.1	35.2	615.7	37.3	443.3	34.2	677.3	55.7	2%	3%	-9%	-33%
42	451.0	47.4	621.9	55.8	444.5	44.1	683.7	73.2	1%	7%	-9%	-24%

Table 8-3 Mooring line tension comparison

Mean value for mooring line tension in the different models show very good agreement with each other. This is because the mooring line pretension is large, and the 10% difference in the thrust is very small compared to the large pretension in the mooring line.

In the extreme condition (Case 42), the mooring line tension is 10% smaller in Model A than in Model B. This is because of the large difference in thrust force in the extreme condition.

There is also large (around 20%) difference in standard deviation analysis.

8.5 Computation time

Computation time for Model B is around 5 hours each case in a PC with 3.33GHz CPU, while it is around 1 hour each case in a PC with 2.93GHz CPU. This is mainly because the computation step for Aerodyn is required to be equal or less than 0.005s.

The computation time is significantly reduced in the TDHmill model. So for simple analyses when fast calculation is needed, TDHmill can provide good time reduction.

Chapter 9. Comparison of Mooring Line Tension for Extreme Conditions

9.1 Summary

In real engineering, maximum structural responses at extreme conditions are usually one important parameter for ULS or ALS design. Statistical uncertainty is significant when maximum response is considered. In this chapter, we focus on the mooring line tension response in extreme conditions, try to reduce statistical uncertainty, and compare the maximum value between these two models.

The load condition for the extreme condition, Case 42 is listed below.

H_s (m)	T_p (s)	U_{mean} (m/s)	I
4.081035	10.79	9	0.164677

Table 9-1 Sample case information, Case 42

9.2 Statistic uncertainty

The analysis above can give an approximate value for response in extreme conditions. This is because the simulation is based on only one seed and short term variability is not yet considered.

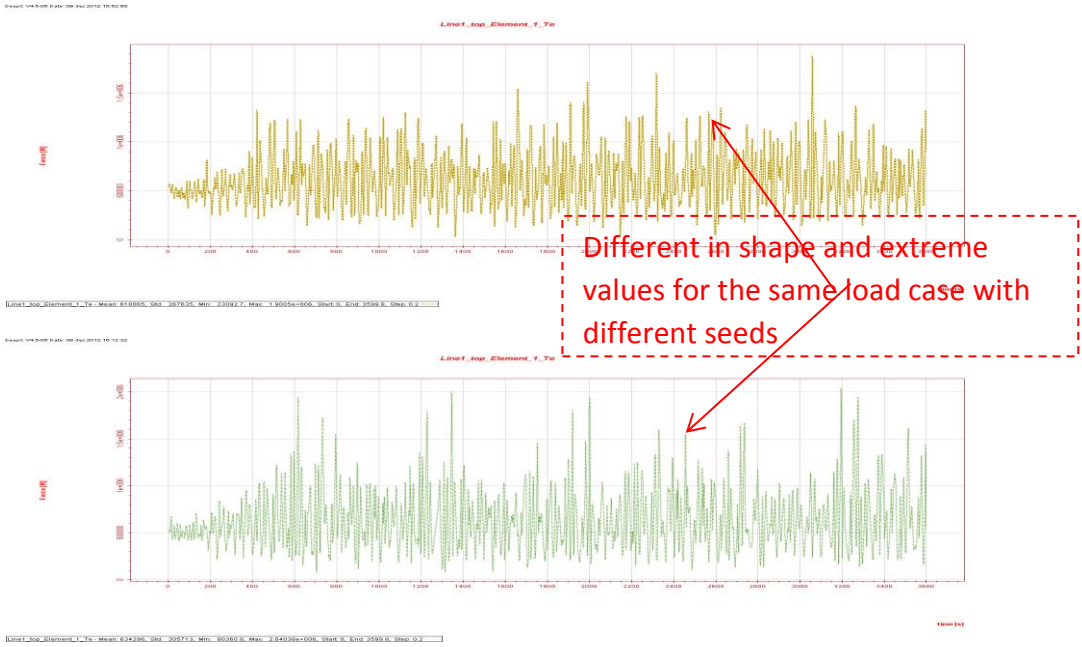

Figure 9-1 Comparison for same case different seeds

Here is an example for short term variability or statistic uncertainty (An example from pre-project). The above are two different time series the same load case with different seeds for both wave condition and wind condition. The time series are totally different in terms of the plotted shape. The maximum values for these two conditions are 1.90E6 and 2.04E6 respectively. Mean value and standard deviation show less difference.

Given a certain load case, H_S, T_P and U, the response can be different due to different seeds. This can be demonstrated by the following formula.

An irregular variable can be considered as the combination of several sinusoidal components, as shown below.

$$\xi = \sum \xi_{0i} \sin(\omega_i t + \varepsilon_i)$$

Each component is associated with an amplitude ξ_{0i}, a frequency ω_i and an initial phase angle ε_i. The initial phase angles are given randomly, and a set of these initial values is called seed. It is seen clearly from the formula that different seeds will result in different maximum values.

The difference in this problem is called short term variability, or statistical uncertainty, and should be avoided when considering extreme responses.

Mean value and standard deviation are not very sensible to statistical uncertainty (see Seaload Stochastic lecture notes for more information). However, the maximum value of response can be very sensitive to statistical uncertainty. And maximum response in extreme conditions is very important for design purpose.

For extreme value analysis, a theoretical way to reduce short term variability is to run many cases for one load case and different seeds, and then fit all the extreme results to a certain distribution. The final extreme value is then obtained from the 5% or 10% exceedance value of the fitted distribution. This method is complicated and it is difficult to evaluate the distribution type of the extreme values. Thus here a simplified method is applied.

The method used in this project is first to run 6 simulations for each load case with different seeds, and get the simple mean of the extreme values, and then multiply this mean extreme value with a factor 1.3. The final value will result in limited error from the complicated fitting method.

9.3 Mean, minimum and maximum results for each case

After the 6 parallel simulations, Mean, minimum and maximum values for the extreme case are presented below. The data is processed with Matlab. See Appendix 8.

		Seed 1	Seed 2	Seed 3	Seed 4	Seed 5	Seed 6	Average
Mean	Line 1 Model A	450.3565	451.1097	450.7674	450.7469	450.2355	450.4601	450.6127
	Line 3 Model A	624.0019	621.5335	619.7452	620.1628	622.2951	621.991	621.6216
	Line 1 Model B	445.3883	444.2551	443.4951	444.6153	443.708	441.6025	443.8441
	Line 3 Model B	609.4036	611.3727	614.955	610.1653	612.9079	622.37	613.5291
Max	Line 1 Model A	713.6449	736.0972	783.1533	766.2076	842.1912	775.794	769.5147
	Line 3 Model A	1065.914	951.2869	956.4713	981.4338	948.4754	1074.829	996.4017
	Line 1 Model B	734.1334	631.7477	731.5162	695.0961	658.1189	673.2077	687.3033
	Line 3 Model B	978.3646	1008.098	979.1384	1113.514	1104.58	975.3041	1026.5
Min	Line 1 Model A	258.1086	285.2723	254.4741	267.9554	255.1638	248.2774	261.5419
	Line 3 Model A	377.12	363.4573	248.2001	295.6172	234.3385	311.6299	305.0605
	Line 1 Model B	307.2697	299.9189	287.5258	264.0101	310.1623	328.1078	299.4991
	Line 3 Model B	255.2702	328.6208	243.0225	294.4698	264.7541	323.5288	284.9444

Table 9-2 Results for parallel simulations in extreme condition

First of all, we examine the minimum value for all mooring lines. As a basic requirement for the mooring line system, mooring line tension must always be positive. If negative mooring line tension is obtained, then snapping problem will occur, resulting in serious problems. In our case of study, we observe that no negative mooring line tension occur, and thus our model meet the non-snapping requirement.

We also see that mean value is not changing much with different seeds. However, the extreme value is quite different for different seeds. This confirms that mean value is not sensitive to statistic uncertainty.

9.4 Mean value comparison

	Model A	Model B	Difference
Line1	450.6127	443.8441	1.5%
Line3	621.6216	613.5291	1.3%

Table 9-3 Comparison of mooring line mean tension at extreme condition

As expected, there is not much difference in the mooring line tension mean value comparison. The number is no big difference that is obtained previously.

9.5 Extreme response comparison

	Characteristic extreme in Model A	Characteristic extreme in Model B	Difference
Line1	1000.369	893.4943	12.0%
Line3	1295.322	1334.45	-2.9%

Table 9-4 Comparison of mooring line characteristic largest tension at extreme condition

We see that there is large difference in the up-wind mooring line and acceptable difference with the down-wind mooring line, which is more important with regard to mooring line extreme value.

According to the thrust mean value analysis before, there is 10% difference in the mean thrust force. The difference in thrust force then is distributed into the four mooring lines to achieve equilibrium. In this analysis the difference in thrust force is more applied on Line 1 than in Line 3, thus there is larger difference in Line 1 than in Line 3 in the comparison.

According to the result, Model A gives a slightly smaller estimation of the extreme value. Thus the result of Model A is on the non-conservative side, but can still be used in concept design or other qualitative estimation, with some safety margin.

However, it must be noted that the characteristic extreme response of mooring line tension is expected to change with different loading conditions. More detailed analysis is needed to confirm the feasibility of TDHmill.

Chapter 10. Spectral Analysis for Sample Cases

10.1 Summary

From the previous chapter, we observed serious difference in standard deviation. In order to give a more detailed look at the result, the time series are transformed to frequency domain spectrum. In this chapter, the spectrum analysis for 3 sample cases, Case 12, Case 27, and Case 42 will be presented with discussions. All these cases are large wave cases. Case 12 is a representative case, with regular results in all the considered responses. Case 27 is the case with large difference between the two models in response mean value. And Case 42 is the extreme case.

Detailed discussion is given for Sample case 1 and the extreme condition sample.

10.2 Sample case 1

The environmental conditions and difference on statistical results for Case 12 are listed below.

H_s (m)	T_p (s)	U_{mean} (m/s)	I
4.081035	10.79	9	0.164677

Table 10-1 Sample case load condition, Case 12

	Difference of statistic results between Model A and B
thrust mean	-3%
thrust std deviation	-24%
surge mean	-2%
surge std deviation	-14%
Line 3 tension mean	0%
Line 3 tension std deviation	-17%

Table 10-2 Difference of statistic results for sample case, Case 12

10.2.1 Comparison of thrust force

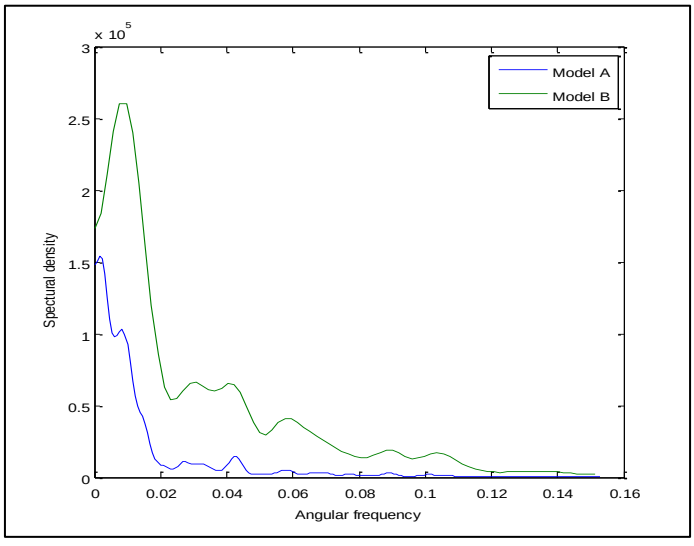

Figure 10-1 Spectrum for thrust force, Case 12

Above is thrust force spectrum.

The spectral results are obtained with a tool box in Matlab called WAFO, developed by Lund University in Sweden. WAFO is a toolbox of Matlab routines for statistical analysis and simulation of random waves and random loads.[1] See Appendix 9 for the Matlab code for data to spectrum transformation.

The shape of the spectrum is similar. However, thrust force in Model A show a much smaller variation than in Model B. Since the wind inputs are exactly the same, this difference is mostly due to the different calculation methods.

10.2.2 Comparison of floater surge motion

The floater surge motion spectrum is shown below.

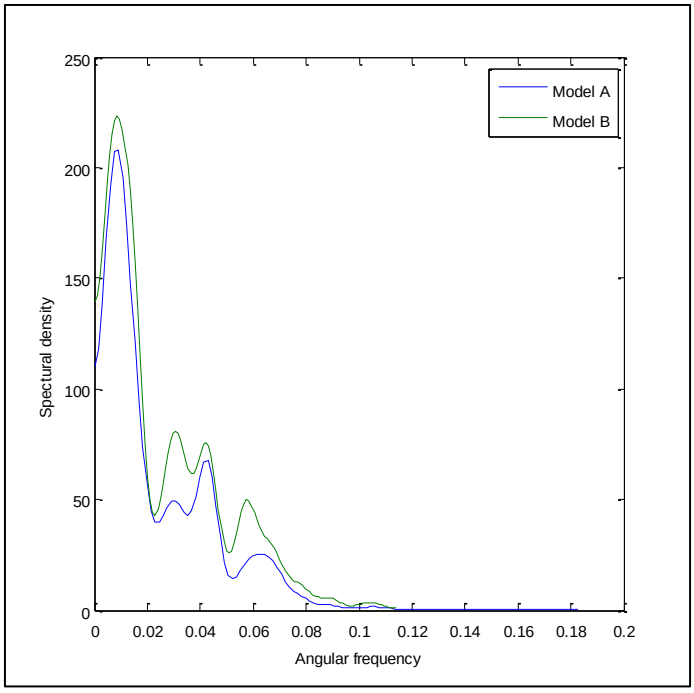

Figure 10-2 Spectrum for floater surge motion, Case 12

From the figure we see again that the shapes of the spectra are similar. At some certain frequencies, for example 0.03 and 0.06, Model A shows smaller spectral density than Model B. These frequencies correspond to period of around 100s and 200s. This means that under such periods TDHmill underestimates the thrust force effect on variation of surge motion.

The difference in surge motion is smaller than the difference in thrust force as the difference area under the spectrum between Model A and Model B is smaller in surge motion. This agrees with the previous result on standard deviations.

For larger frequencies (larger than 0.12, or around 50s in period), the area under the spectrum curve is very small. This means that the system is not sensitive to wind gust of periods less than 50s.

[1] WAFO introduction. http://www.maths.lth.se/matstat/wafo/

10.2.3 Comparison of mooring line tension

The mooring line tension (up-wind mooring line) spectrum is shown below.

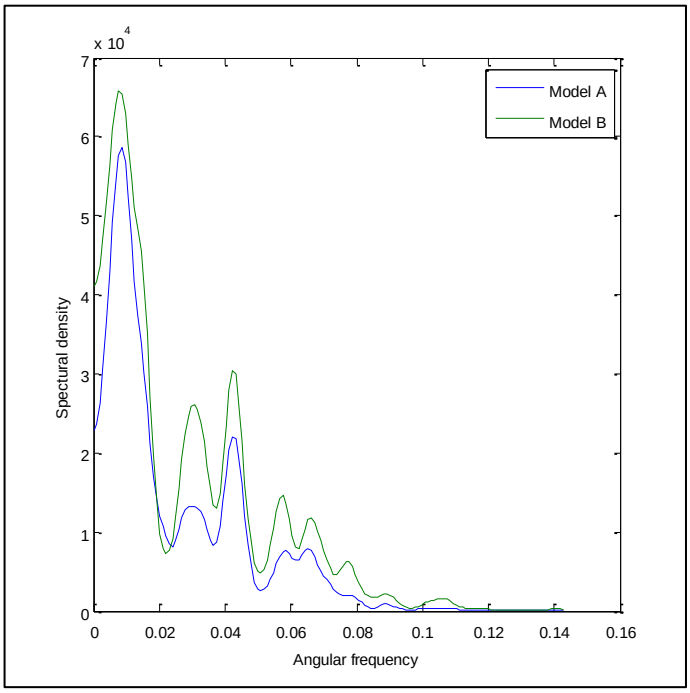

Figure 10-3 Spectrum for mooring line tension, Case 12

Observations from this figure are similar to that of the previous one on floater surge motion. There is slightly larger difference between the two models in this case, which agrees with the standard deviation results.

10.3 Sample case 2

The environmental conditions for Case 27 are listed below.

H_s (m)	T_p (s)	U_{mean} (m/s)	I
5.27	11.36	14	0.138

Table 10-3 Sample case load condition, Case 27

The thrust force, floater surge motion and mooring line tension spectra are shown below.

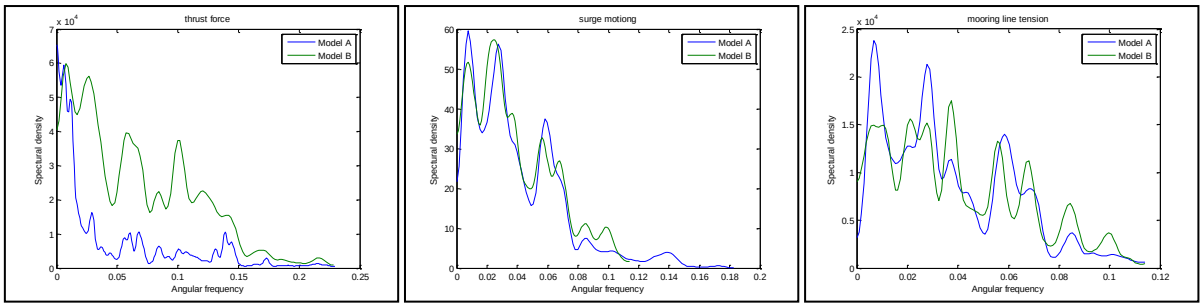

Figure 10-4 Spectra for thrust force, floater surge motion and mooring line tension, Case 27

Similar trend is obtained in this case as in the previous one. The response spectrum of mooring line tension shows larger difference between Model A and Model B than the previous case.

In this load case, there is a bit larger wave than the previous one, and some wave effect is shown if the angular frequency in the spectrum is taken large enough. This will be shown together with the extreme case in the next section.

10.4 Sample case 3

The environmental conditions and difference on statistical results for Case 42 are listed below.

H_s (m)	T_p (s)	U_{mean} (m/s)	I
16.96	15.152	33.59	0.11

Table 10-4 Sample case information, Case 42

	Difference of statistic results between Model A and B
thrust mean	8%
thrust std deviation	-18%
surge mean	7%
surge std deviation	-5%
Line 3 tension mean	-1%
Line 3 tension std deviation	-8%

Table 10-5 Difference of statistic results for sample case, Case 27

The floater surge motion and mooring line tension spectra are shown below. Angular frequencies in this case have been extended to a much larger range to show the features of extreme condition response.

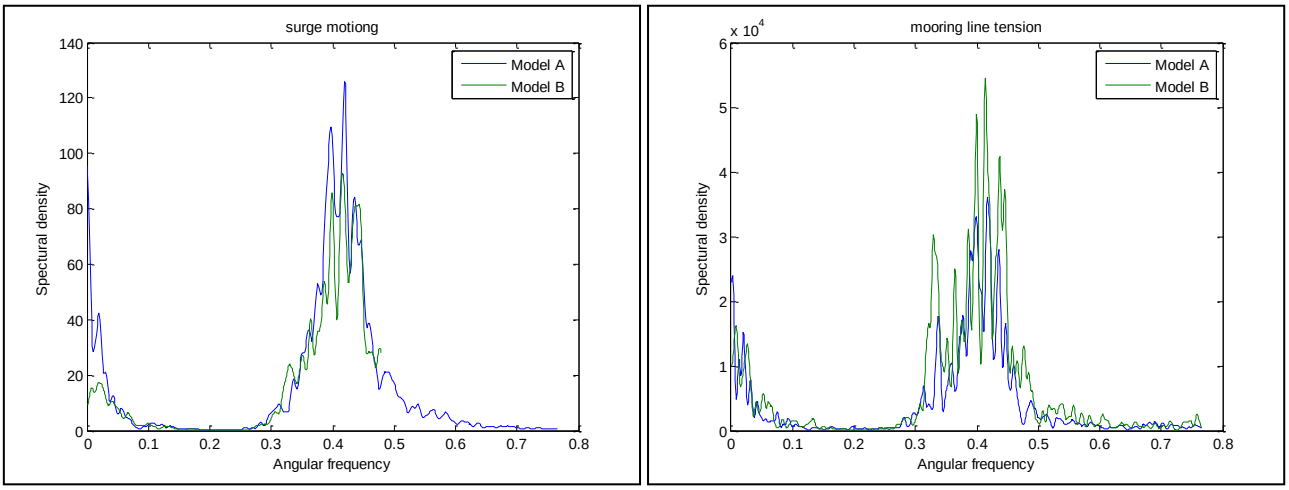

Figure 10-5 Spectrum for floater surge motion and mooring line tension, Case 42

The spectra look very different than what it looks in the previous cases. Apart from the extended angular frequency range, a very obvious observation is that there is significantly large spectral density at angular frequency of about 0.41 for both these two results, and the peak is similar between the two models.

This is because the energy around angular frequency 0.41 is induced by wave effect. Period corresponding to angular frequency 0.41 is about 15s, which is the peak period of the wave spectrum (15.152s). And period around the wave peak period is associated with large wave energy and consequently large motion and tension variance.

The wind effect is comparatively small in this case, because the turbine blades are stalled and the turbine is not in operation. This means that wave effect is more important than wind effect in the extreme case.

It can be seen that the spectrum curve of the two models are similar, which means that the two models have similar performance with regard to wave effect.

Actually, wave effect has already been shown in Case 27. It is just because the effect is very small that we did not include it in the previous section. If we extend the angular frequency range in the previous case, Case 27, the mooring line tension spectrum looks like

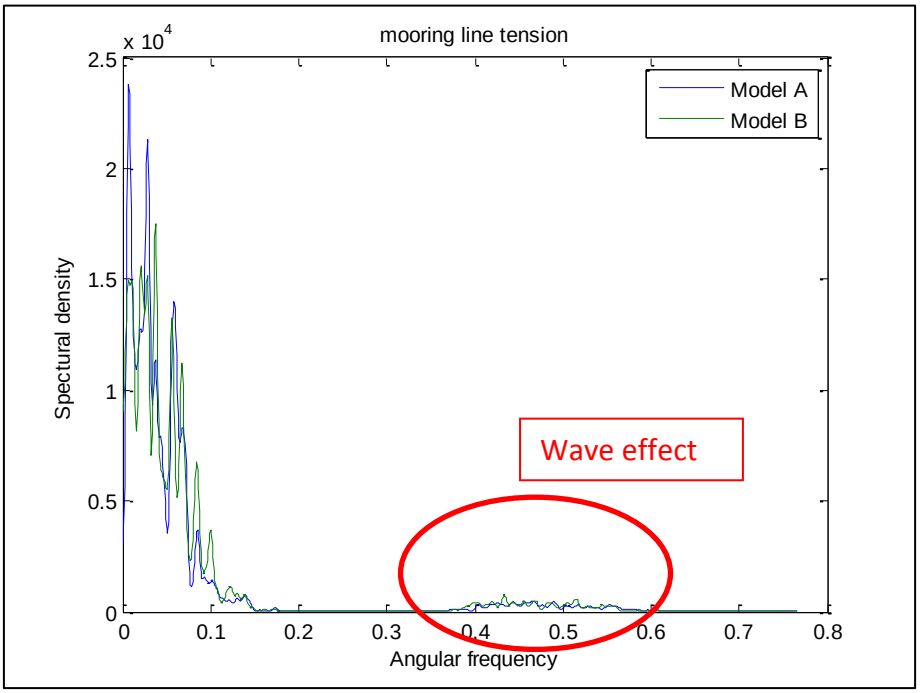

Figure 10-6 Spectra for mooring line tension, Case 27, extended frequency

Some wave induced response is seen in the marked area.

Spectra of other cases look just like Case 12 and Case 27 in this chapter, and thus will not be repeatedly presented herein.

Chapter 11. Conclusion

11.1 Summary of thesis work

This thesis is done in accordance with all the requirements.

First of all, literature review on background and theories involved in this thesis is performed and briefly presented. Next, the two complete models are set up based on different methods. Then, the results are presented and analyzed including time series, statistical values and spectra. At last, conclusions are organized and listed again and future work recommended in this chapter.

11.2 Considerations during the process

1. When changing floater mass model, all mass information including COG, radius of gyration and restoring coefficients must be carefully checked.
2. Thrust coefficients are different for different wind turbines, and thus must be calculated for the turbine in use.
3. Wind input file can be read or generated by TDHmill, and thus processing a wind input file will give the two models exactly the same wind input.
4. Load cases should be chosen to cover all the wind speeds for the turbine in operation, and also the extreme environmental condition should be considered.

11.3 Implications from the results

For the semi-submersible floater in use, we have the following implications of the results:

1. Mean values of thrust force, floater motion and mooring line tension are similar in the two models. TDHmill model shows a slightly larger response.
2. Generally TDHmill model shows less variation than Aerodyn model. This difference is significant (more than 20%).
3. Extreme mooring line tension response is slightly smaller in TDHmill model.
4. Computation time for TDHmill is much shorter than for Aerodyn model.
5. TDHmill give poor estimation of the wind thrust force in extreme conditions.
6. Wave effect is more important than wind effect with regard to motion and mooring line tension in extreme conditions.

11.4 TDHmill model feasibility

Conclusions of TDHmill feasibility for semi-submersible floating offshore wind turbines are:

TDHmill may be used in any environment in turbine working conditions, when mean value is the value of interest and accuracy requirement is not very strict.

TDHmill may not be used in extreme condition analysis, or when extreme value or oscillation range is the value of interest. Neither may it be used when accuracy requirement is strict.

11.5 Uncertainties

Detailed error analysis has already been demonstrated in the discussions in the result analysis chapters. Here the three uncertainties listed are the most important in this project. They can be reduced by some certain methods, but cannot be avoided.

Transient effect:

When the simulation first started, the response will start from the static condition and it will take some time for the system to get rid of the static condition and enter dynamic equilibrium condition. The transient period can be large, and the transient effect still exists in the following simulation time. This error can be reduced by increasing simulation time and take the time series starting point at a later time point.

Truncation error:

The time series taken into consideration can be a relatively short period that does not cover whole oscillation cycles of response components of all periods. For example, when the period taken into account is 500s, and there is a response component of 300s, then this component will not be well represented in this 500s period. Thus statistic values of the response from this 500s period will be exposed to error. This error can also be reduced by increasing simulation time.

Stochastic uncertainty:

This error is due to different seeds used in the simulation. Stochastic uncertainty does not have a strong influence for mean value and standard deviation. But it becomes very important when considering extreme response. Repetition of the same simulation with different seeds can reduce this error.

11.6 Recommendation for future work

First of all, according to the results obtained in this thesis, it is recommended that TDHmill should be used with careful consideration.

Secondly, some of the work done in this thesis can be perfected with more careful consideration and more calculations.

TDHmill thrust coefficients for NREL 5MW can be reevaluated. The thrust coefficients in this project are presented with 29 wind speed points. More points should be included to get a better curve. For each thrust coefficient, 1000s simulation is run and the first 400s are cut off to reduce truncation error. This simulation time may be increased for each wind speed to obtain more accurate thrust force.

Better wind force input data can be achieved by increasing the point numbers on the rotor plain in Turbsim. 16x16 points are used in this project, which is believed to provide sufficient accuracy. But since the wind field is complex and there can be strong turbulence at higher wind speeds, increase of the point numbers will probably give much better results with limited computation time increase.

Longer simulation time for each load case and more parallel simulations for each load case can also be performed to reduce uncertainties as has been discussed in the previous section.

At last, due to limited time and education level of the author, the work done in this thesis is only equivalent to the requirement of master thesis in NTNU. Some other work outside this thesis can also be done to better compare these two models:

Power generation can be compared. Apart from the structural consideration, power generation is also a key feature in offshore floating wind turbines. The power generation calculation methods in these two models are also different, with TDHmill the simplified method and Aerodyn the refined. It would be of interest to first model the wind generation carefully in these two models and then conduct an analysis on the power generation results.

Tower can be modeled as flexible structure and bending moment of the tower can be compared. More work is involved if the tower in TDHmill model is also to be modeled with flexible elements. But the bending moment at the bottom of the tower is one of the most important structural features, and it is of interest to see this result.

Fatigue analysis can also be performed. A very important reason for structural failure of offshore floating structures is the fatigue damage of floater or mooring line. So it would also be interesting to analyze the features of these two methods in fatigue considerations. More calculation cases will be needed then for this purpose.

References

[1] Principle Power. Inc. http://www.principlepowerinc.com/products/windfloat.html Windfloat description.

[2] Roddier D, Peiffer A. A Generic 5 MW Windfloat for Numerical Tool Validation & Comparison Against a Generic Spar. OMAE2011-50278, Rotterdam: 2011.

[3] Jonkman J, Butterfield S. Definition of a 5 MW Reference Wind Turbine for Offshore System Development. Technical Report NREL/TP-500-38060. 2009.

[4] H. Tennekes and J.L Lumley. A First Course in Turbulence. The MIT Press. 1972.

[5] Rune Yttervik. TDHMILL3D User documentation. Statoil internal document, 2009.

[6] Martin O. L. Hansen. Aerodynamics of Wind Turbines, second edition. Earthscan, 2008.

[7] P.J. Moriarty. AeroDyn Theory Manual

[8] SINTEF. Simo introduction. http://www.sintef.no/upload/MARINTEK/PDF-filer/Sofware/Simo.pdf

[9] MARINTEK. Rifelx. http://www.sintef.no/home/MARINTEK-old/Software-developed-at-MARINTEK/RIFLEX/

[10] Statoil. TDHMILL3D User Documentation

[11] Kelley N, Jonkman B. TurbSim description. http://wind.nrel.gov/designcodes/preprocessors/turbsim/

[12] Chenyu Luan. Pre-project for Master's Thesis. Norwegian University of Science and Technology: 2010.

[13] Erin Bachynski. Simo-Riflex-Aerodyn User's Manual. January, 2012

[14] Li L, Gao Z, Moan T. Environmental Data at Five Selected Sites for Concept Comparison. CeSOS: 2012

[15] WAFO introduction. http://www.maths.lth.se/matstat/wafo/

[16] Det Norske Veritas (DNV). GeniE user manual, 2008.

[17] Det Norske Veritas (DNV). HydroD user manual, 2008.

[18] Det Norske Veritas (DNV). WADAM user manual, 2005.

[19] Det Norske Veritas (DNV). DeepC user manual, 2010.

[20] Det Norske Veritas (DNV). DNV-RP-C205 Environmental conditions and environmental loads, October 2010.

[21] Det Norske Veritas (DNV). DNV-OS-E301 Position Mooring. October 2010

[22] Chenyu Luan. Dynamic response analysis of a semi-submersible floating wind turbine. Master thesis, NTNU, June 2011.

[23] Dag Myrhaug. Marin Dynamikk – uregelmessig sjø. Department of Marine Technology, NTNU, 2007

[24] Dag Myrhaug. Stochastic Seaload compendium. Department of Marine Technology, NTNU, 2011

[25] Rui Zhang. Mooring Analysis of Semi-submersible Wind Turbine. Master project, NTNU, 2012

Appendix

Several steps in this thesis require calculations based on Excel or Matlab. The detailed calculations are presented. Also presented are sample input files of Turbsim. Input files for Simo or Riflex are extremely long with much repetitive information. The key points of inputs for Simo and Riflex have been mentioned in the main text of this thesis, and thus will not be presented here in the Appendix.

List of appendices

Appendix 1. Mass calculation for floater in Model B

TOW	6.5E+02					TOTAL	4640											
	2.6E+01	-3E-07	6.9E+01				-2.78E-01	0	3.73									
	4.5E+05	2.2E+04	3.6E+06	1.2E+06			5.65E+06	5.59E+06	3.3E+06	0.00								
FLOA	4.0E+03					FLOAT	4000											
MY	-4.59	4E-08	-6.78			LUAN	-4.53	0	-6.71									
	2.2E+06	1.7E+06	2.8E+06	-1.2E+06			2.15E+06	1.66E+06	2.79E+06	-1.2E+06								
tower																		
num	length	center				diast	thst	densst	weight				Ixx	Iyy	Izz	Izx		
13	5	26.56	0	10	12.5	5.696	0.034	8.5	25.6	2.3	0.0	1.1	1.8E+04	0	4.0E+03	8.5E+03		
14	5	26.56	0	15	17.5	5.574	0.033	8.5	24.6	2.2	0.0	1.5	1.7E+04	0	7.5E+03	1.1E+04		
15	5	26.56	0	20	22.5	5.453	0.032	8.5	23.6	2.1	0.0	1.8	1.7E+04	0	1.2E+04	1.4E+04		
16	5	26.56	0	25	27.5	5.331	0.032	8.5	22.7	2.0	0.0	2.1	1.6E+04	0	1.7E+04	1.7E+04		
17	5	26.56	0	30	32.5	5.210	0.031	8.5	21.7	2.0	0.0	2.4	1.5E+04	0	2.3E+04	1.9E+04		
18	5	26.56	0	35	37.5	5.088	0.031	8.5	20.8	1.9	0.0	2.6	1.5E+04	0	2.9E+04	2.1E+04		
19	5	26.56	0	40	42.5	4.967	0.030	8.5	19.9	1.8	0.0	2.9	1.4E+04	0	3.6E+04	2.2E+04		
3	5	26.56	0	45	47.5	4.845	0.029	8.5	19.1	1.7	0.0	3.1	1.3E+04	0	4.3E+04	2.4E+04		
4	5	26.56	0	50	52.5	4.723	0.029	8.5	18.2	1.6	0.0	3.2	1.3E+04	0	5.0E+04	2.5E+04		
5	5	26.56	0	55	57.5	4.602	0.028	8.5	17.4	1.6	0.0	3.4	1.2E+04	0	5.7E+04	2.7E+04		
6	5	26.56	0	60	62.5	4.480	0.028	8.5	16.6	1.5	0.0	3.5	1.2E+04	0	6.5E+04	2.7E+04		
7	5	26.56	0	65	67.5	4.359	0.027	8.5	15.8	1.4	0.0	3.6	1.1E+04	0	7.2E+04	2.8E+04		
8	5	26.56	0	70	72.5	4.237	0.026	8.5	15.0	1.3	0.0	3.7	1.1E+04	0	7.9E+04	2.9E+04		
9	5	26.56	0	75	77.5	4.116	0.026	8.5	14.2	1.3	0.0	3.7	1.0E+04	0	8.5E+04	2.9E+04		
10	5	26.56	0	80	82.5	3.994	0.025	8.5	13.5	1.2	0.0	3.8	9.5E+03	0	9.2E+04	3.0E+04		
11	2.6	26.56	0	85	86.3	3.902	0.025	8.5	6.7	0.6	0.0	2.0	4.7E+03	0	5.0E+04	1.5E+04		
12	1.96	26.56	0	87.6	88.58	3.902	0.025	0	0.0	0.0	0.0	0.0	0	0	0	0		
	79.56			89.56					295.3	26.6	0.0	44.3	2.1E+05	0	7.2E+05	3.5E+05		
shaft																		
	length	center			center			unit w	weight									
shaft1	0.5	21.56	0	90	21.809	0	89.98	4.66	2.33	22	0	90	1108	0	18864	4572		
shaft2	0.5	22.058	0	89.96	22.307	0	89.93	0.01	0.005	0	0	0	2	0	40	10		
		22.556	0	89.91					2.335	22	0	90	1111	0	18904	4582		
		cent 1			cent 2			center 3					Ixx	Iyy	Izz			
		21.5	1.5	90.0	21.6	-0.7	91.3	21.4	-0.7	88.713			3025	27	53356	12702		
num	length	18.8	62.9	90.2	23.6	-31.5	144.5	14.1	-31.5	35.939	unit w	wei	2366	81	42262	9995		
1	2.7333	21.4	2.9	90.0	21.7	-1.4	92.5	21.2	-1.4	87.54	0.80	2.19	1577	122	28554	6705	1	0
2	2.7333	21.3	5.6	90.0	21.7	-2.8	94.8	20.9	-2.8	85.19	0.63	1.74	2429	377	44770	10411	4	0
3	2.7333	21.2	8.3	90.0	21.8	-4.2	97.2	20.6	-4.2	82.85	0.43	1.17	1978	568	37307	8564	7	0
4	4.1	21.0	11.7	90.0	21.9	-5.9	100.2	20.2	-5.9	79.92	0.45	1.83	1868	864	36137	8180	10	0
5	4.1	20.9	15.8	90.1	22.1	-7.9	103.7	19.7	-7.9	76.40	0.37	1.51	1744	1190	34635	7721	14	0
6	4.1	20.7	19.9	90.1	22.2	-10.0	107.3	19.2	-10.0	72.88	0.35	1.45	1570	1490	32069	7034	18	0
7	4.1	20.5	24.0	90.1	22.3	-12.0	110.8	18.7	-12.0	69.36	0.34	1.37	1375	1739	28936	6237	23	0
8	4.1	20.3	28.1	90.1	22.5	-14.1	114.4	18.2	-14.1	65.84	0.31	1.26	1221	1991	26509	5611	27	0
9	4.1	20.2	32.2	90.1	22.6	-16.1	117.9	17.7	-16.1	62.33	0.27	1.12	986	2021	22119	4593	31	1
10	4.1	20.0	36.3	90.1	22.7	-18.2	121.5	17.2	-18.2	58.81	0.25	1.01	811	2045	18814	3830	35	1
11	4.1	19.8	40.4	90.2	22.9	-20.2	125.0	16.8	-20.2	55.29	0.20	0.82	669	2042	16091	3210	39	1
12	4.1	19.6	44.5	90.2	23.0	-22.3	128.6	16.3	-22.3	51.77	0.17	0.69	505	1836	12577	2457	43	1
13	4.1	19.4	48.6	90.2	23.1	-24.3	132.1	15.8	-24.3	48.25	0.14	0.58	281	1172	7223	1386	47	1
14	4.1	19.3	52.7	90.2	23.2	-26.3	135.7	15.3	-26.3	44.73	0.11	0.44	217	1006	5727	1083	51	1
15	2.7333	19.1	56.1	90.2	23.4	-28.1	138.6	14.9	-28.1	41.80	0.09	0.25	147	752	3974	741	55	1
16	2.7333	19.0	58.8	90.2	23.4	-29.4	141.0	14.6	-29.4	39.46	0.07	0.19	22767	1932	451060	100462	57	1
17	2.7333	18.9	61.6	90.2	23.5	-30.8	143.4	14.2	-30.8	37.11	0.05	0.13					60	1
												17.74	21	0	90		61	
LOCAL																		
26.56	0	87.6	0	0	0													
1.9	0	1.75																
RM	RIXX	RIYX	RIYY	RIZX	RIZY	RIZZ												
240	1695	0	2895	-798	0	3026.4	28.46	0	89.35									
LOCAL							Ixx	Iyy	Izz	Ixz								
21.56	0	90	0	0	0		196088	2895	1919048	609498								
0	0	0																
RM	RIXX	RIYX	RIYY	RIZX	RIZY	RIZZ												
54	110	0	0	0	0	0	25211.01	0	437400	104782								

Appendix 2. Matlab code for thrust coefficients

```
clear all
clc
fid=fopen('data.txt','w');
for k=1:29;
    e=importdata(sprintf('Z:/Dokument/masterthesis/7/tdhmill coefficients/full
aerodyn - Copy - Copy (%d)/DLL_WTdata.txt',k),' ',1);
    f=e.data(:,8);
    g=e.data(1,2);
    d=mean(f(2000:4999));
    b=d/7.284/(g^2);
    fprintf(fid,'%d\t %d\n',[g,d]);
end
```

Appendix 3. Matlab code for TDHmill wind input file generation

```
clear all;
clc
for k=1
    data=importdata(sprintf('wind%d.u',k),' ',11);
    % data=importdata('wind1.u');
    [m,n]=size(data.data);
    for i=0:m/17-1
        t(i+1,1)=data.data(17*i+1,1);
        t(i+1,2)=data.data(17*i+1,2);
        temp1=zeros(17,16);
        temp1=data.data([17*i+2:17*i+17],:);
        t(i+1,3)=mean(temp1(:));
    end
    fid=fopen(sprintf('wind%d.dat',k),'w')
    % fid=fopen('wind1.dat','w');
    fprintf(fid,'%4d %4d\n',[m/17 1])
    for j=1:m/17
        fprintf(fid,'%4d %4d %4d\n',[t(j,1),t(j,2),t(j,3)])
    end
end
```

Appendix 4. Matlab code for constant wind test data process

```
clear all
clc
fid=fopen('data.txt','w');
for k=1:29;
    e=importdata(sprintf('Z:/Dokument/masterthesis/7/tdhmill coefficients/full
aerodyn - Copy - Copy (%d)/DLL_WTdata.txt',k),' ',1);
    f=e.data(:,8);
    g=e.data(1,2);
    d=mean(f(2000:4999));
    b=d/7.284/(g^2);
    fprintf(fid,'%d\t %d\n',[g,d]);
end
```

Appendix 5. Matlab code for frequency analysis in yaw decay test

```
clear all
clc
a=importdata('yaw.txt');
y=a(2000:5000);
```

```
[m,n]=size(y);
NFFT = 100000;
Y=fft(y,NFFT)/m;
f=2.5*linspace(0,1,(NFFT/2+1));
g=f.';
% Plot single-sided amplitude spectrum.
t=2*abs(Y(1:(NFFT/2+1)));
plot(g,t);
title('Single-Sided Amplitude Spectrum of y(t)')
xlabel('Frequency (Hz)')
ylabel('|Y(f)|')
```

Appendix 6. Matlab code for peak period selection

```
clear all;
clc
data=importdata('data.txt');
% syms x y z
[m,m1]=size(data);
x1=0.001:0.001:50;
n=max(size(x1));
for i=1:m
    a=data(i,1);
    b=data(i,2);
    for j=1:n
        y(j)=1/(sqrt(2*pi)*b*x1(j))*exp(-1/2*((log(x1(j))-a)/b)^2);
    end
    t(i)=x1(find(y==max(y)));
end
```

Appendix 7. Matlab code for statistics process

Model A

```
clear all
clc
fid=fopen('data.txt','w');
for k=1:42;
    a=importdata(sprintf('Z:/Dokument/master thesis/DeepC
workspace/11,18/Analysis%d/surge.asc',k),' ',4);
    b=importdata(sprintf('Z:/Dokument/master thesis/DeepC
workspace/11,18/Analysis%d/pitch.asc',k),' ',4);
    c=importdata(sprintf('Z:/Dokument/master thesis/DeepC
workspace/11,18/Analysis%d/heave.asc',k),' ',4);
    e=importdata(sprintf('Z:/Dokument/master thesis/DeepC
workspace/11,18/Analysis%d/thrust.asc',k),' ',4);
    d(1)=mean(a.data(6401:7200));
    d(2)=std(a.data(6401:7200));
    d(3)=mean(b.data(6401:7200));
    d(4)=std(b.data(6401:7200));
    d(5)=mean(c.data(6401:7200));
    d(6)=std(c.data(6401:7200));
    d(7)=mean(e.data(6401:7200));
    d(8)=std(e.data(6401:7200));
    fprintf(fid,'%4d %4d %4d %4d %4d %4d %d %d\n',d);
end
```

Model B

```
clear all
clc
fid=fopen('data.txt','w');
for k=1:42;
    a=importdata(sprintf('Z:/Dokument/masterthesis/6/%d/surge.asc',k),' ',4);
    b=importdata(sprintf('Z:/Dokument/masterthesis/6/%d/pitch.asc',k),' ',4);
    c=importdata(sprintf('Z:/Dokument/masterthesis/6/%d/heave.asc',k),' ',4);
    e=importdata(sprintf('Z:/Dokument/masterthesis/6/%d/DLL_WTdata.txt',k),' ',1);
    f=e.data(:,8);
    d(1)=mean(a.data(16000:18000));
    d(2)=std(a.data(16000:18000));
    d(3)=mean(b.data(16000:18000));
    d(4)=std(b.data(16000:18000));
    d(5)=mean(c.data(16000:18000));
    d(6)=std(c.data(16000:18000));
    d(7)=mean(f(32001:35999));
    d(8)=std(f(32001:35999));
    fprintf(fid,'%4d %4d %4d %4d %4d %4d %d %d\n',d);
end
```

Appendix 8. Matlab code for extreme condition analysis

```
clear all
for k=0:5
    a=importdata(sprintf('Z:/Dokument/master thesis/DeepC
workspace/11,18/Analysis42%d/tension.asc',k));
    [m,n]=size(a);
    meanA1(k+1)=mean(a((round(m/6)):m,2));
    meanA3(k+1)=mean(a((round(m/6)):m,3));
    maxA1(k+1)=max(a(1:m,2));
    maxA3(k+1)=max(a(1:m,3));
    minA1(k+1)=min(a(1:m,2));
    minA3(k+1)=min(a(1:m,3));
end
for k=0:5
    a=importdata(sprintf('Z:/Dokument/masterthesis/6/42 - Copy (%d) -
Copy/A030200_elmfor.asc',k));
    [m,n]=size(a);
    meanB1(k+1)=mean(a((round(m/6)):m,2));
    meanB3(k+1)=mean(a((round(m/6)):m,3));
    maxB1(k+1)=max(a(1:m,2));
    maxB3(k+1)=max(a(1:m,3));
    minB1(k+1)=min(a(1:m,2));
    minB3(k+1)=min(a(1:m,3));
end
```

Appendix 9. Matlab code for spectral anlsysis

```
clear all
clc
a1=importdata('Z:/Dokument/master thesis/DeepC
workspace/11,18/Analysis12/surge.asc',' ',4);
[m1,n1]=size(a1.data);
b1=a1.data(round(m1/4):m1);
c1=mean(b1);
[p1,q1]=size(b1);
for i=1:p1
    t1(i,1)=i*3600/m1;
    t1(i,2)=b1(i)-c1;
end
```

```
a2=importdata('Z:/Dokument/masterthesis/6/12/surge.asc',' ',4);
[m2,n2]=size(a2.data);
b2=a2.data(round(m2/4):m2);
c2=mean(b2);
[p2,q2]=size(b2);
for j=1:p2
    t2(j,1)=j*3600/m2;
    t2(j,2)=b2(j)-c2;
end
S11=dat2spec2(t1,2000);
S12=dat2spec2(t2,5000);
%%
clc
a1=importdata('Z:/Dokument/master thesis/DeepC
workspace/11,18/Analysis12/tension.asc');
[m1,n1]=size(a1);
b1=a1(round(m1/4):m1,3);
c1=mean(b1);
[p1,q1]=size(b1);
for i=1:p1
    t1(i,1)=i*3600/m1;
    t1(i,2)=b1(i)-c1;
end
a2=importdata('Z:/Dokument/masterthesis/6/12/A030200_elmfor.asc');
[m2,n2]=size(a2);
b2=a2(round(m2/4):m2,3);
c2=mean(b2);
[p2,q2]=size(b2);
for j=1:p2
    t2(j,1)=j*3600/m2;
    t2(j,2)=b2(j)-c2;
end
S21=dat2spec2(t1,15000);
S22=dat2spec2(t2,15000);
%%
clc
a1=importdata('Z:/Dokument/master thesis/DeepC
workspace/11,18/Analysis12/thrust.asc',' ',4);
[m1,n1]=size(a1.data);
b1=a1.data(round(m1/4):m1);
c1=mean(b1);
[p1,q1]=size(b1);
for i=1:p1
    t1(i,1)=i*3600/m1;
    t1(i,2)=b1(i)-c1;
end
a2=importdata('Z:/Dokument/masterthesis/6/12/DLL_WTdata.txt',' ',1);
[m2,n2]=size(a2.data);
b2=a2.data(round(m2/4):m2,8);
c2=mean(b2);
[p2,q2]=size(b2);
for j=1:p2
    t2(j,1)=j*3600/m2;
    t2(j,2)=b2(j)-c2;
end
S31=dat2spec2(t1,4000);
S32=dat2spec2(t2,8000);
%%
plot(S11.w(1:500),S11.S(1:500),S12.w(1:500),S12.S(1:500));
title('surge motiong')
xlabel('Angular frequency')
```

```
ylabel('Spectural density')
legend('Model A', 'Model B')
legend('Location','NorthEast')
plot(S21.w(1:800),S21.S(1:800),S22.w(1:800),S22.S(1:800));
title ('mooring line tension')
xlabel('Angular frequency')
ylabel('Spectural density')
legend('Model A', 'Model B')
legend('Location','NorthEast')
plot(S31.w(1:1000),S31.S(1:1000),S32.w(1:400),S32.S(1:400));
title('thrust force')
xlabel('Angular frequency')
ylabel('Spectural density')
legend('Model A', 'Model B')
legend('Location','NorthEast')
```

Appendix 10. Sample input file for Turbsim (Case 1)

TurbSim Input File. Valid for TurbSim v1.06.00, 21-Sep-2012

---------Runtime Options-----------------------------------
2318573 RandSeed1 - First random seed (-2147483648 to 2147483647)
RANLUX RandSeed2 - Second random seed (-2147483648 to 2147483647) for intrinsic pRNG, or an alternative pRNG: "RanLux" or "RNSNLW"
False WrBHHTP - Output hub-height turbulence parameters in binary form? (Generates RootName.bin)
False WrFHHTP - Output hub-height turbulence parameters in formatted form? (Generates RootName.dat)
False WrADHH - Output hub-height time-series data in AeroDyn form? (Generates RootName.hh)
False WrADFF - Output full-field time-series data in TurbSim/AeroDyn form? (Generates Rootname.bts)
True WrBLFF - Output full-field time-series data in BLADED/AeroDyn form? (Generates RootName.wnd)
False WrADTWR - Output tower time-series data? (Generates RootName.twr)
True WrFMTFF - Output full-field time-series data in formatted (readable) form? (Generates RootName.u, RootName.v, RootName.w)
True WrACT - Output coherent turbulence time steps in AeroDyn form? (Generates RootName.cts)
True Clockwise - Clockwise rotation looking downwind? (used only for full-field binary files - not necessary for AeroDyn)
0 ScaleIEC - Scale IEC turbulence models to exact target standard deviation? [0=no additional scaling; 1=use hub scale uniformly; 2=use individual scales]

--------Turbine/Model Specifications----------------------
16 NumGrid_Z - Vertical grid-point matrix dimension
16 NumGrid_Y - Horizontal grid-point matrix dimension
0.05 TimeStep - Time step [seconds]
4600 AnalysisTime - Length of analysis time series [seconds] (program will add time if necessary: AnalysisTime = MAX(AnalysisTime, UsableTime+GridWidth/MeanHHWS))
4600 UsableTime - Usable length of output time series [seconds] (program will add GridWidth/MeanHHWS seconds)
90 HubHt - Hub height [m] (should be > 0.5*GridHeight)
160.00 GridHeight - Grid height [m]
160.00 GridWidth - Grid width [m] (should be >= 2*(RotorRadius+ShaftLength))
0 VFlowAng - Vertical mean flow (uptilt) angle [degrees]
0 HFlowAng - Horizontal mean flow (skew) angle [degrees]

--------Meteorological Boundary Conditions-------------------
"IECKAI" TurbModel - Turbulence model ("IECKAI"=Kaimal, "IECVKM"=von Karman, "GP_LLJ", "NWTCUP", "SMOOTH", "WF_UPW", "WF_07D", "WF_14D", or "NONE")
"3" IECstandard - Number of IEC 61400-x standard (x=1,2, or 3 with optional 61400-1 edition number (i.e. "1-Ed2"))
31.4 IECturbc - IEC turbulence characteristic ("A", "B", "C" or the turbulence intensity in percent) ("KHTEST" option with NWTCUP model, not used for other models)
"NTM" IEC_WindType - IEC turbulence type ("NTM"=normal, "xETM"=extreme turbulence, "xEWM1"=extreme 1-year wind, "xEWM50"=extreme 50-year wind, where x=wind turbine class 1, 2, or 3)
default ETMc - IEC Extreme Turbulence Model "c" parameter [m/s]
default WindProfileType - Wind profile type ("JET","LOG"=logarithmic,"PL"=power law,"IEC"=PL on rotor disk,LOG elsewhere, or "default")
90 RefHt - Height of the reference wind speed [m]

```
3               URef          - Mean (total) wind speed at the reference height [m/s] (or "default" for JET wind profile)
default         ZJetMax       - Jet height [m] (used only for JET wind profile, valid 70-490 m)
default         PLExp         - Power law exponent [-] (or "default")
default         Z0            - Surface roughness length [m] (or "default")

--------Non-IEC Meteorological Boundary Conditions------------
default         Latitude      - Site latitude [degrees] (or "default")
0.05            RICH_NO       - Gradient Richardson number
default         UStar         - Friction or shear velocity [m/s] (or "default")
default         ZI            - Mixing layer depth [m] (or "default")
default         PC_UW         - Hub mean u'w' Reynolds stress (or "default")
default         PC_UV         - Hub mean u'v' Reynolds stress (or "default")
default         PC_VW         - Hub mean v'w' Reynolds stress (or "default")
default         IncDec1       - u-component coherence parameters (e.g. "10.0  0.3e-3" in quotes) (or "default")
default         IncDec2       - v-component coherence parameters (e.g. "10.0  0.3e-3" in quotes) (or "default")
default         IncDec3       - w-component coherence parameters (e.g. "10.0  0.3e-3" in quotes) (or "default")
default         CohExp        - Coherence exponent (or "default")

--------Coherent Turbulence Scaling Parameters-------------------
"D:\chrome downloads\TURBSIM\Test\EventData"  CTEventPath    - Name of the path where event data files are located
"Random"        CTEventFile   - Type of event files ("LES", "DNS", or "RANDOM")
true            Randomize     - Randomize the disturbance scale and locations? (true/false)
 1.0            DistScl       - Disturbance scale (ratio of wave height to rotor disk). (Ignored when Randomize = true.)
 0.5            CTLy          - Fractional location of tower centerline from right (looking downwind) to left side of the dataset. (Ignored
when Randomize = true.)
 0.5            CTLz          - Fractional location of hub height from the bottom of the dataset. (Ignored when Randomize = true.)
30.0            CTStartTime   - Minimum start time for coherent structures in RootName.cts [seconds]

================================================
NOTE: Do not add or remove any lines in this file!
================================================
```